AD

USAAMRDL TECHNICAL REPORT 72-31

AIRCRAFT CLUTCH ASSEMBLIES, RAMP ROLLER

By

Jules G. Kish

July 1972

EUSTIS DIRECTORATE
U. S. ARMY AIR MOBILITY RESEARCH AND DEVELOPMENT LABORATORY
FORT EUSTIS, VIRGINIA

CONTRACT DAAJ02-71-C-0026
SIKORSKY AIRCRAFT
DIVISION OF UNITED AIRCRAFT CORPORATION
STRATFORD, CONNECTICUT

Approved for public release; distribution unlimited.

98

DISCLAIMERS

The findings in this report are not to be construed as an official Department of the Army position unless so designated by other authorized documents.

When Government drawings, specifications, or other data are used for any purpose other than in connection with a definitely related Government procurement operation, the United States Government thereby incurs no responsibility nor any obligation whatsoever; and the fact that the Government may have formulated, furnished, or in any way supplied the said drawings, specifications, or other data is not to be regarded by implication or otherwise as in any manner licensing the holder or any other person or corporation, or conveying any rights or permission, to manufacture, use, or sell any patented invention that may in any way be related thereto.

Trade names cited in this report do not constitute an official endorsement or approval of the use of such commercial hardware or software.

DISPOSITION INSTRUCTIONS

Destroy this report when no longer needed. Do not return it to the originator.

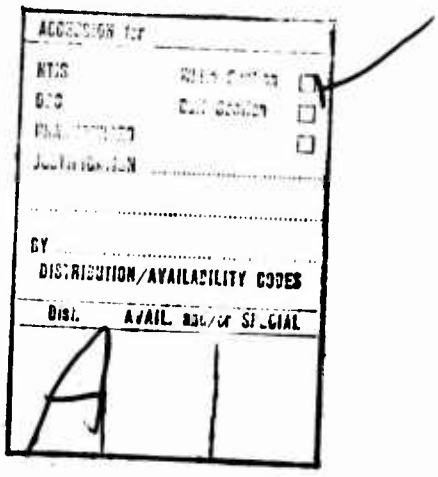

Unclassified
Security Classification

DOCUMENT CONTROL DATA - R & D

(Security classification of title, body of abstract and indexing annotation must be entered when the overall report is classified)

1. ORIGINATING ACTIVITY (Corporate author)	2a. REPORT SECURITY CLASSIFICATION
Sikorsky Aircraft Division of United Aircraft Corp. Stratford, Connecticut	Unclassified
	2b. GROUP

3. REPORT TITLE

AIRCRAFT CLUTCH ASSEMBLIES, RAMP ROLLER

4. DESCRIPTIVE NOTES (Type of report and inclusive dates)

Final Report

5. AUTHOR(S) (First name, middle initial, last name)

Jules G. Kish

6. REPORT DATE	7a. TOTAL NO. OF PAGES	7b. NO. OF REFS
July 1972	93	8

8a. CONTRACT OR GRANT NO.	9a. ORIGINATOR'S REPORT NUMBER(S)
DAAJ02-71-C-0026	USAAMRL Technical Report 72-31
b. PROJECT NO. 1G162207AA72	
c.	9b. OTHER REPORT NO(S) (Any other numbers that may be assigned this report) SER 50767
d.	

10. DISTRIBUTION STATEMENT

Approved for public release; distribution unlimited.

11. SUPPLEMENTARY NOTES	12. SPONSORING MILITARY ACTIVITY
	Eustis Directorate, U.S. Army Air Mobility Research and Development Laboratory, Fort Eustis, Virginia

13. ABSTRACT

The results of a 12-month program to evaluate a ramp roller clutch operating at engine input conditions of 26,500 rpm and 1500 hp are contained herein. The purpose of this design, manufacture, and test program was to evaluate clutch operation at the high speeds of advanced technology engines.

The ramp roller clutch was designed using the most advanced state-of-the-art technology available. Several new features were added to enhance high-speed operation. The most outstanding results were obtained from hollow rollers, which were used for the first time in a ramp roller clutch.

Although the ramp roller clutches tested operated well within acceptable limits for full-speed overrunning and engagement conditions, differential-speed overrunning tests resulted in excessive roller and housing wear.

Further exploratory development effort is required in the housing and roller retainer assembly elements of the ramp roller clutch.

12

DD FORM 1 NOV 68 1473

Unclassified
Security Classification

14. KEY WORDS	LINK A		LINK B		LINK C	
	ROLE	WT	ROLE	WT	ROLE	WT
Ramp Roller Clutch						
Transmission						
Overrunning Clutch						
Clutch						
Freewheel Unit						
Gearbox						
Helicopter Drive System						

i 2

DEPARTMENT OF THE ARMY
U. S. ARMY AIR MOBILITY RESEARCH & DEVELOPMENT LABORATORY
EUSTIS DIRECTORATE
FORT EUSTIS, VIRGINIA 23604

The research described herein was conducted by Sikorsky Aircraft under the terms of Contract DAAJ02-71-C-0026. The work was performed under the technical management of Mr. E. R. Givens, assisted by Mr. D. P. Lubrano, Propulsion Division, Eustis Directorate, U.S. Army Air Mobility Research and Development Laboratory.

VTOL drive systems must incorporate an overrunning (freewheel) clutch unit so that in the event of engine malfunction the aircraft can safely autorotate or, in the case of multiengines, proceed on singe-engine operation. Current overrunning speeds are limited to speeds of approximately 12,000 rpm or less depending on the torque transmitted. The objective of this program was to evaluate a ramp roller clutch operating at engine input conditions of 26,500 rpm and 1500 hp.

Appropriate technical personnel of this Directorate have reviewed this report and concur with the conclusions contained herein.

Project 1G162207AA72
Contract DAAJ02-71-C-0026
USAAMRDL Technical Report 72-31
July 1972

AIRCRAFT CLUTCH ASSEMBLIES, RAMP ROLLER

Final Report

Sikorsky Engineering Report 50767

By

Jules G. Kish

Prepared by

Sikorsky Aircraft
Division of United Aircraft Corporation
Stratford, Connecticut

for

EUSTIS DIRECTORATE
U.S. ARMY AIR MOBILITY
RESEARCH AND DEVELOPMENT LABORATORY
FORT EUSTIS, VIRGINIA

SUMMARY

The results of a 12-month program to evaluate a ramp roller clutch operating at engine input conditions of 26,500 rpm and 1500 hp are contained herein. The purpose of this design, manufacture, and test program was to evaluate clutch operation at the high speeds of advanced technology engines.

The ramp roller clutch was designed using the most advanced state-of-the-art technology available. Several new features were added to enhance high-speed operation. The most outstanding results were obtained from hollow rollers which were used for the first time in a ramp roller clutch.

Although the ramp roller clutches tested operated well within acceptable limits for full-speed overrunning and engagement conditions, differential-speed overrunning tests resulted in excessive roller and housing wear.

Further exploratory development effort is required in the housing and roller retainer assembly elements of the ramp roller clutch.

FOREWORD

The program reported herein was conducted during an 11-month period from February 22, 1971 to January 22, 1972 for the Eustis Directorate, U.S. Army Air Mobility Research and Development Laboratory (USAAMRDL), Fort Eustis, Virginia, under Contract DAAJ02-71-C-0026, Project 1G162207AA72.

USAAMRDL technical direction was provided by Mr. L. M. Bartone, Mr. E. R. Givens and Mr. D. Lubrano of the Eustis Directorate, Propulsion Division.

The program was conducted at Sikorsky Aircraft, Stratford, Connecticut, and Bridgeport, Connecticut, under the technical supervision of Mr. Lester R. Burroughs, Supervisor, Transmission Design and Development Section. Principal investigators for the program were Mr. T. Lally and Mr. R. Costanzo of the Transmission Design and Development Section, Mr. D. Wilson and Mr. R. Mack of the Mechanical Test Section, and Mr. J. Bucci of the Materials Section.

TABLE OF CONTENTS

LIST OF ILLUSTRATIONS

LIST OF TABLES

INTRODUCTION

An overrunning clutch permits the output or driven member of the clutch to freewheel whenever the input or driving member is stopped or is rotating at a slower speed. In a helicopter transmission, overrunning clutches are used to disengage the engines from the rotor, thus allowing the rotors to turn without engine drive. In multiple-engine aircraft, the overrunning clutch permits individual engines to be started without rotating the remaining engines. Safe landings may be executed by autorotation without the use of engines because the overrunning clutch automatically disconnects the engines from the rotor head when the engines are stopped.

One type of overrunning clutch is the ramp roller clutch, which is the subject of this report. The principal components of a ramp roller overrunning clutch are the cam, rollers, outer housing, and cage as shown in Figure 1. A spring and plunger mechanism acts on the roller retainer, which in turn forces the rollers up the ramps and against the outer housing. Driving action is obtained by wedging the rollers between the circular outer housing and the flats of the cam. This wedging of the rollers will occur only when the driving member attempts to turn faster than the driven member. Overrunning occurs whenever the driven member attempts to drive faster than the driving member. In the overrunning condition, the rollers theoretically roll on the outer housing and slide on the cam. However, in practice, the rollers do some sliding on the outer housing which reduces sliding on the cam.

The driving member may be either the cam or the housing. Each arrangement has its own advantages and disadvantages. The advantage of designing the outer housing as the driving member and the cam as the overrunning member is that lubricant can be fed from the center of the rotating cam and out to rollers, cage, and housing by centrifugal force. The disadvantage of cam overrunning is that the rollers are subjected to centrifugal load, which increases wear of rollers and housing. In the design with the cam driving, centrifugal roller loads during full-speed overrunning are eliminated, but the lubrication system must be pressurized to assure lubrication when the cam is stationary. In the high-speed ramp roller clutch design of this program, the configuration with the cam as driving member has been chosen since roller wear at the high speeds encountered is an overriding factor.

The purpose of this program was to test a ramp roller clutch at the high speeds of advanced technology engines. The helicopter overrunning clutch designed to operate at engine speed will be lighter than it would be when designed to operate on the second stage gear shaft (which is the usual case). Present state-of-the-art clutches generally operate at 6000 to 8000 rpm with 12,000 rpm the upper limit. Thus with the 26,500 rpm speed of the test clutch centrifugal effects are an order of magnitude higher since centrifugal load is proportional to speed squared.

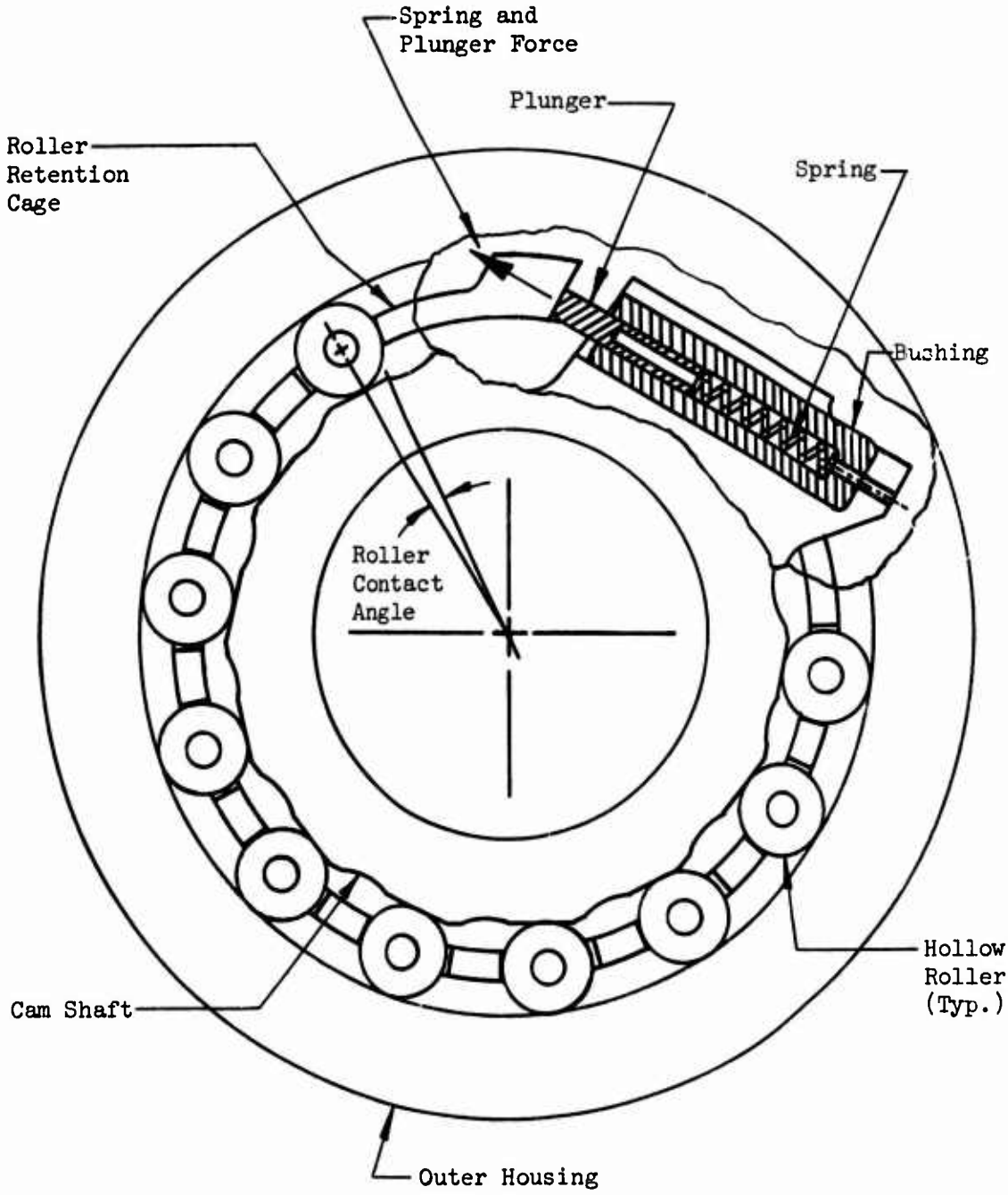

Figure 1. Principal Components of a Ramp-Roller Clutch.

DESIGN

DISCUSSION

The ramp roller clutch was designed using the methods and practices developed by Sikorsky Aircraft through years of successful ramp roller overrunning clutch applications. The clutch was designed for reliable operation in a helicopter transmission compatible with 26,500 rpm and 3,570 inch-pounds of torque. MIL-L-7808 lubricant was used at 195°F minimum oil inlet temperature and 100 psi maximum oil inlet pressure. Several new features make it possible to operate at the 20,850-fpm pitch-line velocity encountered during the 26,500-rpm differential speed overrunning tests. Three new design features are used for the first time on a Sikorsky Aircraft ramp roller clutch: oil-exchange ports, hollow rollers, and close-tolerance concentricity. Other recent design features also incorporated include pressurized lubrication system, tungsten-carbide flame-plated outer housing, straddle-mounted roller retainer, lubricated roller retainer return-spring-pin assembly, and outer housing oil dam. Table I summarizes the clutch design criteria, design geometry, and component stresses. Appendix I presents a structural analysis of major clutch components. Figure 2 is a cross section of the ramp roller clutch assembly indicating design features.

TABLE I. SUMMARY OF DESIGN CRITERIA, GEOMETRY, AND COMPONENT STRESS, RAMP ROLLER CLUTCH

Item	Minimum Roller Contact Angle	Maximum Roller Contact Angle
No-load roller contact angle	3 deg 52 min	4 deg 51 min
Roller contact angle (1500 hp)	5 deg 9 min	5 deg 50 min
RPM	26,500	26,500
HP (normal)	1,500	1,500
HP (static)	3,000	3,000
Housing outside radius	1.8800 in.	1.8700 in.
Housing bore radius	1.5030 in.	1.5035 in.
Cam flat to centerline	1.1250 in.	1.1240 in.
Cam inside radius	0.795 in.	0.805 in.
Roller radius	0.1875 in.	0.1874 in.
Effective roller length	0.56 in.	0.56 in.
Number of rollers	14	14
Roller load (1500 hp)	3770 lb	3320 lb
Roller Hertz stress (1500 hp)	433,600 psi	407,300 psi
Roller load (3000 hp)	6,540 lb	5,940 lb
Roller Hertz stress (3000 hp)	571,300 psi	544,700 psi
Clutch assembly weight	9.34 lb	9.34 lb

CRITICAL SPEED

As shown in Figure 2, the basic design has a low length-to-diameter ratio, resulting in the benefit of high natural frequency of lateral vibration for the system. This was verified during the design phase of the program using a computer program which determines natural frequency of rotating shaft systems. The first bending natural frequency was found analytically to be 35,060 cpm, which is well above the 26,500 cpm operating frequency. Concentricity tolerances on the outer housing were closely controlled during manufacture since this component creates the highest unbalance forces because it has the largest mass and polar moment of inertia.

FLAME PLATING

The outer housing of the ramp roller clutch is coated with tungsten-carbide, and the inner cam surface is case carburized. On the outer housing, the tungsten-carbide coating prevents excessive wear on the rolling surface. The coating process used on the outer housing conforms to Aeronautical Material Specification 2435. Previous tests conducted at Sikorsky Aircraft have shown that the inner cam flats can not be tungsten-carbide coated because of poor plating adhesion properties on the noncircular cam surfaces.

LUBRICATION

The shape of the inside of the cam shaft provides a natural chamber for oil flow to all clutch components. This chamber is pressurized to assure oil flow when the clutch overruns and the shaft is stationary. A single, fixed jet supplies oil to the chamber, which in turn supplies oil to clutch rollers, bearings, roller cage, and cage return-spring pin assembly. The clutch theoretical oil flow may be calculated by empirical methods which determine the friction horsepower. In practice, the most efficient oil flow may vary substantially from the theoretical. Windage and churning create a back pressure at the oil jet outlets which cannot be predicted by known analsis. As a result of windage and churning losses, the calculated oil flow of 1.42 gpm was reduced to .83 gpm. A further discussion is presented in the "TEST RESULTS" section of this report.

Each bearing has an oil port directed to the gap between bearing cage and inner race outside diameter. On the outer spacer of the matched spacer set between bearings, four 0.125-inch-diameter holes provide a rapid drain of oil between bearings. This rapid drain port reduces heat generation from churning.

A lubrication feature used for the first time on the clutch of this program is the oil-exchange port concept. Two 0.040-inch-diameter holes drain oil from the clutch roller area at approximately 0.6 gpm at 26,500 rpm and under the influence of pressure created by centrifugal force in the area of the oil dam (see Figure 2). This is less than the flow being fed to the roller area, spilling part of the oil over the oil dam and part of the oil through the oil-exchange ports. A constant turnover of new, cool oil is presented to the roller contact area; stagnant, trapped oil is prevented. Field experience has shown that frequently this area of the ramp-roller clutch outer

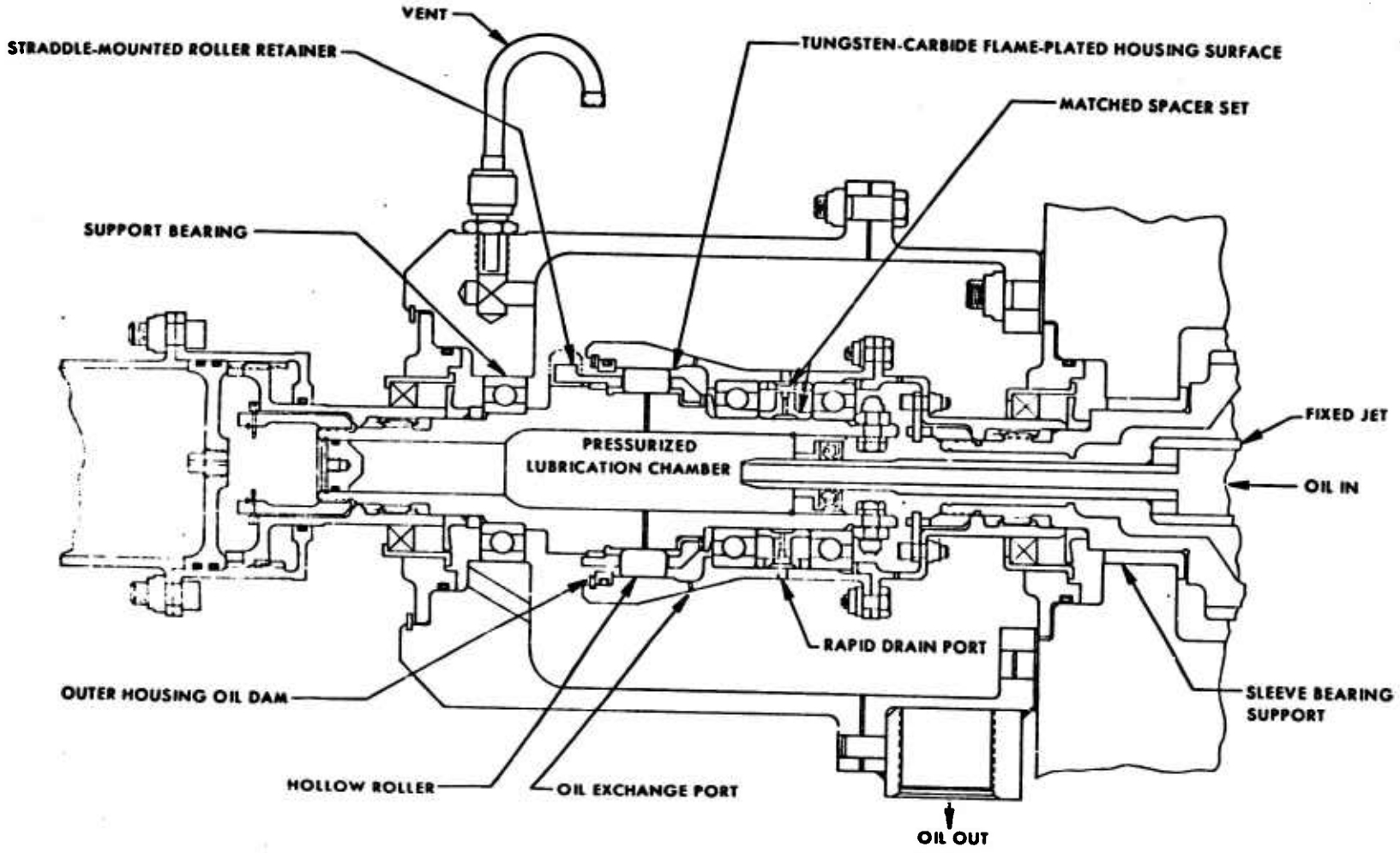

XXXXXXXXXXXXXXXXXXXXXXXXX
See the following pages
for greater detail.
XXXXXXXXXXXXXXXXXXXXXXXXX

Figure 2. Section View, Ramp Roller Clutch in Test Facility.

5.1 5.2 5.3

A

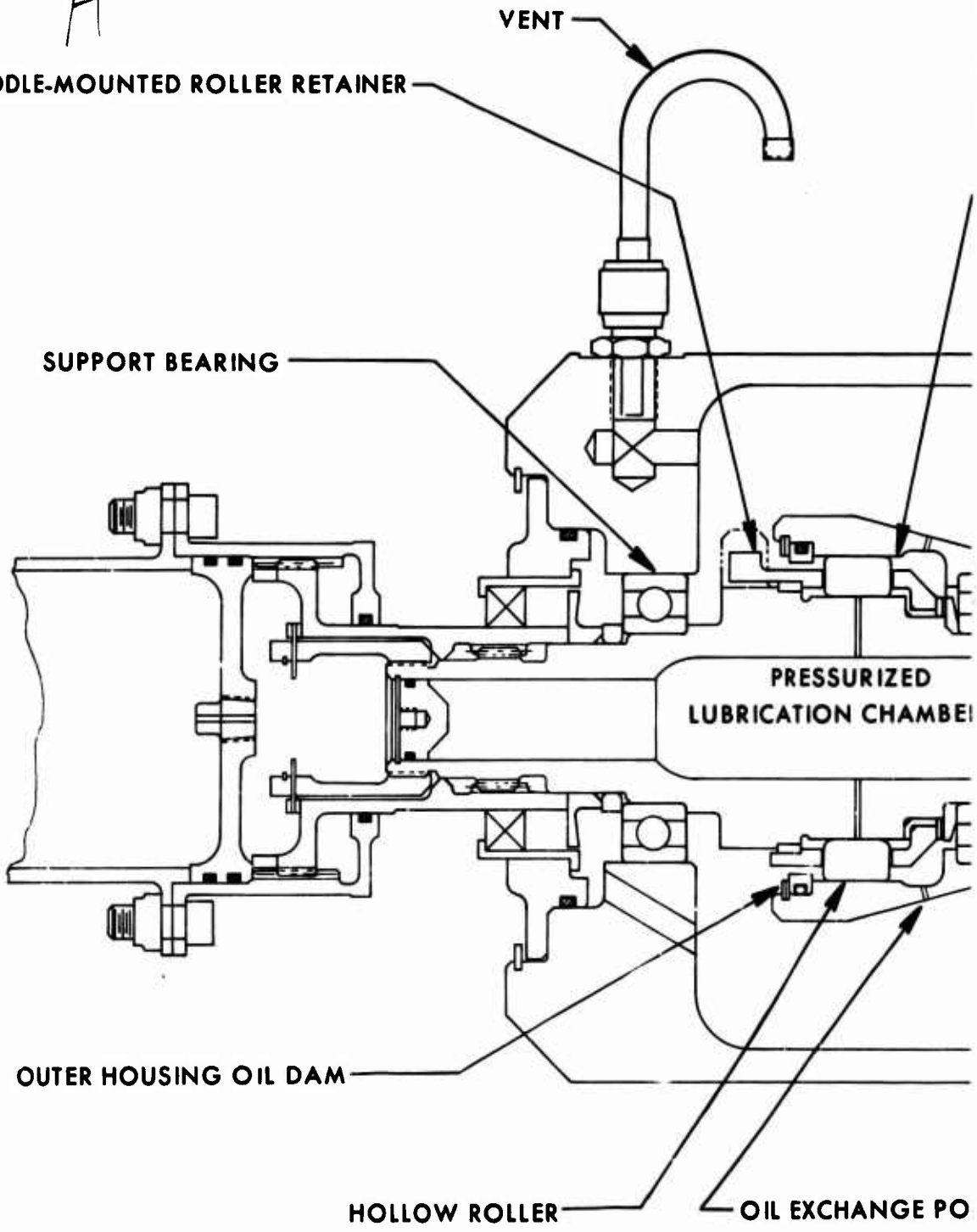
VENT
STRADDLE-MOUNTED ROLLER RETAINER
SUPPORT BEARING
PRESSURIZED
LUBRICATION CHAMBE
OUTER HOUSING OIL DAM
HOLLOW ROLLER
OIL EXCHANGE PO

5.1

Figu

5.2

B

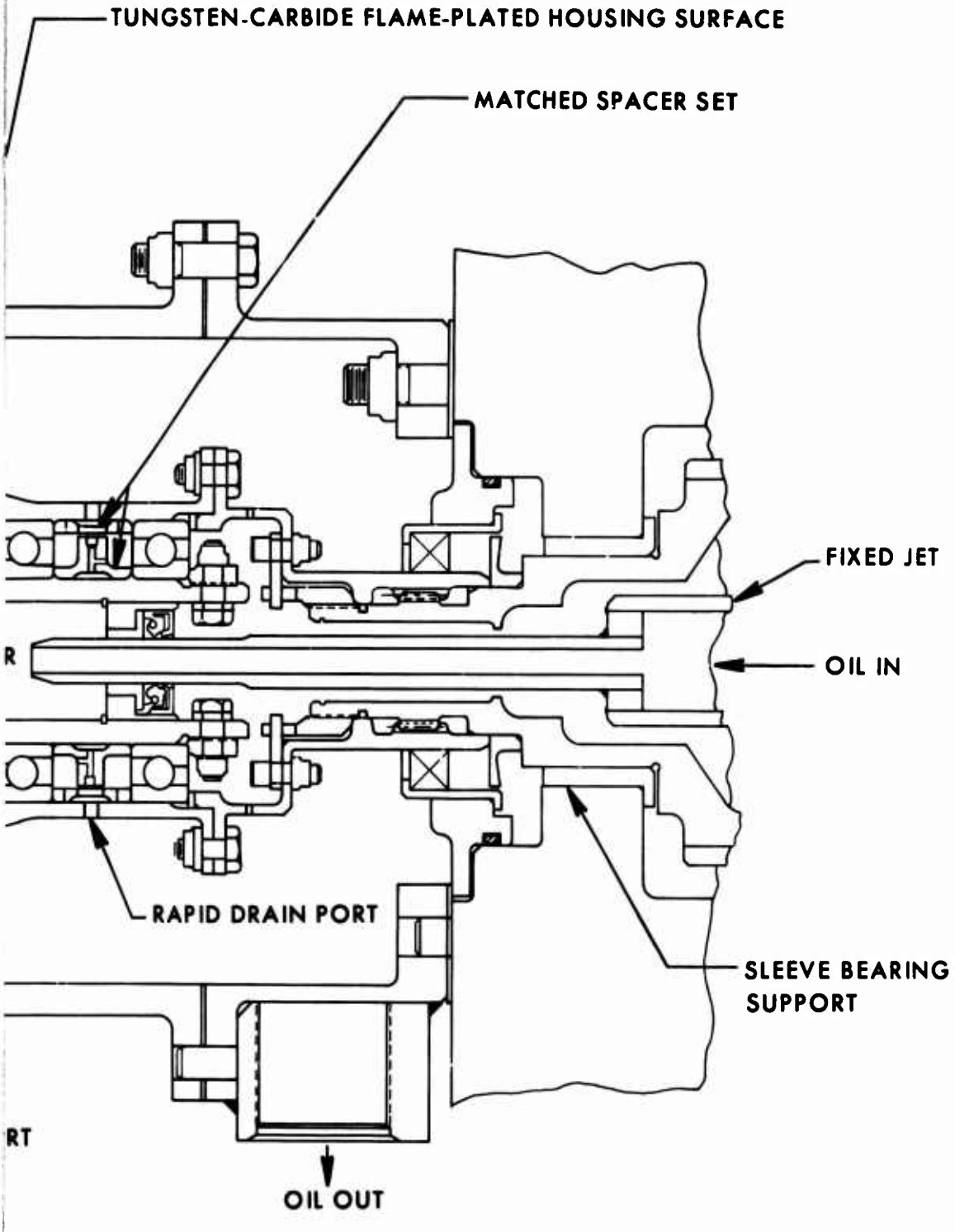

ıre 2. Section View, Ramp Roller Clutch in Test Facility.

housing builds up a sludge deposit which further reduces clutch efficiency, creates heat, and increases wear.

The pressurized lubrication chamber also provides oil for the roller retainer return-pin-spring assembly to reduce fretting created by the relative motion between pin and bushing.

The axially restrained roller retainer is straddle-mounted on oilite bushings and is free to rotate about its own axis. Straddle mounting helps to prevent misalignment of rollers on the cam during overrunning and also creates a chamber which forces oil to flow to the rollers.

HOLLOW ROLLERS

Hollow rollers have been incorporated into the design of the ramp-roller clutch. Although hollow rollers have previously been used in cylindrical roller bearings, this is the first time this concept has been used in a ramp-roller clutch. Hollow rollers reduce centrifugal load, increase heat dissipation, and improve load sharing as a result of increased roller flexibility.

The 0.125-inch-diameter hole in the 0.375-inch-diameter roller reduces solid roller weight by 12.5 percent. Since centrifugal roller load is directly proportional to roller mass, the load of the rollers on the housing at differential overrunning is reduced by 12.5 percent. Reduced centrifugal loads reduce wear of rollers and housing.

The most important advantage of the hollow roller accrues from greater roller flexibility. Small roller deflections greatly increase the contact area between rollers and housing and rollers and cam. Increased area of contact reduces surface compressive (Hertz) stress. The magnitude of the compressive stress is the overriding factor which controls the housing roller and cam cross-sectional dimensions. Hence, the overall freewheel unit size may be reduced when hollow rollers are used. A detailed analysis of hollow rollers is presented in Appendix II.

TEST FACILITY

DYNAMIC

The ramp-roller clutch dynamic test facility was used to conduct full-speed overrunning, differential-speed overrunning, and engagement tests. The test facility is shown in Figure 3.

The facility is a back-to-back open-loop configuration consisting of two Sikorsky H-3 helicopter main transmission input gearbox sections with separate electric drive motors. The ramp roller clutch test specimen is installed in a separate casing between drive transmissions. The clutch outer housing is belt driven through the H-3 rotor brake flange with a two-speed 40-hp electric motor. The rotor brake takeoff, normally operated at 3195 rpm, is driven at 4464 rpm, which corresponds to 26,500 rpm at the gearbox high-speed shafts. The ramp-roller input cam shaft is belt driven by a variable-speed 75-hp electric motor and has the capability of driving at any speed from 8500 rpm to 26,500 rpm.

Separate lubrication systems are supplied for the ramp-roller clutch and the drive transmission. The test clutch lubrication system with instrumentation is shown schematically in Figure 4. The clutch lubrication supply pump is capable of delivering 6 gpm at 100 psi at the clutch inlet. Flow and pressure are controlled by a bypass valve. A thermostatically controlled electrical heater is located between the lubrication supply pump and clutch oil inlet. This heater maintains oil inlet temperature at 195° F minimum, simulating extreme gearbox operating temperature.

The measurement of clutch drag torque is taken as shown in Figure 5. The linear potentiometer, which is rigidly connected to the spring scale, provides an accurate, remote measurement of spring deflection and hence load on the arm.

The test equipment and measurement instrumentation for the ramp-roller clutch dynamic test facility are listed in Table II.

STATIC

The ramp-roller clutch static test facilities were used to conduct the static cyclic clutch test and the ultimate load test of the ramp-roller clutch. The static test facility is shown in Figure 6.

The same clutch mounting fixture was installed on two different loading facilities to conduct the static cyclic and ultimate load tests. The clutch mounting fixture was installed on an IVY-4 Universal Fatigue Testing Machine during the static cyclic test and on a Static Universal Test Fixture with hydraulic cylinder during the overload test.

Cyclic torque of 7140 $\pm$ 900 inch-pounds is applied at 1800 cpm through a 12-inch torque arm mounted to the clutch camshaft. The clutch outer housing is bolted to a fixed support to react torque through the clutch. Load is continuously monitored by a calibrated load cell located between the torque arm

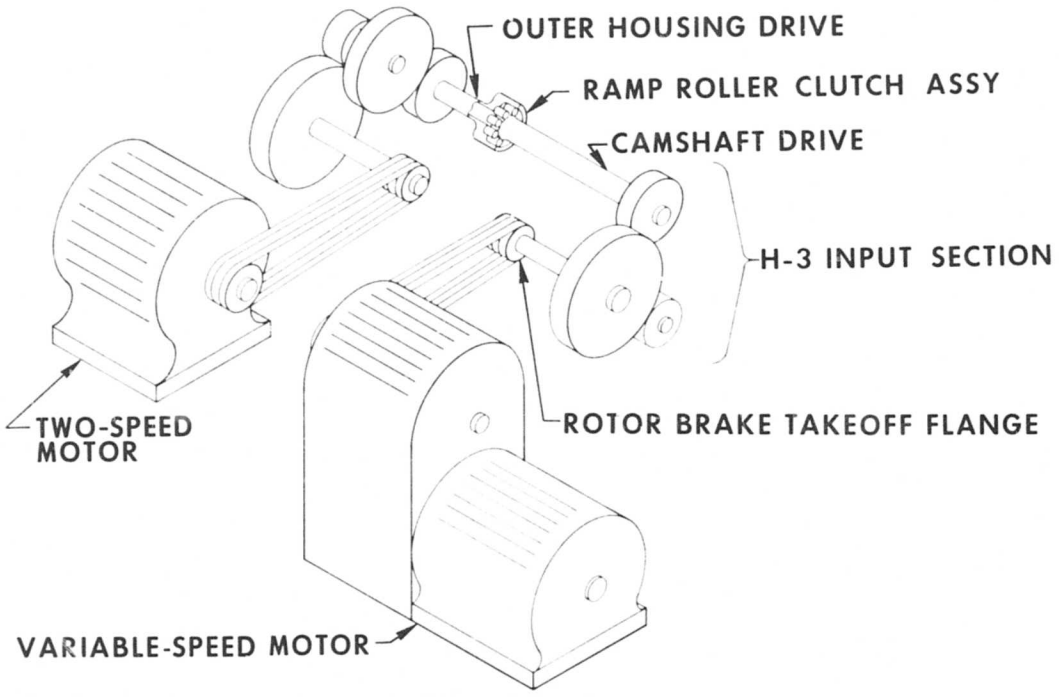

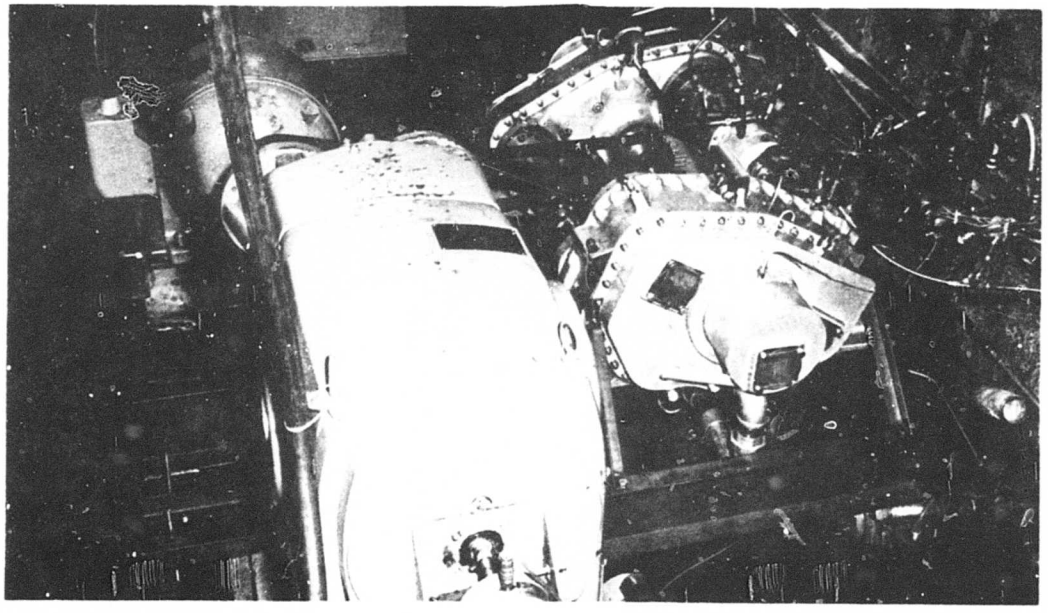

Figure 3. Schematic Arrangement, Dynamic Test Facility.

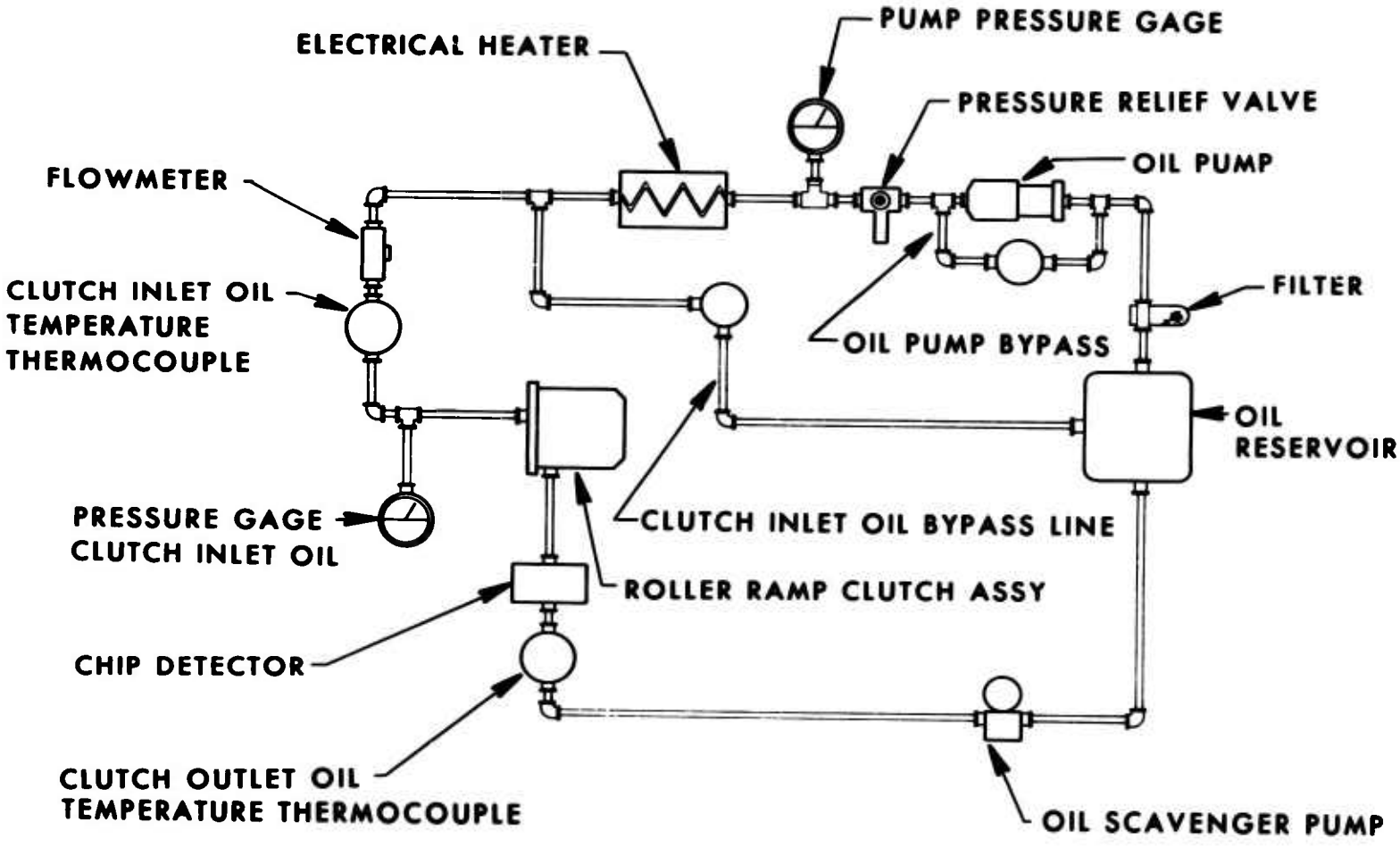

Figure 4. Lubrication Schematic, Ramp Roller Clutch Dynamic Facility.

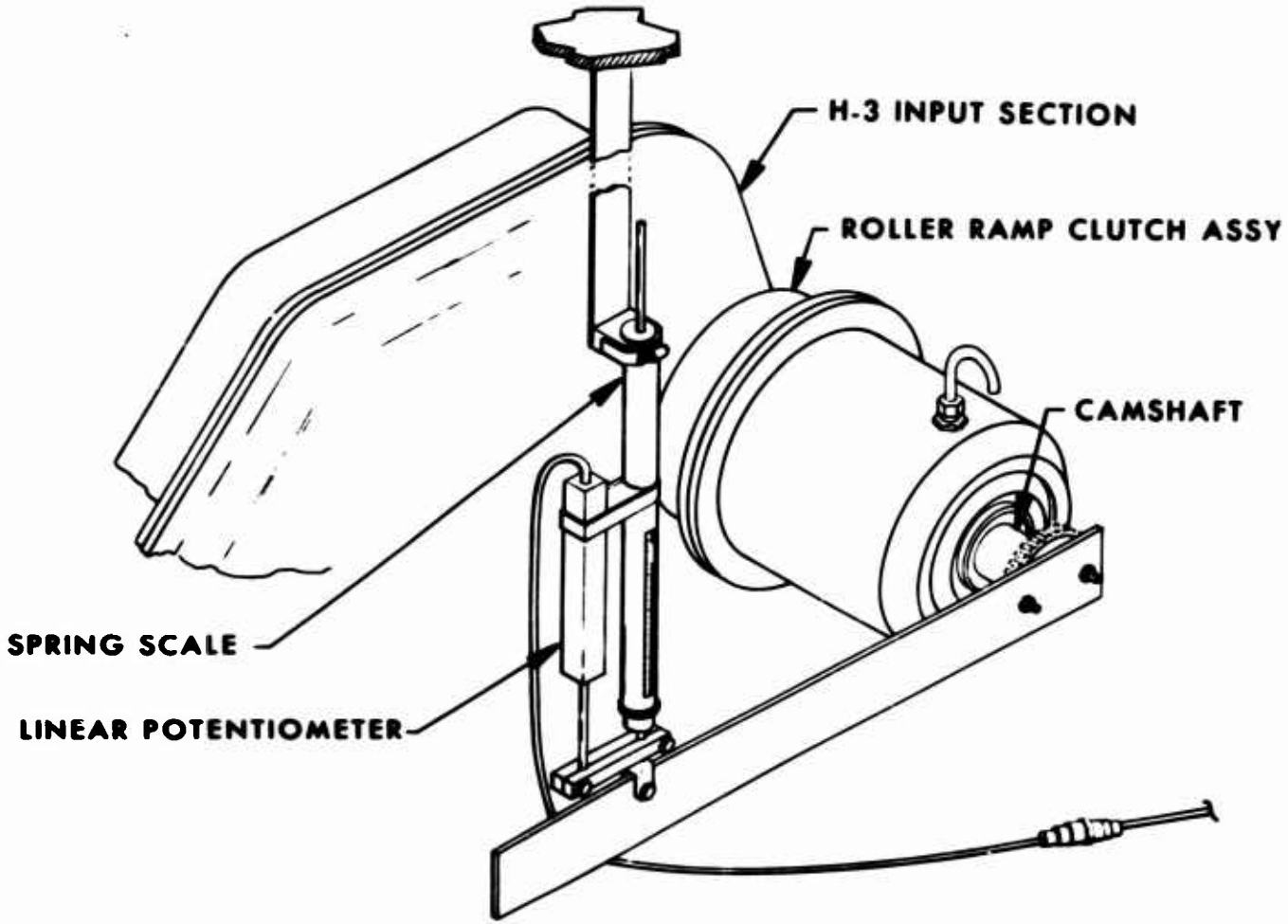

Figure 5. Full-Speed Overrunning Drag Torque Measurement.

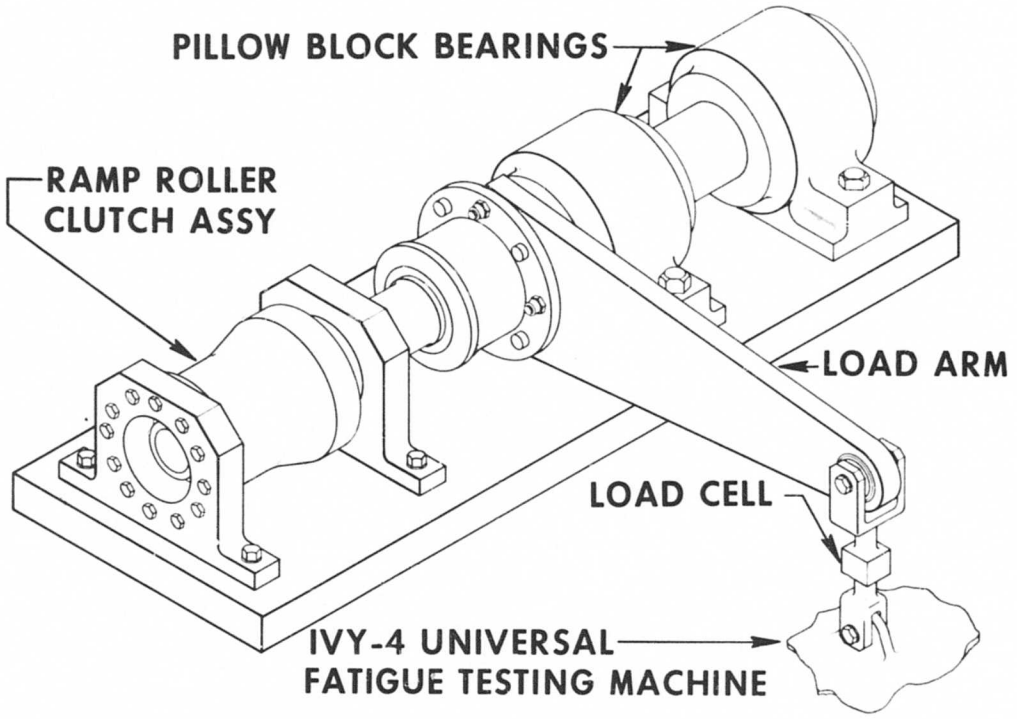

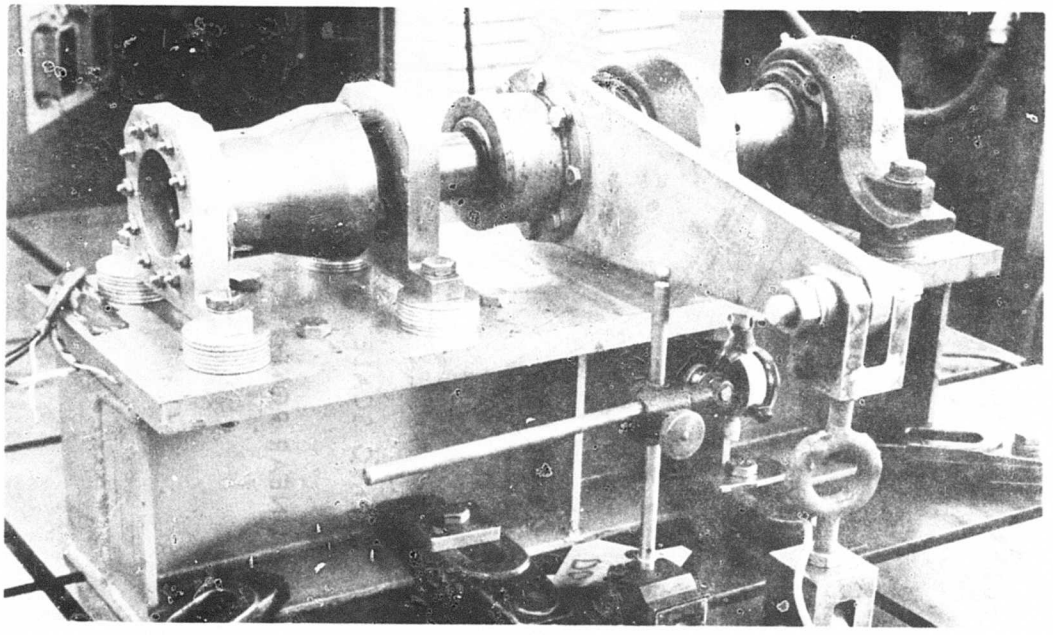

Figure 6. Schematic Arrangement, Static Test Facility.

TABLE II. TEST EQUIPMENT AND MEASUREMENT INSTRUMENTATION - RAMP-ROLLER CLUTCH DYNAMIC TEST FACILITY

Item	Equipment
Input drive motor	75-hp "Varidrive" electric motor
Output drive motor	40-hp two-speed electric motor
Input gearbox	H-3 main transmission input section with left-side input spur and left-side freewheel unit shaft removed and special fabricated rear cover
Output gearbox	H-3 main transmission input section with right-side input spur and right-side freewheel unit shaft removed and special fabricated rear cover
Clutch test specimen	Ramp roller clutch
H-3 transmission lubrication pump	5-hp electric-motor-driven vane pump
Clutch lubrication supply pump	2-hp electric-motor-driven vane pump
Clutch lubrication scavenge pump	0.5-hp electric-motor-driven vane pump
Input gearbox rpm	Pulse pickup and converter
Output gearbox rpm	Pulse pickup and converter
Test clutch oil flow rate	Flowmeter
Clutch oil-in temperature	Immersed thermocouple - strip chart recorder
Clutch oil-out temperature	Immersed thermocouple - strip chart recorder
Clutch oil-in pressure	Pressure gage
Drag torque (full-speed override test only)	Linear potentiometer and 0- to 2-lb spring scale
Drive gearboxes bearing temperature	Lug type thermocouples
Drive gearboxes oil flow	Flowmeter
Drive gearboxes manifold pressure	Pressure gage
Drive gearboxes inlet and outlet oil temperature	Immersion type thermocouples

and the testing machine. Microwire and limit switches automatically terminate testing if failure occurs.

Ultimate load is applied by a Static Universal Test Fixture with hydraulic cylinder using the same support structure of the static cyclic test.

The test equipment and measurement instrumentation for the ramp-roller clutch static test facility is listed in Table III.

TABLE III. TEST EQUIPMENT AND MEASUREMENT INSTRUMENTATION - RAMP-ROLLER CLUTCH STATIC TEST FACILITY

Item	Equipment
Ultimate load applicator	Static Universal Test Fixture with hydraulic cylinder
Static cyclic load applicator	IVY-4 Universal Fatigue Test Machine
Clutch test specimen	Ramp-roller clutch
Input torque	Load cell with Ellis Console
Radial housing displacement	Dial indicator, micrometer
Angular displacement	Dial gage
Cycles	Cycle converter

TEST PROCEDURE

DYNAMIC

Full-Speed Override

The purpose of the full-speed override test was to determine the optimum oil flow rate for the ramp-roller clutch test specimen and to subject the components to extreme speed differential. The tests were conducted on the ramp-roller clutch dynamic test facility. Prior to the start of testing, a checkout was conducted to verify test stand operation at 26,500 rpm, to check out the test stand instrumentation, and to determine characteristics of the H-3 main transmission input section lubrication system.

MIL-L-7808 oil was used as the lubricant during all dynamic testing. During the full-speed override tests, the input cam was held stationary while the output housing was rotated at 26,500 rpm. Four tests of 5 hours duration each were conducted at progressively lower oil flow conditions. After each 5-hour test, the test specimen was disassembled and inspected. Measurements were taken of the diameter of each roller, diameter of housing, and depth of wear of cam flats. Each roller was numbered and assembled into its corresponding numbered slot in the roller retainer. Full-speed overrunning test conditions are listed in Table IV.

TABLE IV. FULL-SPEED OVERRUNNING TEST PLANNED OPERATING CONDITIONS

Test	Oil Flow (%)	Input Speed (rpm)	Output Speed (rpm)
1	300	0	26,500
2	200	0	26,500
3	100	0	26,500
4	67	0	26,500
5*	33	0	26,500

* Test not conducted - see discussion in "TEST RESULTS" section

Each test was run for 5 hours after temperature conditions had stabilized. The minimum oil inlet temperature was 195°F for all tests and was thermostatically controlled by a heater in the clutch lubrication system. At 15-minute intervals, measurements were taken of total running time, temperature at the oil inlet and outlet lines, pressure of oil in, flow of oil in, and clutch drag torque. The test specimen outer casing was insulated during each full-speed overrunning test to determine heat rejection.

Differential-Speed Override

The purpose of the differential-speed override test was to determine the clutch maximum drag condition and to ascertain the effects of centrifugal force on clutch operation. The ramp-roller clutch dynamic test facility was used to conduct the differential-speed tests.

During the differential-speed tests, the clutch output housing was rotated at 26,500 rpm while the input cam was rotated at 50 percent, 67 percent and 75 percent of output. Rotation of the input cam subjected the rollers, cam, cage, and cage return-spring-pin assembly to the effects of centrifugal force for the first time. Three tests were scheduled to be conducted for 5 hours each at progressively higher input cam speed at the oil flow condition established during the full-speed overrunning tests. The test conditions of the differential-speed overrunning tests are listed in Table V.

TABLE V. DIFFERENTIAL-SPEED OVERRUNNING TEST PLANNED OPERATING CONDITIONS

Test	Oil Flow (%)	Input Speed (rpm)	Output Speed (rpm)
6	100	13,250	26,500
7	100	17,667	26,500
8*	100	19,875	16,500

* Test not conducted - see discussion in "TEST RESULTS" section

Each test was run for 5 hours after temperature conditions had stabilized. Oil inlet temperature was maintained at 195°F minimum with a thermostatically controlled heater. At 15-minute intervals, measurements were taken of total running time, temperature at the oil inlet and outlet lines, pressure of oil-in, and flow of oil-in.

After each 5-hour test, the clutch test specimen was disassembled and inspected. Each roller was numbered and assembled into its corresponding numbered slot in the cage. Measurements were taken of each roller diameter, depth of wear of cam flats, and outer housing diameter (average of two readings). The test specimen outer casing was insulated during each differential-speed overrunning test to determine heat rejection.

Engagement

Engagement tests were conducted on the ramp-roller clutch to verify operation under various dynamic conditions. All engagement tests were conducted on the ramp-roller clutch dynamic facility. Engagement tests were conducted by first rotating the outer housing above the engagement speed. The input cam was then rotated at the required engagement speed. The output electric

drive motor was then shut off, allowing the outer housing speed to decay until engagement occurred at zero housing and cam speed differential. Table VI lists the engagement speed and number of engagements.

TABLE VI. ENGAGEMENT TEST PLANNED OPERATING CONDITIONS

Test Number	Engagement Speed (rpm)	Percent (%)	Number of Engagements
9	13,250	50	2
10*	19,875	75	2
11	26,500	100	5

* Test not conducted - see discussion in "TEST RESULTS" section

After each engagement test, the clutch was disassembled and inspected. Measurements were taken of each roller diameter, depth of brinelling in cam flats, and diameter of outer housing bore (average of two readings). The rollers, housing, and cam flats were examined for brinelled areas. The cage was examined for cracks or brinelling in roller slots.

STATIC

Cyclic Load

Cyclic load tests of the ramp roller clutch were conducted to verify structural integrity of the clutch components. During this test the ramp roller clutch outer housing was fixed while the input cam was subjected to 7140 $\pm$ 900 inch-pounds torque in the engagement direction. The test was conducted for 10 million cycles with the test specimen installed in the ramp-roller clutch static facility on an IVY-4 Universal Fatigue Test Machine. Torque was applied at the rate of 1800 cpm.

Torque was continuously monitored by a calibrated load cell and oscillograph readout. Microwire and load monitoring units were installed to automatically shut the test machine off. The load monitor was set at $\pm$ 2 percent load deviation. At 60-minute intervals, readings were taken of clutch torque, number of cycles, clutch creep, and outer housing radial displacement. Clutch creep is defined as angular displacement of input relative to output. At the completion of testing, the clutch was disassembled and inspected.

Overload

An ultimate load test of the ramp-roller clutch test specimen was conducted to verify static structural integrity. The clutch was installed in the ramp roller clutch static facility on the static universal test fixture. A steady load was applied in the engaging direction in increments of 1800

inch-pounds up to 10,800 inch-pounds and in increments of 900 inch-pounds thereafter until slippage or failure occurred. At each load increment, readings were taken of clutch torque, housing radial displacement, and clutch creep. Two separate tests were conducted: one with a case carburized outer housing without tungsten-carbide flame plating and one with tungsten-carbide flame plating on the outer housing.

TEST RESULTS

DYNAMIC TESTS

Full-Speed Override

Analysis of the friction horsepower absorbed by the ramp roller clutch during overrunning indicated that 1.42 gpm would be required to remove heat for the 100-percent oil flow condition. During the actual initial trial runs with the input cam fixed and the output housing rotating, it was found that with flow rates greater than 0.83 gpm, a choking phenomenon occurred inside the clutch pressurized chamber. As the rpm of the outer housing increased, churning and windage losses also increased in the area of the rollers, creating a back pressure which restricted flow from the jets. Figures 7 and 8 show pressure and flow versus speed of the output housing with the input cam fixed. Note that the choking effect does not occur below approximately 0.83 gpm final flow rate. On this basis, the 100-percent flow condition was chosen to be 0.83 gpm.

Once the 100-percent flow condition was established, the 300-percent flow test at 2.5 gpm was conducted. After temperatures were stabilized with the input cam fixed and the output housing rotating at 26,500 rpm, 5 hours of overrunning time were accumulated. The clutch was disassembled and visually inspected for signs of wear. Measurements were taken of all roller diameters, depth of depressions on cam flats, and outer housing diameter. Visual inspection showed negligible wear on all components. Inspection of rollers and cam showed that the black oxide surface was partially removed. Depth of wear did not exceed 0.0001 inch on any component.

The same ramp roller clutch specimen was assembled, and the test at 200-percent flow condition of 1.66 gpm was conducted. Disassembly and inspection after 5 hours of running again showed negligible wear. On the tungsten-carbide flame plating of the outer housing, a hard line appeared approximately 0.03 inch wide and 30 percent of the circumference with no measurable depth.

Similar results were obtained during the third 5-hour run at the 100-percent flow condition. Roller wear again measured less than 0.0001 inch. The hard line experienced during the 200-percent flow test was enlarged to approximately 0.04 inch wide and 40 percent of the circumference with no measurable depth.

The fourth test run of 5 hours duration was conducted at the 67-percent flow condition of 0.55 gpm. Post-test inspection results were markedly different from those of the previous tests. Total roller diametral wear from all previous tests ranged from 0.0003 to 0.0005 inch. During the 67-percent test, the roller diametral wear ranged from 0.0066 to 0.0103 inch. Roller wear data is shown in Figure 9 for all full-speed overrunning tests. Heavy sludge deposits were found in the oil-exchange-port area of the outer housing. Figure 10 shows the condition of the rollers after the 67-percent flow test. Although high wear was measured, as shown in Figure 9, the rollers were highly polished and perfectly round. The flame-plated outer housing, shown in Figure 11, showed wear for 360° and the full length of the roller

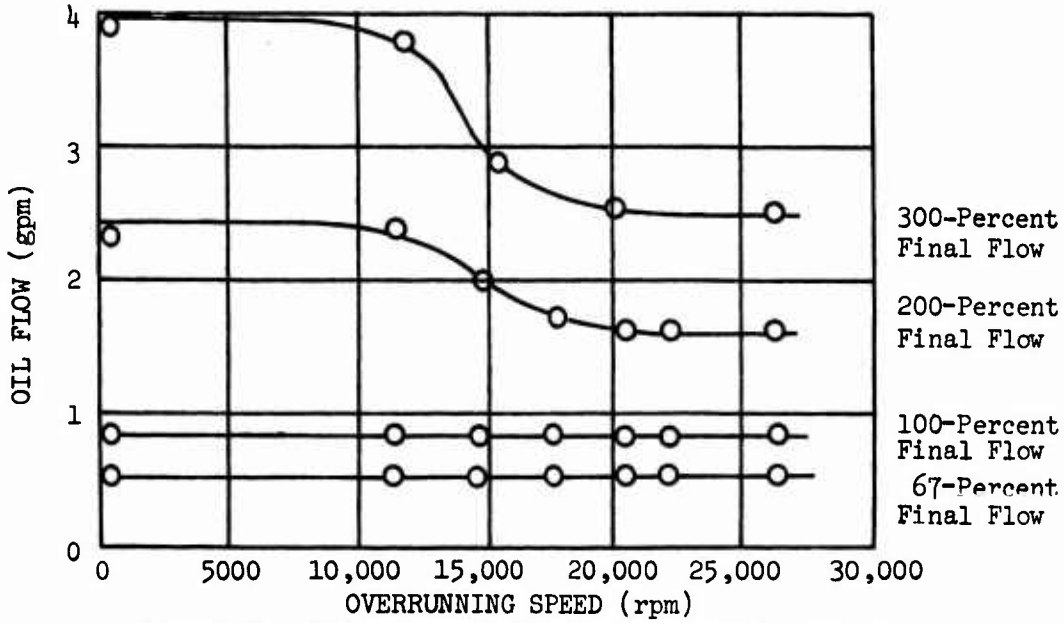

Figure 7. Influence of Housing Overrunning Speed on Pressurized Chamber Oil Flow.

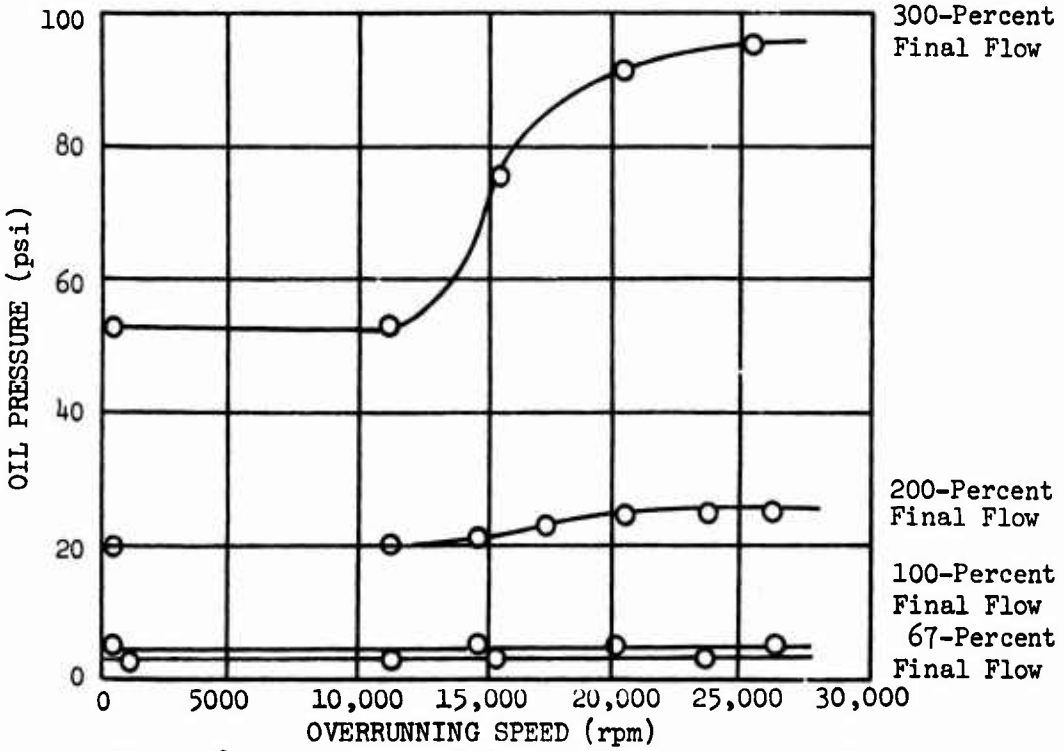

Figure 8. Influence of Housing Overrunning Speed on Clutch Inlet Oil Pressure.

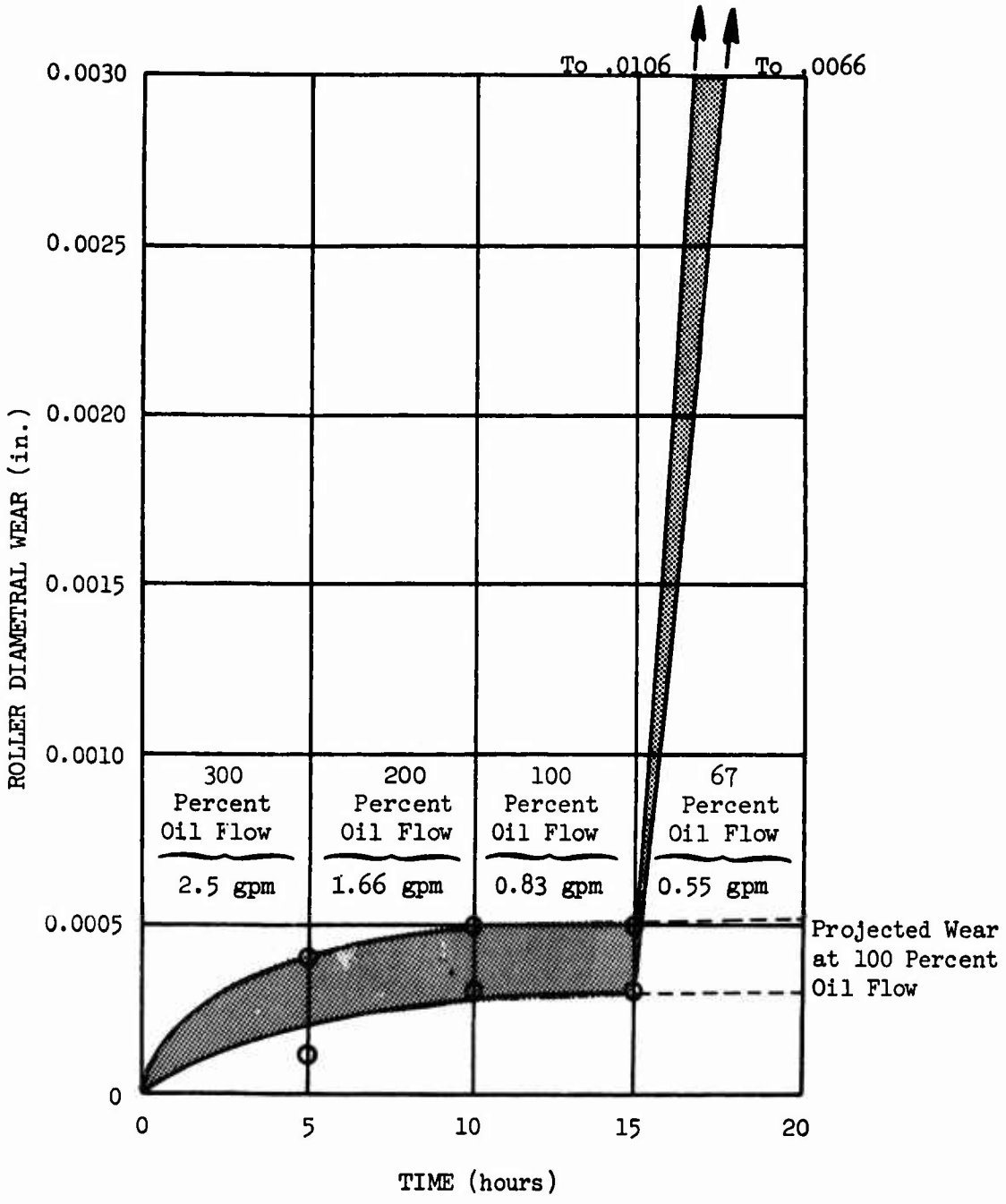

Figure 9. Full-Speed Overrunning Test Roller Wear.

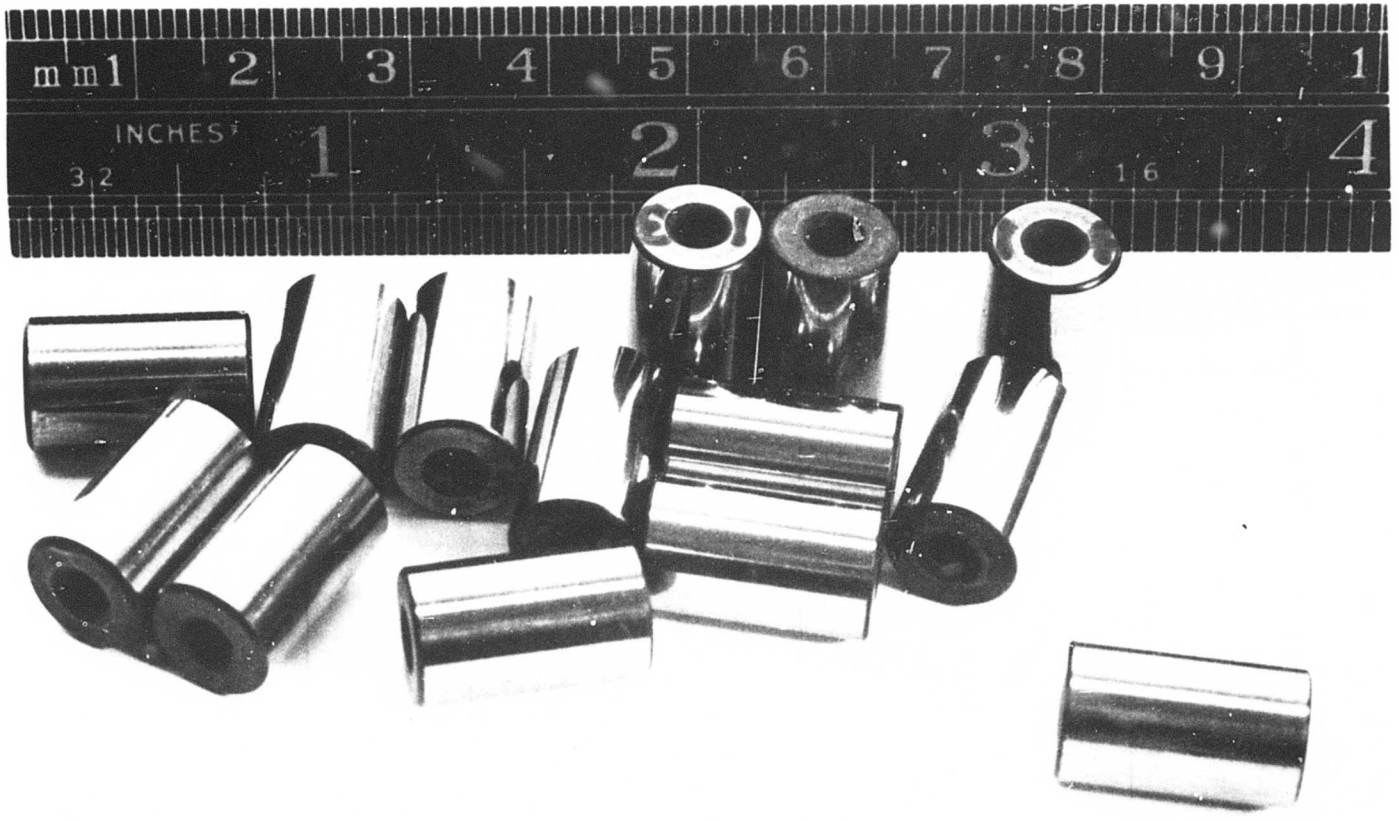

Figure 10. Condition of Rollers at Completion of Full-Speed Overrunning Tests.

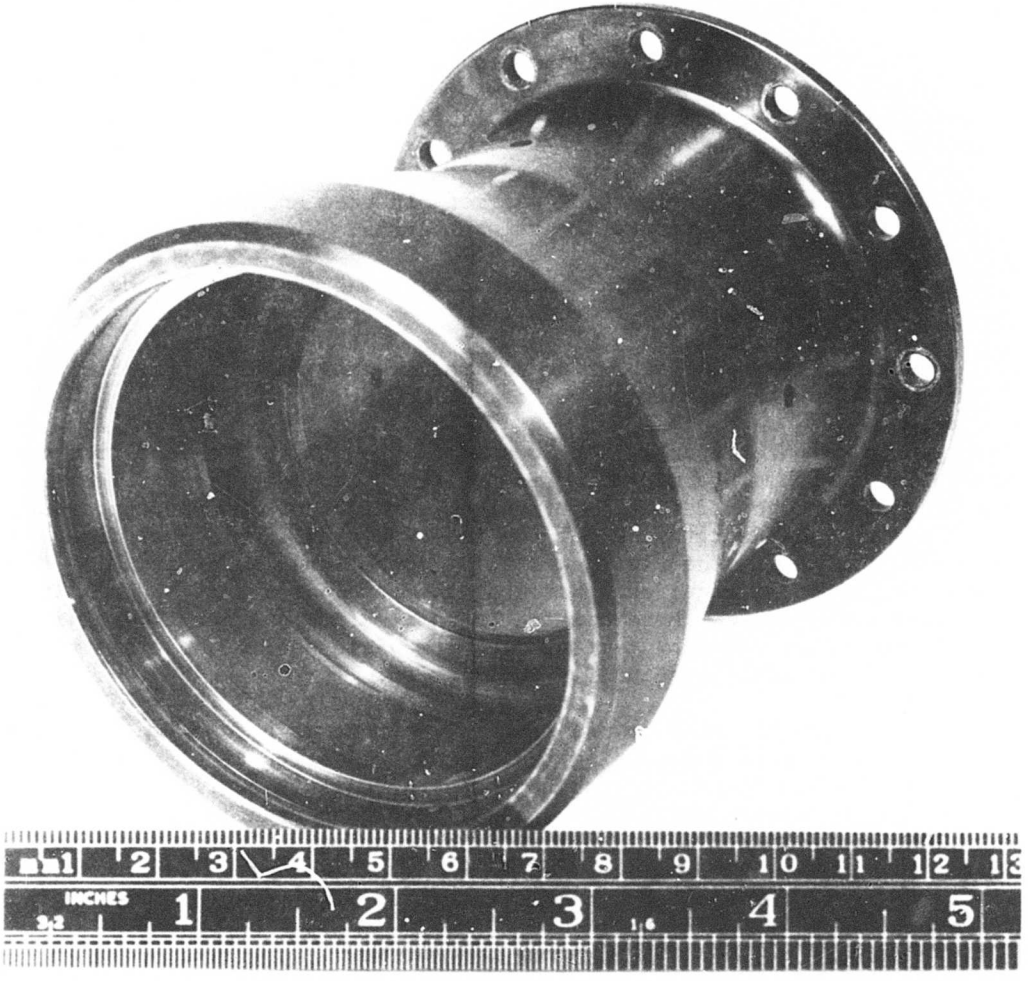

Figure 11. Condition of Outer Housing at Completion of Full-Speed Overrunning Tests.

contact area for a depth of 0.0002 inch. The cam flats exhibited a polished surface, as shown in Figure 12, but the depth of wear was less than 0.0001 inch. The outer housing support bearing nearest the clutch rollers had extensive heat and deformation damage as shown in Figure 13. Discoloration of the inner race showed a maximum temperature of 475° when matched to a standard temperature color comparator for 52100 bearing steel. Figure 14 shows all ramp roller clutch components after the 67-percent flow test of 0.55 gpm.

Examination of all clutch components showed that the high wear of rollers and overheating of the duplex bearing nearest the rollers were caused by insufficient quantity of lubrication. This conclusion is based on the following facts:

1. The bearing discoloration was heat induced and was typical of a failure due to insufficient lubrication.

2. The only test variable changed during the 67-percent flow test was the flow, which was reduced from 0.83 gpm to 0.55 gpm.

3. Marked increase in housing and roller wear rate occurred only after oil flow was reduced to 0.55 gpm.

The magnetic chip detector switch located in the oil return line from the ramp roller clutch contained magnetic particles but not of sufficient magnitude to cause the chip detector to indicate. No other outward appearances of failure were evident throughout the test. Even with the heat damage and wear indicated above, the clutch was fully operational and capable of transmitting full load if required. Based on the conclusion that the results of the 67-percent flow test were created by an insufficient quantity of lubrication, the 33-percent flow test at 0.28 gpm was cancelled, as this test would provide no additional useful information.

Figure 15 depicts the average oil temperature rise as a function of flow during the full-speed overrunning tests. The reduction at 0.55 gpm indicates that the heat generated was not transferred to the oil. The velocity of the bearing lubricating jet stream may have been reduced to the point where lubricant was not in contact with the bearing.

Drag torque data for each flow condition of the full-speed overrunning tests are given in Appendix III.

Figure 16 is a graph of full-speed overrunning drag torque as a function of flow.

Analysis of the roller wear curves and the heat rejection curves leads to the conclusion that the design flow condition should be chosen as low as possible for minimum heat generation but must be of sufficient magnitude to maintain lubrication on all surfaces. Projected roller wear with proper lubrication as shown in Figure 9 shows that wear of rollers during full-speed overrunning is approximately 0.000005 inch per overrunning hour after initial break in wear of 0.0005 inch in a period of 15 hours. Assuming 0.005 diametral wear life of rollers, this leads to 915 hours roller

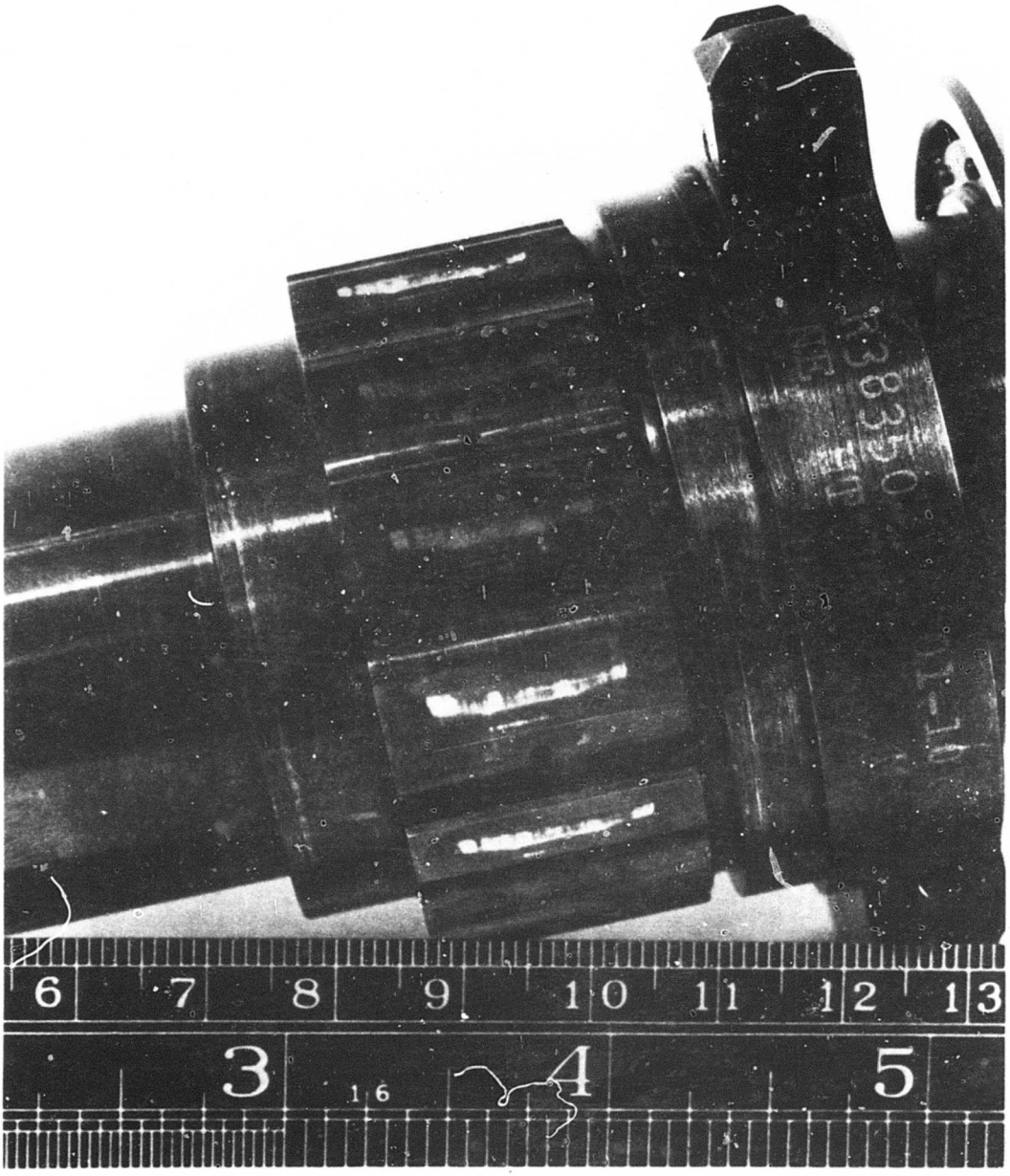

Figure 12. Condition of Cam Flats at Completion of Full-Speed Overrunning Tests.

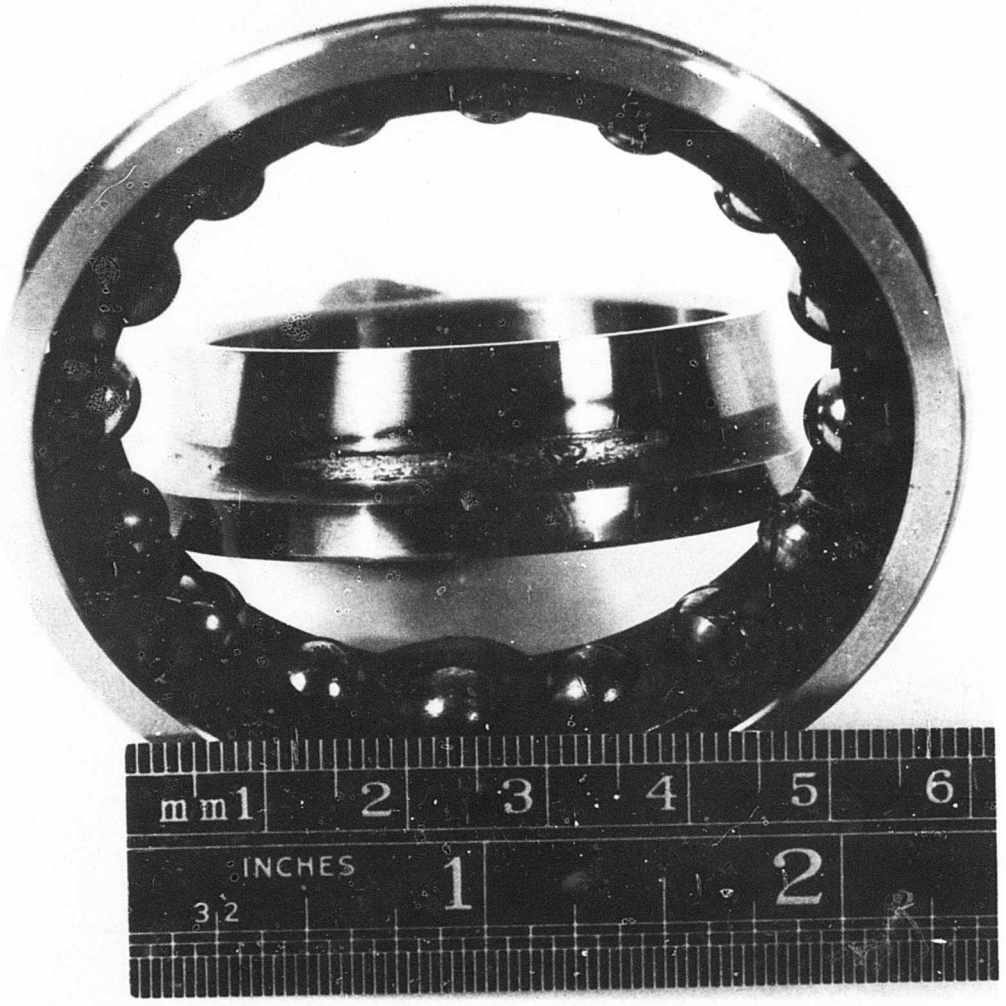

Figure 13. Forward Support Bearing Heat Damage, 67-Percent Oil Flow Overrunning Tests.

Figure 14. Clutch Components After Full-Speed Overrunning Tests.

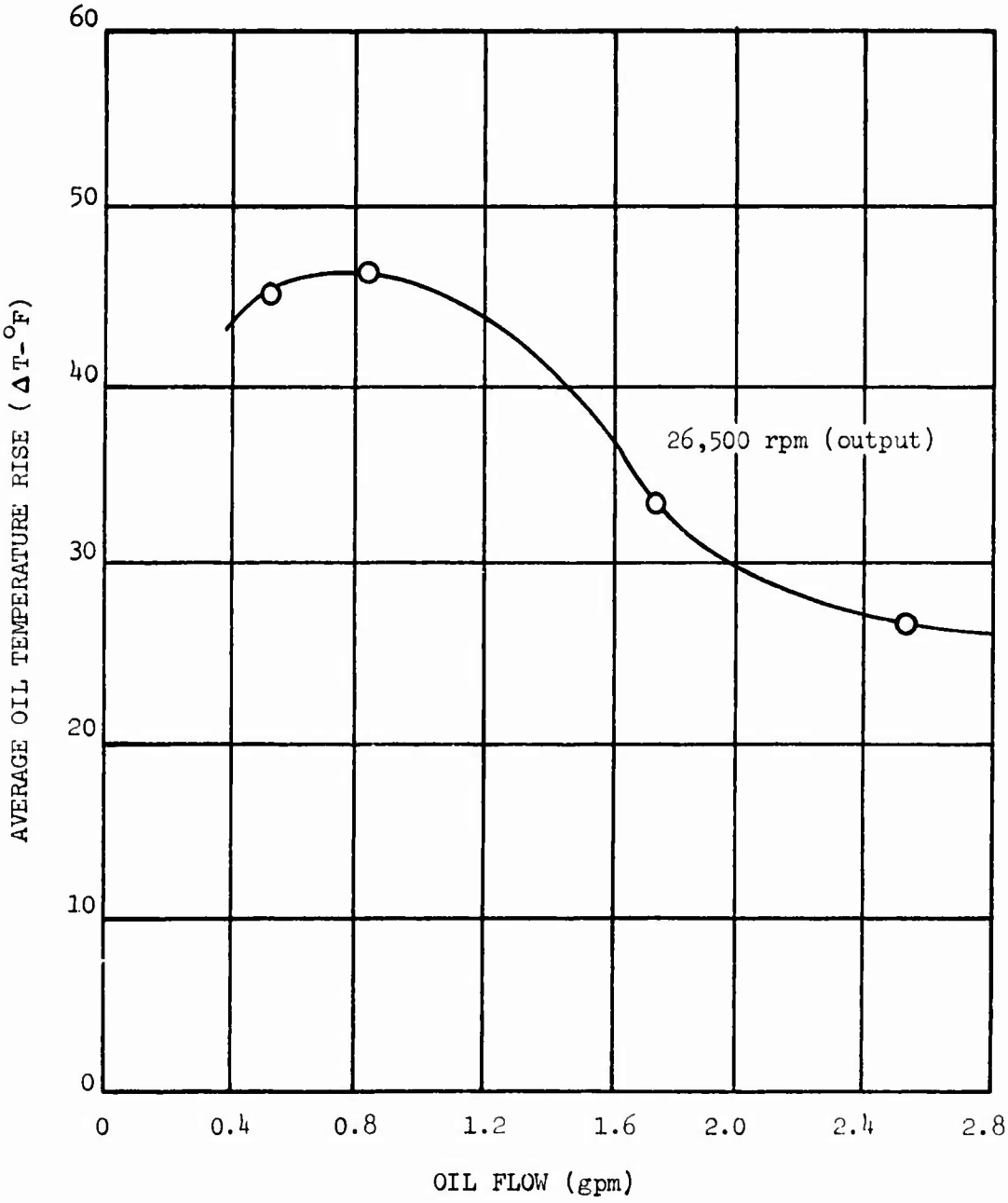

Figure 15. Variation of Oil Temperature Rise With Oil Flow at Full-Speed Overrunning. (Input Stationary)

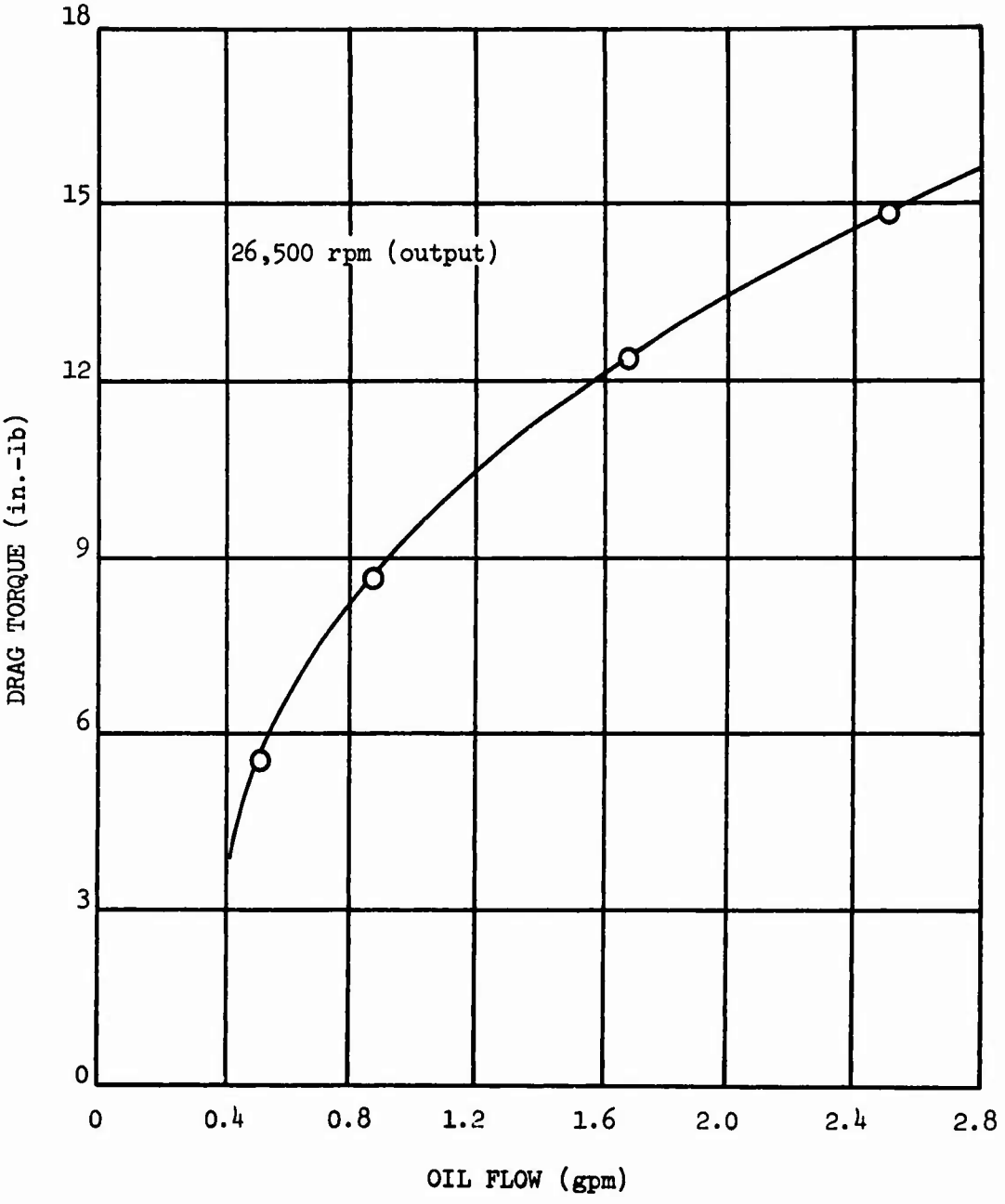

Figure 16. Effect of Oil Flow on Drag Torque, Full-Speed Overrunning. (Input Stationary)

full-speed overrunning life. This exceeds expected transmission life on a typical helicopter, since overrunning is estimated to occur less than 5 percent of the time.

Differential-Speed Override

The rollers, housing, and bearing which were damaged during the full-speed overrunning test at 0.55 gpm were replaced with new parts. The first differential-speed test was conducted with the cam at 13,250 rpm and outer housing at 26,500 rpm for 5 hours after temperatures had stabilized.

Based on the results of the full-speed overrunning tests, the 100-percent flow rate for the first differential-speed overrunning test was set at 1.1 gpm. This provided a 100% flow margin above the inadequate flow experienced during the 0.55-gpm full-speed overrunning test and was not detrimental to wear, as shown by the wear rates at higher flow conditions during the full-speed overrunning tests.

Disassembly inspection after the first 5-hour test revealed wear on rollers, cam, cage and housing. The tungsten-carbide flame plating on the outer housing was worn through, as shown in Figure 17. The edges were chipped and peeled but not beyond the parent material. The roller diametral wear experienced during the 50-percent differential-speed overrunning tests ranged from 0.0051 to 0.0070 inch. The original roller diameters ranged from 0.3749 to 0.3750 inch.

Roller cocking caused wear on the ends of the rollers as shown by the typical example of Figure 18. Another example of roller cocking may be found on the ends of the cage roller slots as shown in Figure 19.

The cam flats were rounded at the intersection of the flat and undercut section as shown in Figure 20. The wide band area at approximately the center of the flat was formed previously during the full-speed overrunning tests and had no measurable depth. The rounded area on the flat corner indicated that the roller was not located at the proper overrunning position but was running partially in the undercut and partially on the flat of the cam. Thus, without intimate contact between housing and cam, the roller was assumed to be "fluttering" between cam and housing. During the test, no measurable vibration was recorded on vibration pickups mounted to the clutch housing. The depth of wear of the tungsten-carbide coated outer housing, which was suspiciously even with the coating depth and not beyond, may have been created by the impacts of the fluttering rollers against the housing. The tungsten-carbide coating is vulnerable to impact type loading. The residue from the worn coating may have acted as a grinding abrasive compound, creating accelerated roller and cage wear.

The tests were temporarily halted so that the outer housings could be replated with tungsten-carbide; the testing was then continued.

To correct the cocking of the rollers and the roller flutter problem, the cage return spring which preloads the roller retainer and holds the roller in intimate contact between housing and cam was changed to a larger size, increasing the load per pin from 1.0 pound to 1.5 pounds at installed length

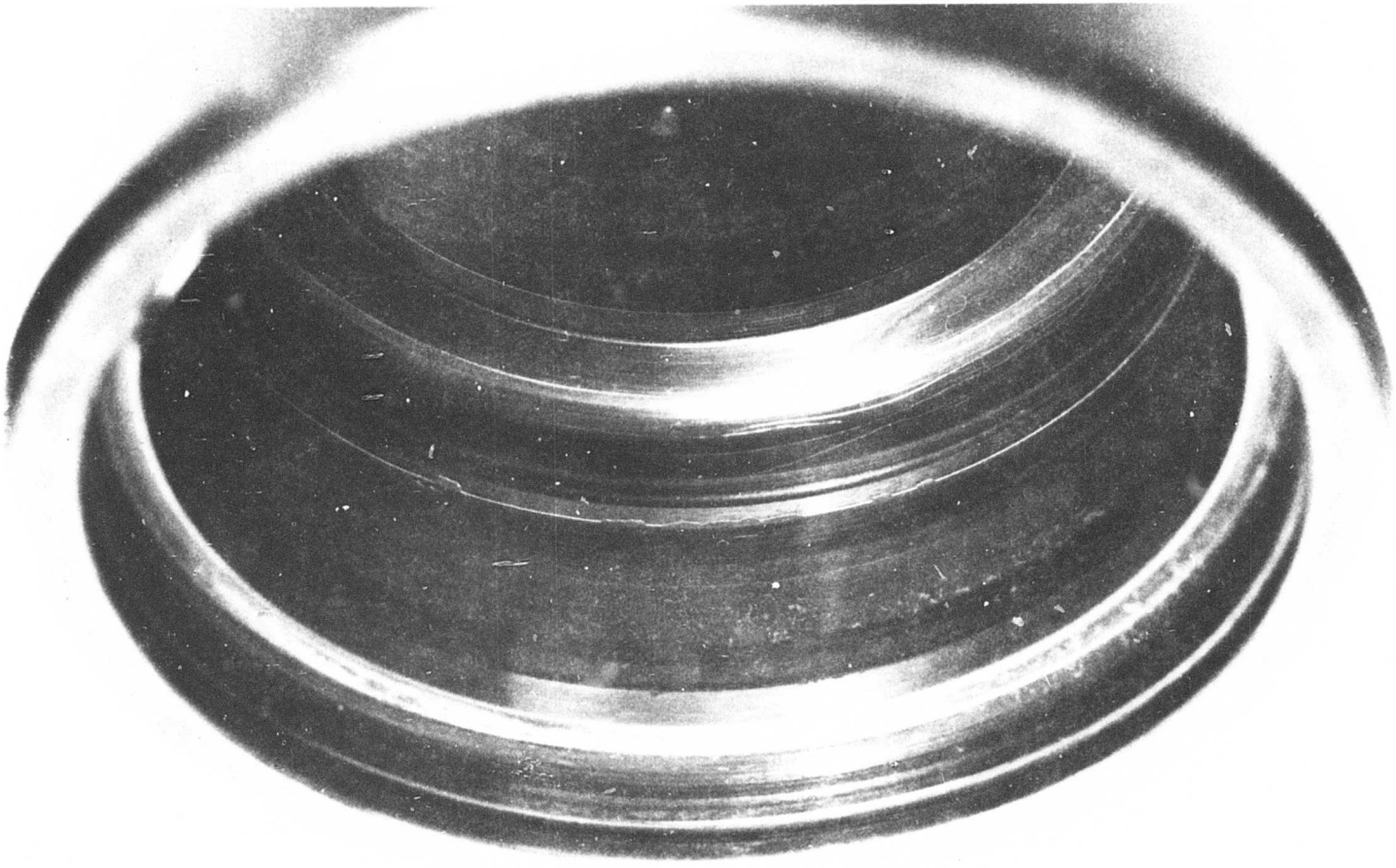

Figure 17. Wear of Tungsten-Carbide Flame Plating on Outer Housing After 50-Percent Differential-Speed Overrunning Test.

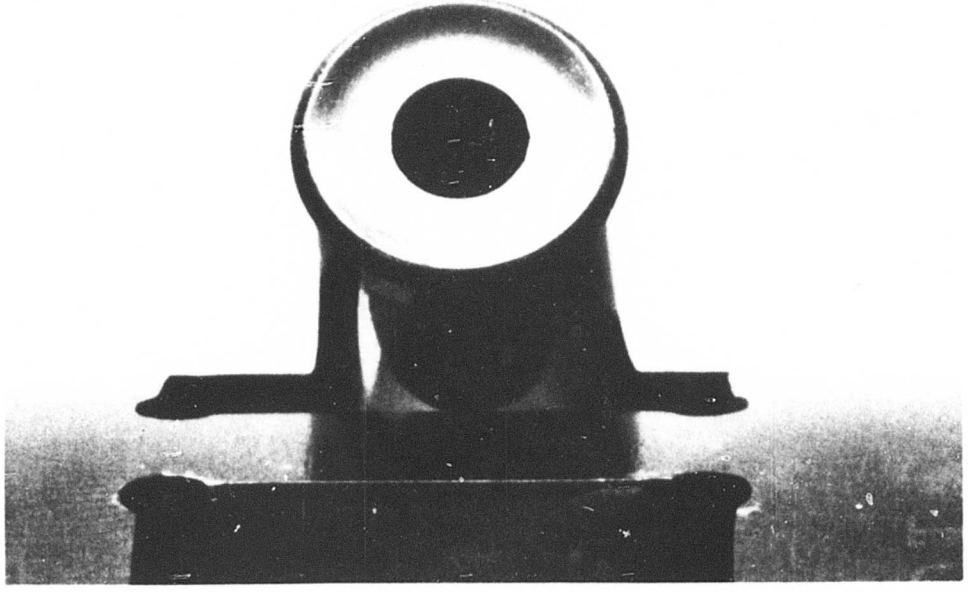

Figure 18. Roller End Wear, 50-Percent Differential-Speed Overrunning Test.

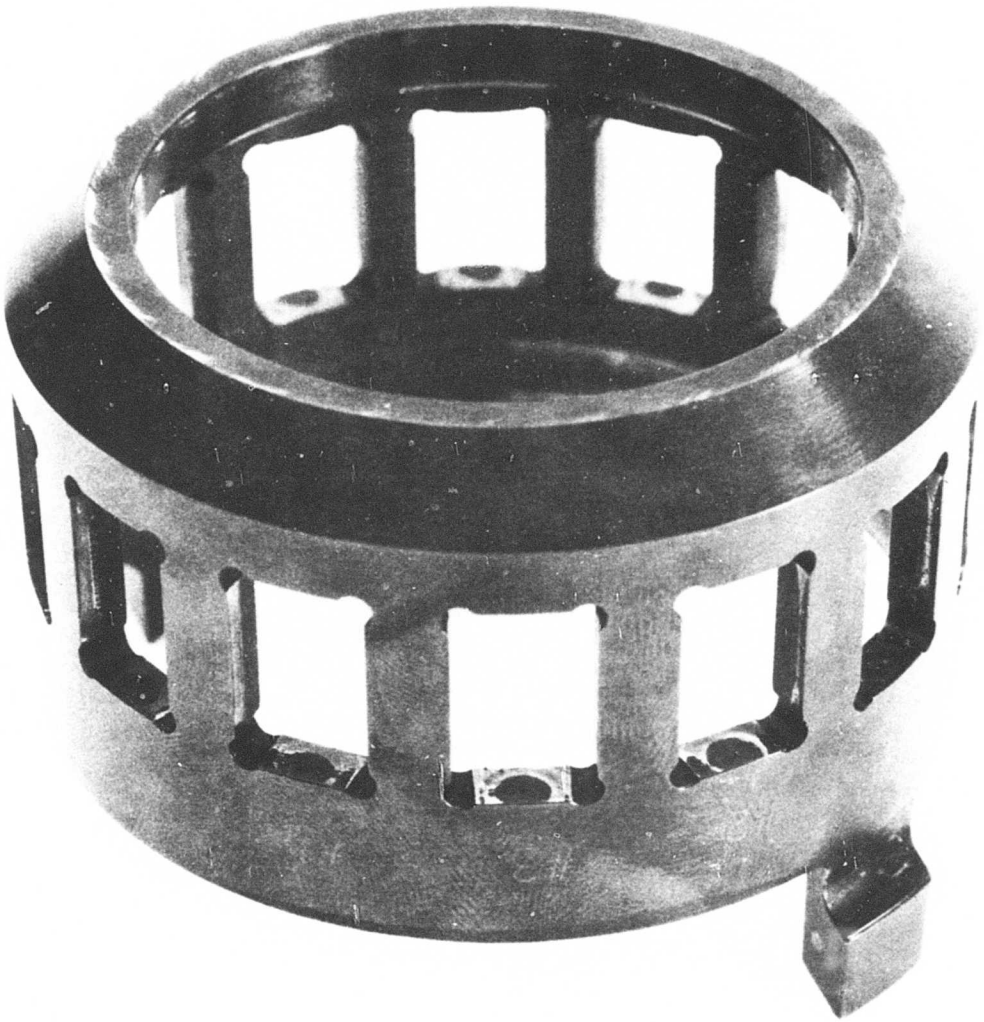

Figure 19. Roller Retention Cage Wear, 50-Percent Differential-Speed Overrunning Test.

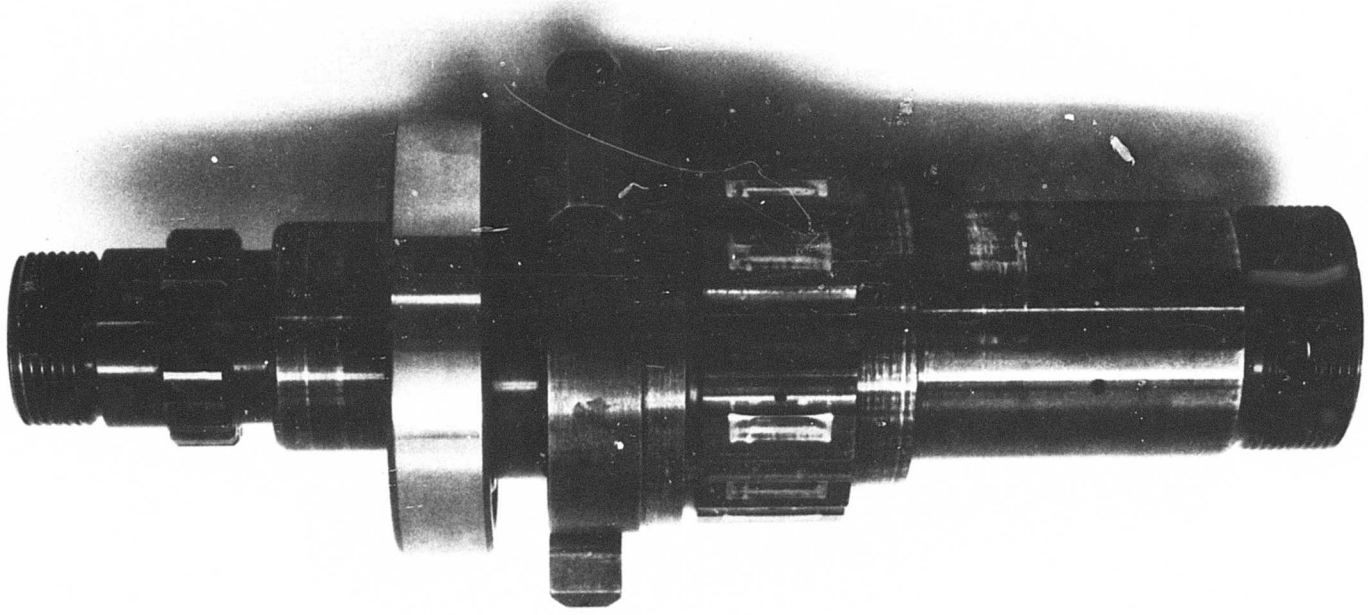

Figure 20. Cam at Completion of 50-Percent Differential-Speed Overrunning Test.

in the overrunning condition.

A new set of hollow rollers with reworked outer housing was installed, and the 67-percent differential-speed overrunning test was conducted with output housing rotation at 26,500 rpm and input cam rotating at 17,667 rpm. The flow condition of 1.1 gpm for the 50-percent differential-speed test was increased to 1.8 gpm for the 67-percent differential-speed test to increase roller lubrication.

Disassembly inspection after the 67-percent differential-speed overrunning test again revealed wear on rollers, cam, cage, and housing, but to a lesser extent than that found after the 50-percent test. Roller diametral wear, which ranged from 0.0051 to 0.0071 inch after the 50-percent differential-speed test, now ranged from 0.0013 to 0.0035 inch after the 67-percent differential-speed overrunning test.

The housing flame plating was worn through, with measurements of 3.0063 inches prior to test and 3.0134 inches diameter after test. As in the 50-percent differential-speed overrunning test, no wear was noted in the parent metal. The roller wear, which was lower in the 67-percent speed test than in the 50-percent speed test, may be attributed to the higher, 1.8-gpm, oil flow rate used, which probably flushed the flame plating abrasive compound away from the roller contact area.

Drag torque data for the 50-percent and 67-percent differential-speed overrunning tests is shown in Appendix III. Drag torque versus speed of input cam as a percentage of housing speed is shown in Figure 21. Temperature rise (ΔT) as a percent of housing speed is shown in Figure 22.

With the output housing rotating at 100 percent and with the input cam rotating at speeds greater than 67 percent, the drag torque decreases until the minimum value is reached when the freewheel unit is in the locked driving position. This low-drag condition at locked position is created by the absence of churning in the roller contact area. The zero point was obtained from the full-speed overrunning tests at the 1.8 gpm flow condition.

Note the small decrease in drag torque shown from 0 percent to 75 percent in Figure 21. As cam speed increases, churning losses are counterbalanced by higher centrifugal roller loads. At cam speeds greater than 75 percent, the churning losses become less important even though centrifugal load is increasing as the square of speed.

Based on the wear rates experienced during the 50-percent and 67-percent differential-speed overrunning tests, a third test scheduled to be conducted at 75-percent differential speed overrunning was cancelled since it was expected that the flame-plated outer housing would again experience high wear.

The wear improvement shown in the 67-percent test indicates that the flame-plated outer housings may create the wear problem. This conclusion is based on the fact that the wear advanced to the thickness of the plating and not into the parent metal. Also, the higher flow rate carried the abrasive wear particles away faster, indicating that the particles of flame plating may be

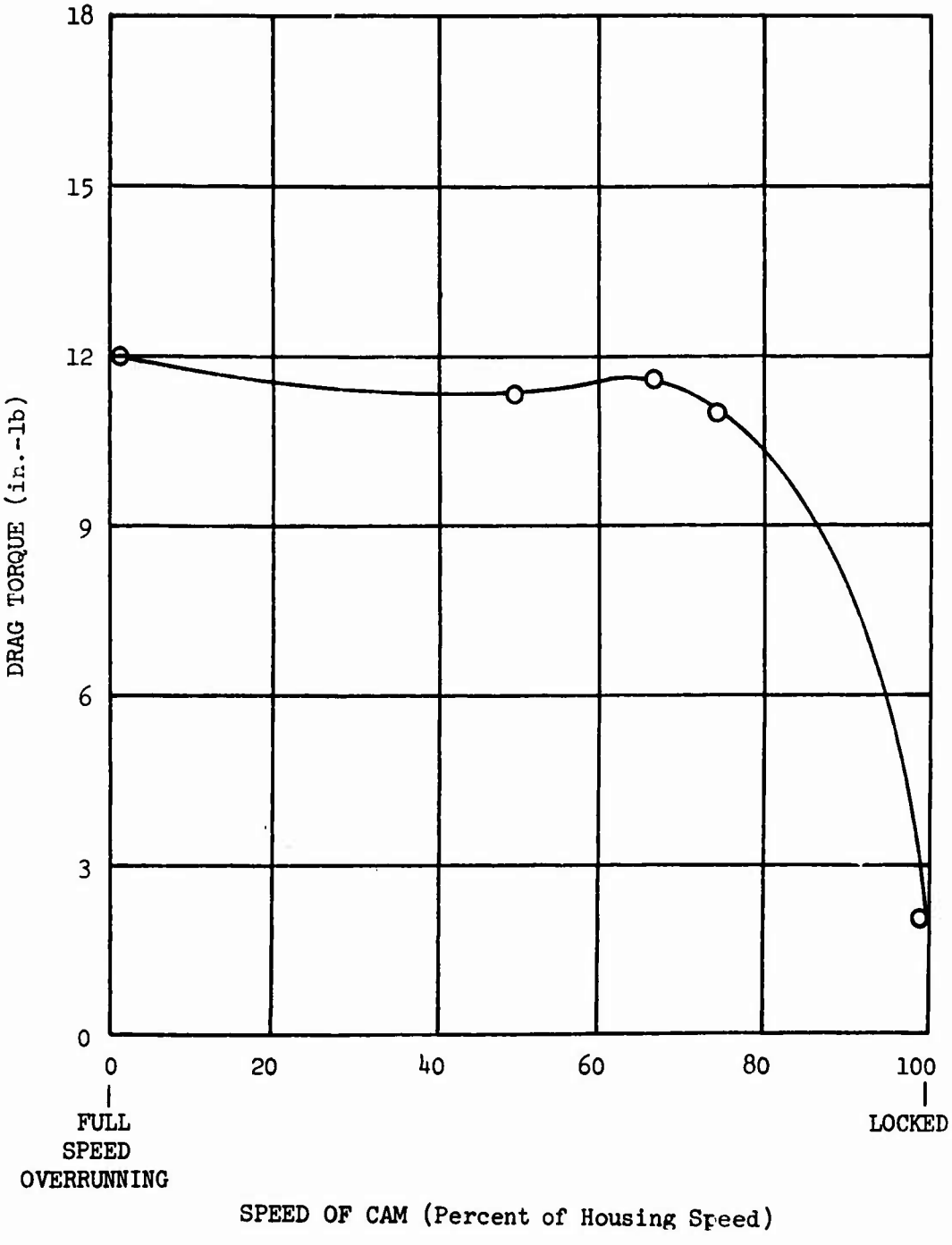

Figure 21. Drag Torque as a Function of Overrunning Speed at 1.8 gpm Flow.

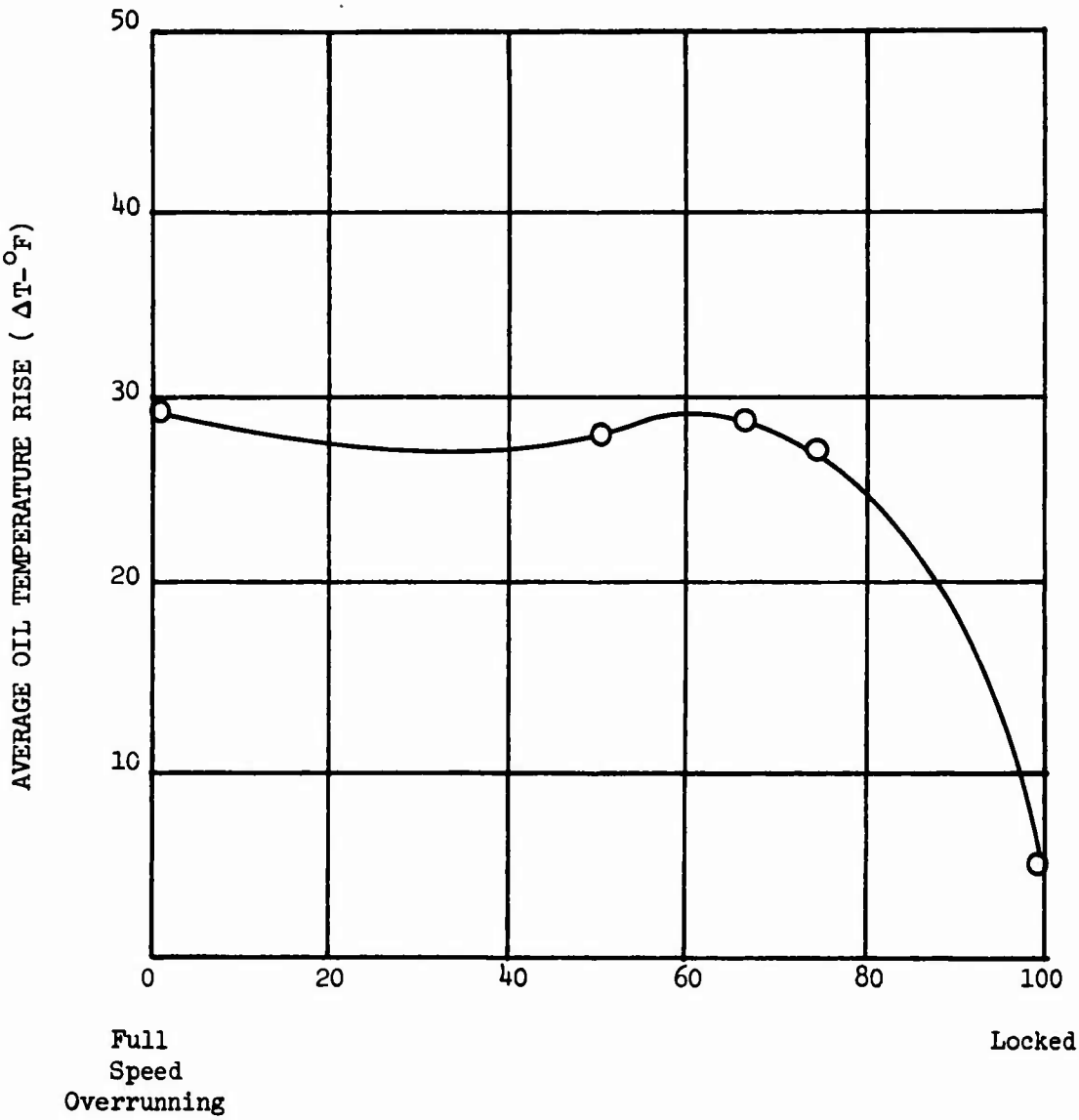

Figure 22. Variation of Oil Temperature Rise, ΔT, as a Function of Overrunning Speed at 1.8 gpm Flow.

the cause of high roller wear.

Dynamic Engagement

The hollow rollers were replaced with new rollers, and the ramp roller clutch was reassembled for dynamic engagement testing.

With the output housing rotating at 13,250 rpm, the input cam speed was brought up to 12,640 rpm. The output electric drive motor was then shut off, allowing the output housing to coast down to 12,640 rpm, at which time engagement occurred. The input cam then drove the entire assembly for a period of 5 minutes. The engagement was smooth with no unusual noise, vibration, temperature, or other adverse condition. The procedure was repeated for a total of two engagements at the 50-percent engagement speed condition. Disassembly and inspection revealed no measurable wear or other abnormalities.

The components were reassembled and installed in the test facility for the 100-percent engagement tests. The above procedure was repeated with the output housing rotating at 26,500 rpm and with the input cam rotating at 25,440 rpm. After engagement, the input cam was allowed to drive the entire test stand. As with the 50-percent engagement test, the engagement was smooth with no unusual noise, vibration, temperature, or other adverse condition.

Approximately one minute after the engagement with the input cam driving the entire test stand, an abnormal noise was heard and the stand was shut down. Disassembly revealed a broken adapter shaft which connects the ramp roller clutch assembly to the H-3 input gearbox assembly. This shaft is not a clutch test component but is used to couple the drive gearbox to the clutch housing. Figure 23 shows the failed adapter.

A new adapter shaft and nut were installed and the testing continued. A second successful and smooth engagement was made at 100 percent without abnormalities. On the attempt at the third engagement, the output housing did not engage at the speed of the input cam but was delayed substantially below the cam speed. This "delayed engagement" created an impact or shock load when the cam attempted to instantaneously accelerate the housing to 100-percent speed. The chip detector light was on after the delayed engagement.

The clutch was disassembled and inspected after the delayed engagement. The cam is shown in Figure 24. Indentations were found on all flats at approximately the center of the flat where the roller had jammed into the cam. These indentations measured 0.0018 inch maximum in depth. The rollers were brinnelled, with changes in original diameter ranging from 0.0013 to 0.0014 inch. The new adapter shaft failed in the same location as on the previous engagement tests. The cam, housing, rollers, and flange are shown in Figure 25.

Adapter flange fractures were caused by fatigue bending with multiple origins as discovered in post-test metallurgical evaluations. The adapter

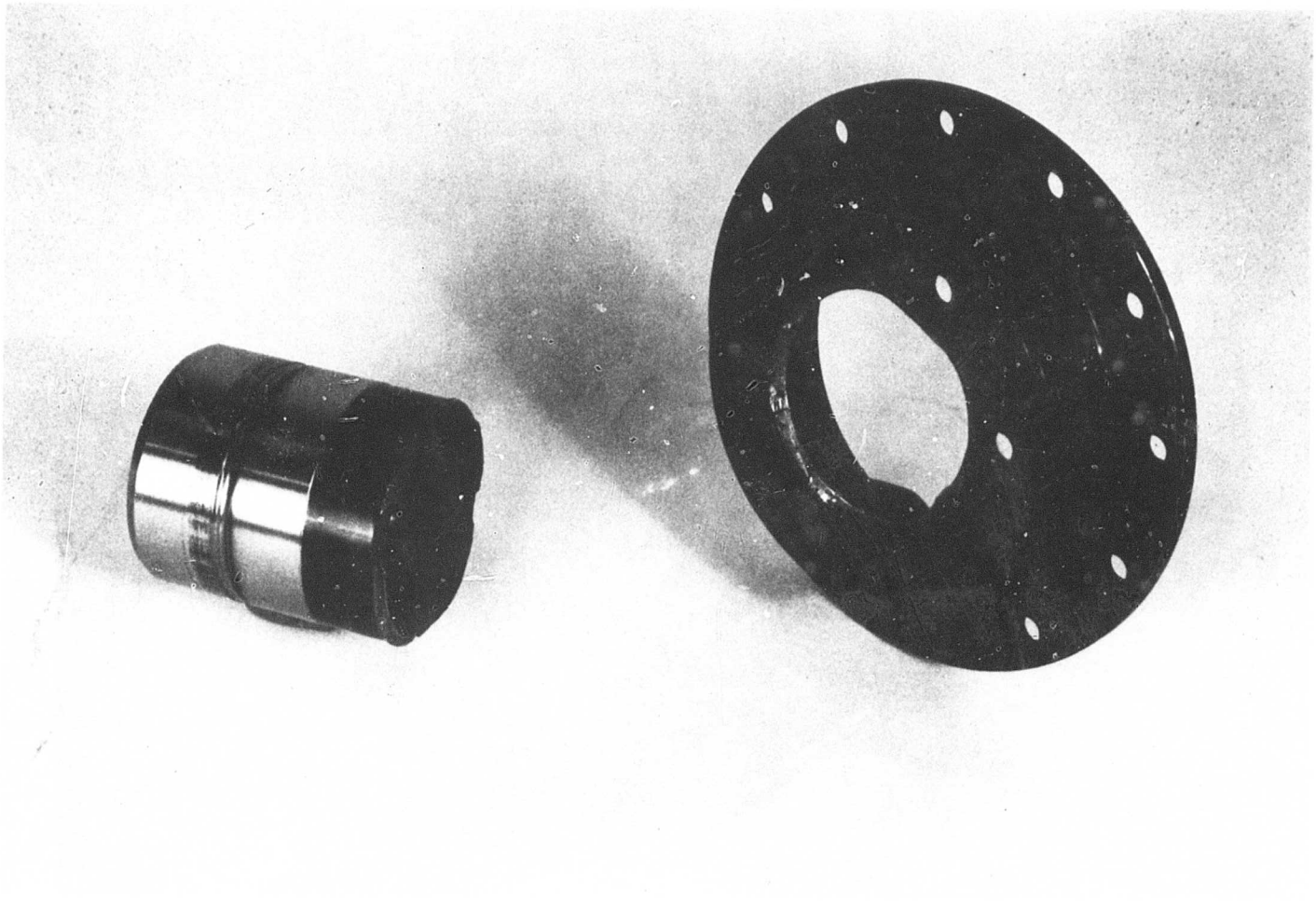

Figure 23. Adapter Flange Fracture, 100-Percent Speed Engagement Test.

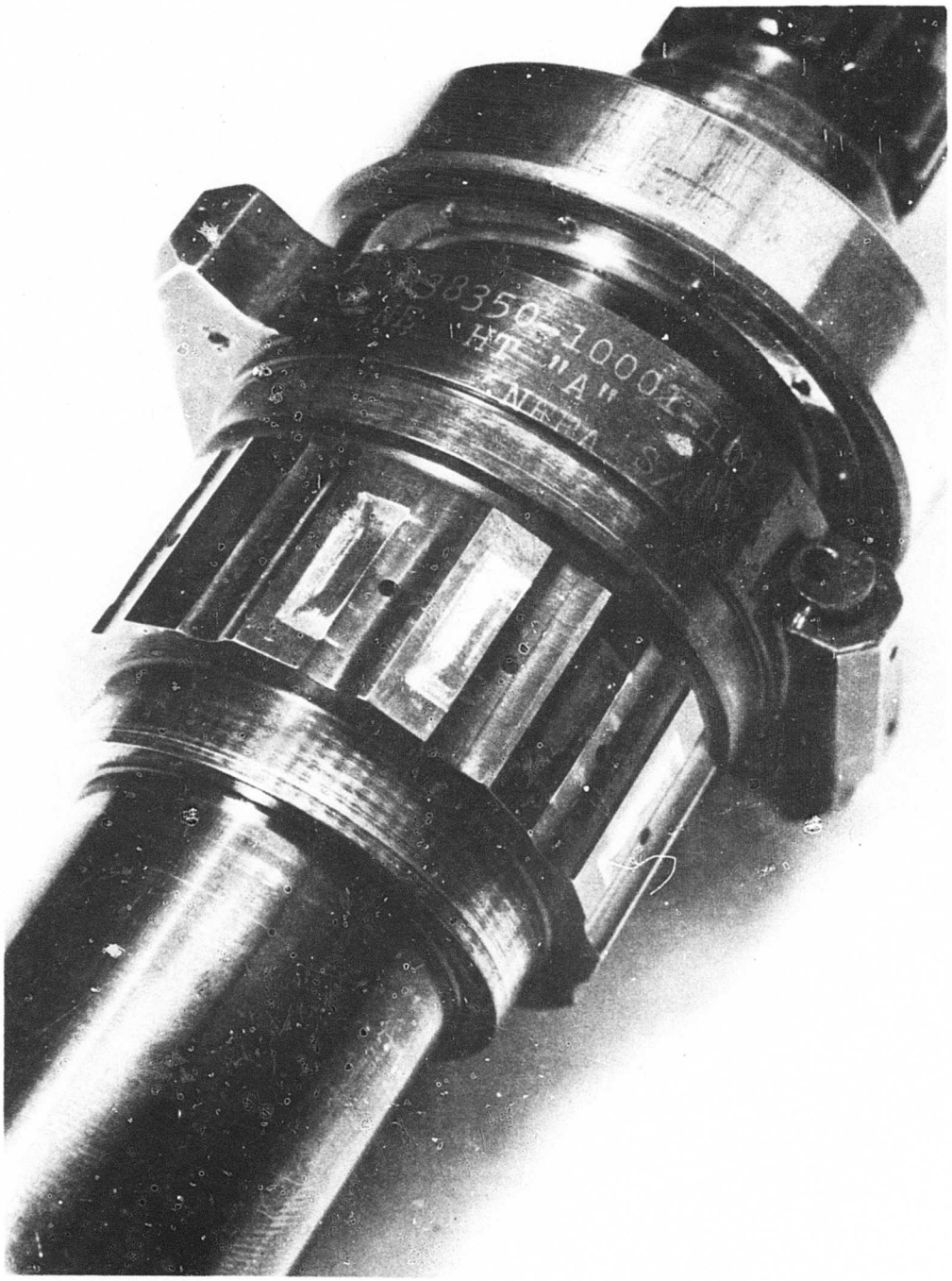

Figure 24. Cam Condition After Delayed Engagement.

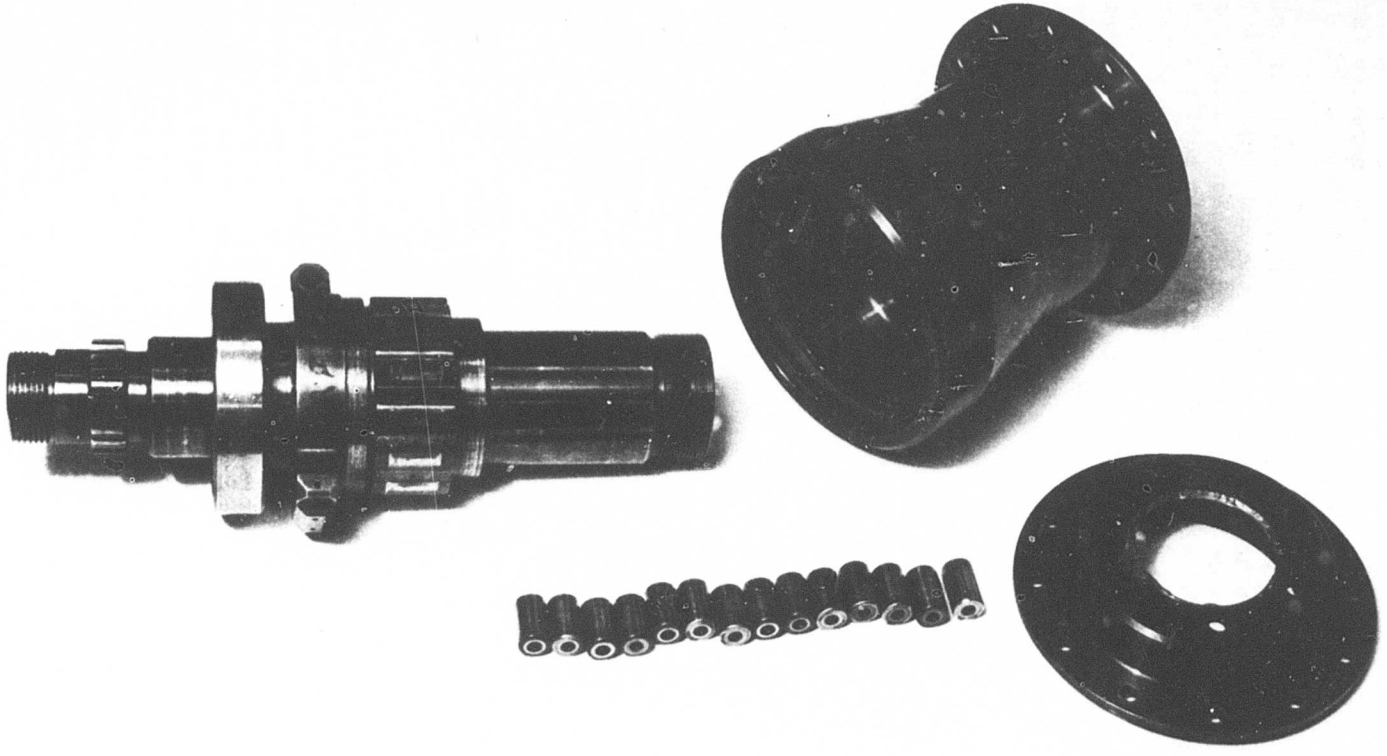

Figure 25. Clutch Components After Delayed Engagement.

flange failures were traced to a worn sleeve bearing in the H-3 gearbox facility. The sleeve bearing failure induced high bending stresses in the adapter shaft. The sleeve bearing is shown in Figure 26.

It was assumed that the delayed engagement was a direct result of rollers not riding in the proper engagement position on the cam ramps. This condition is attributed to the worn sleeve bearing and fractured adapter flange. With proper support from the sleeve bearing, the adapter shafts would probably not have failed and the delayed engagement would not have occurred.

The remaining engagement test scheduled to be conducted at 75-percent engagement speed was cancelled due to lack of adapter flanges.

STATIC TESTS

Cyclic Load

Static cyclic testing was conducted for 10 million cycles at a torque of 7140 ± 900 inch-pounds on the ramp roller clutch static test facility. An IVY-4 Universal Fatigue Test Machine was used to apply the torque through a 12-inch load arm as shown in the "TEST FACILITY" section of this report.

Clutch creep, defined as the angular displacement of the input cam shaft relative to output housing, is shown in Figure 27 as it progressed through the cyclic test. This creep is an indication of wear, yielding or fretting of cam, rollers, or housing. Angular displacement can not change with constant load unless the cam, rollers, or housing experience dimensional changes. Each reading of angular deflection was taken at the steady torque condition of 7140 inch-pounds. As shown by Figure 27, the maximum clutch creep was .30 degree and was essentially at a constant rate to 8 million cycles, where an increase in slope occurred.

Readings of housing radial displacement were taken throughout the test. As expected, the housing radial displacement did not change during the test from the initial setting of 0.0016 inch at 7140 inch-pounds torque.

Disassembly inspection of the cam after the 10 million cycle test revealed slight fretting of the cage oilite bushing on the bushing journal as shown in Figure 28. Three of fourteen cam flats had brinnell marks measuring 0.0004, 0.0003, and 0.0003 inch in depth. The housing, shown in Figure 29, experienced heavy chafing and wear of the contacting surface between rollers and housing. The tungsten-carbide flame coating was damaged to a depth of 0.005 inch, which was through the coating to the carburized surface beneath. The rollers had slight spalling on the side in contact with the cam and heavy spalling on the side in contact with the housing, although compressive stresses are lower on the housing side due to the housing radius of curvature (concave/convex contact on housing and flat/convex contact on cam). One roller of the fourteen was fractured as shown in Figure 30. The roller was fractured by fatigue stresses with origins on the outer surfaces. Therefore, it was assumed that stress concentrations introduced by breakdown of the tungsten-carbide coating on the contacting roller surfaces caused the roller failure. The maximum roller stress is at the inside on

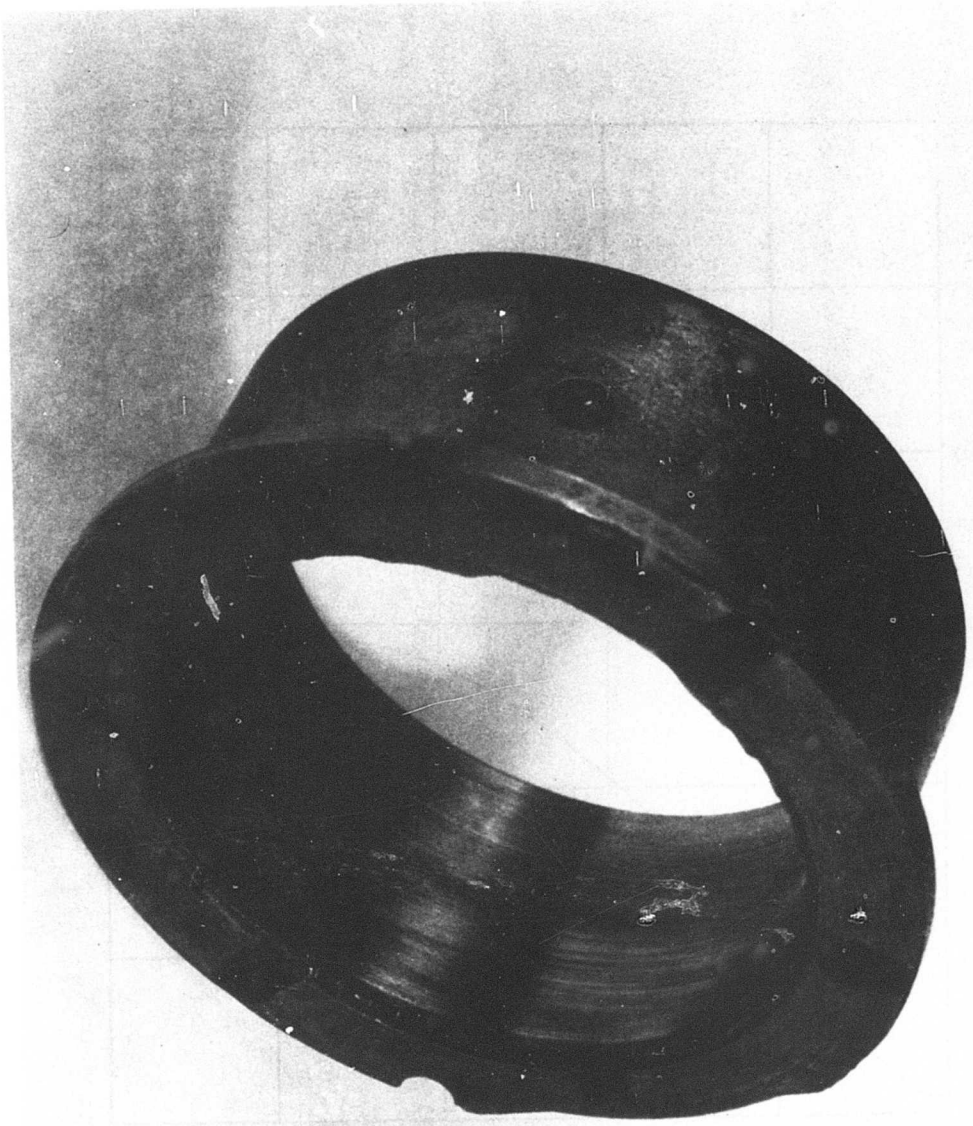

Figure 26. Sleeve Bearing at Completion of Dynamic Engagement Test.

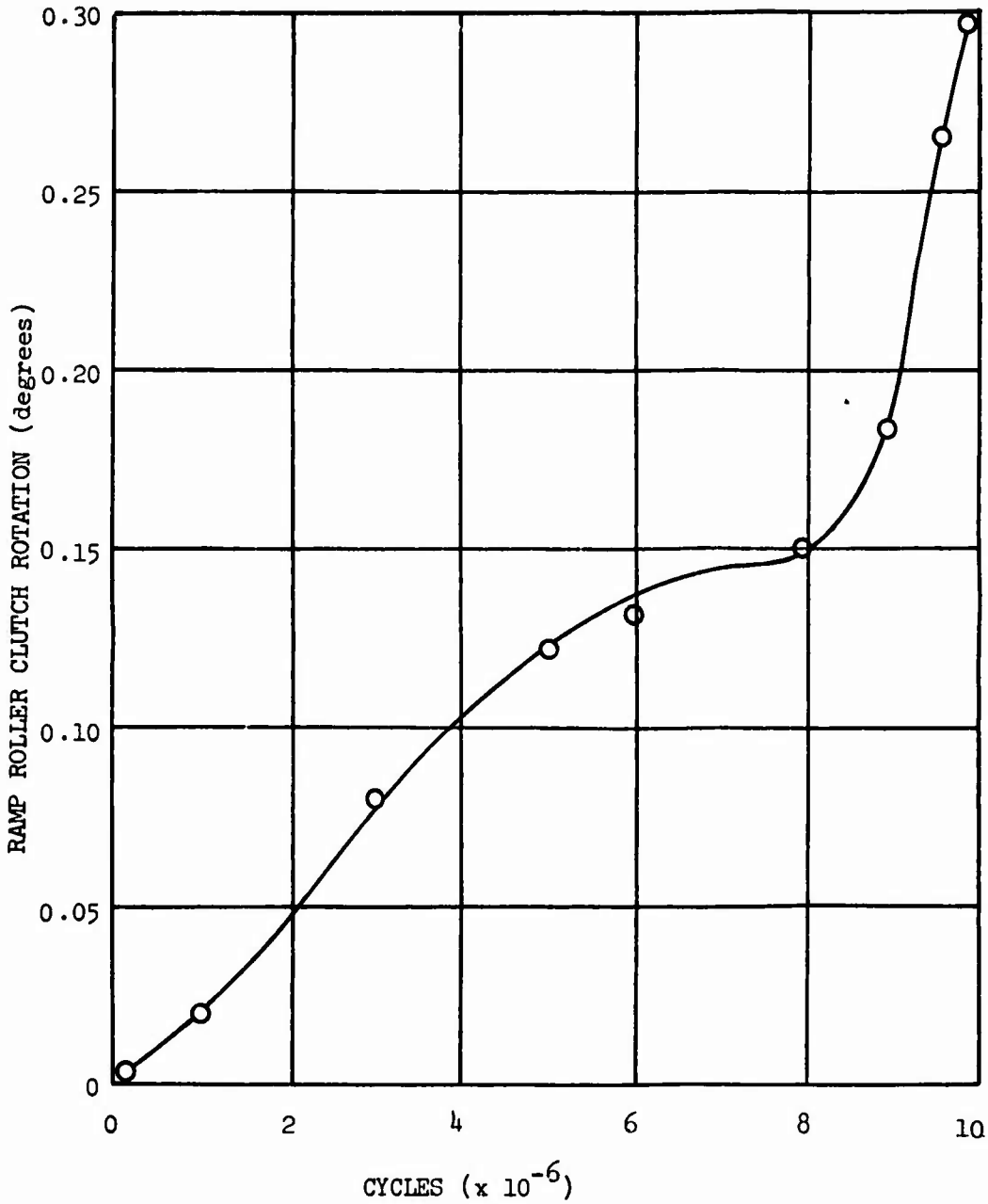

Figure 27. Clutch Creep Under the Influence of Cyclic Loading.

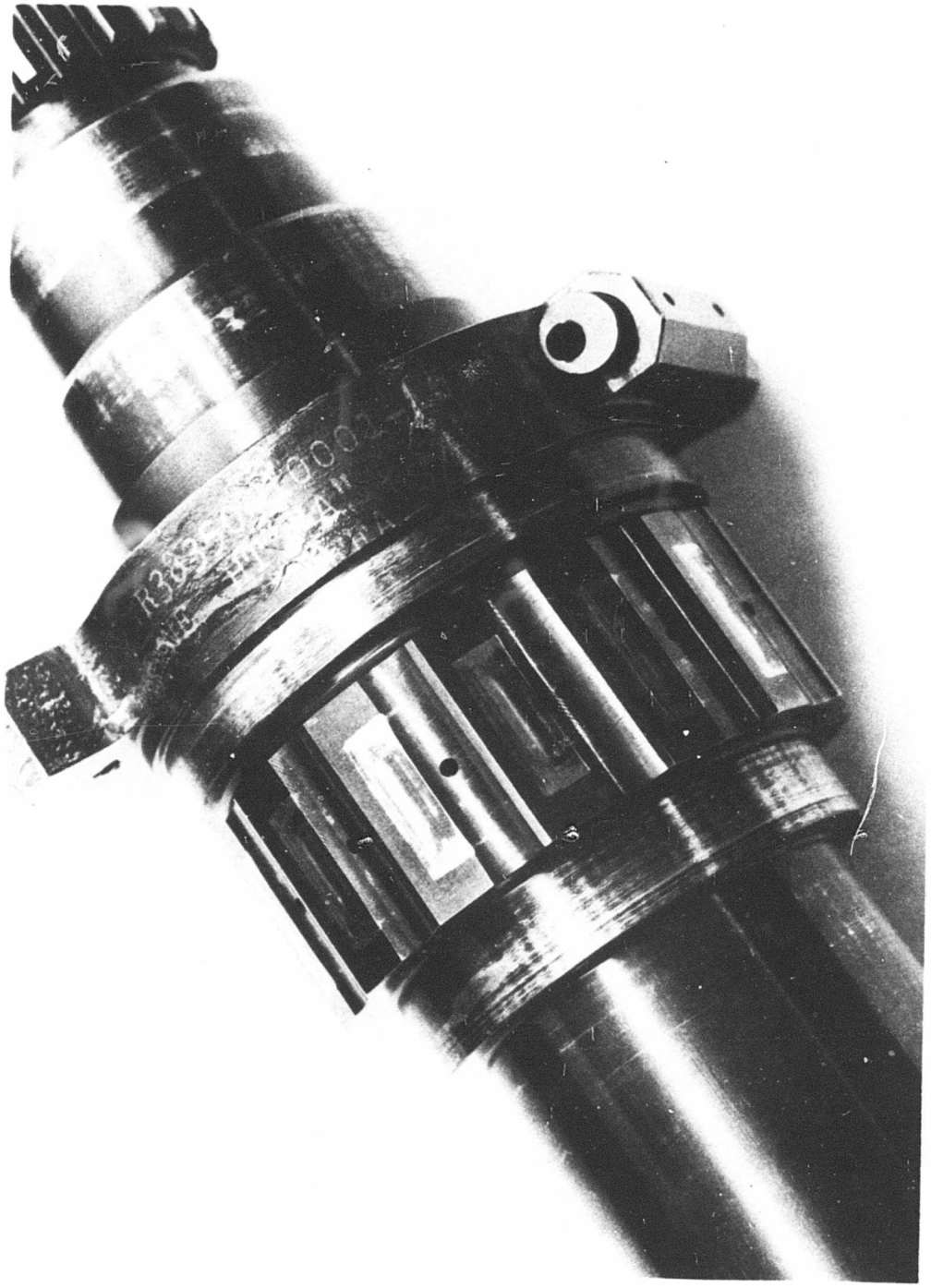

Figure 28. Clutch Cam After Static Cyclic Test.

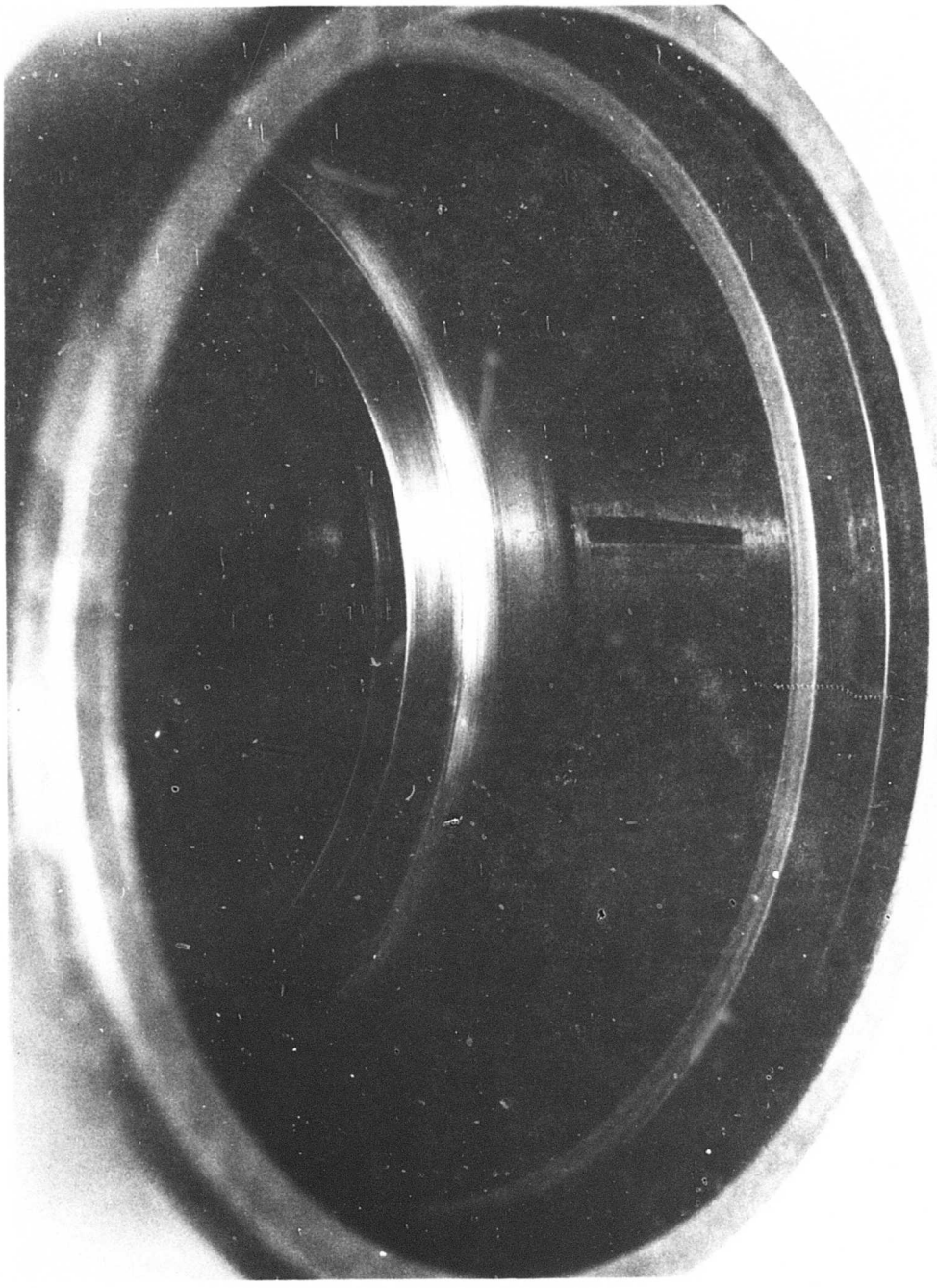

Figure 29. Outer Housing Wear Pattern in Tungsten-Carbide Flame Plating, Static Cyclic Test.

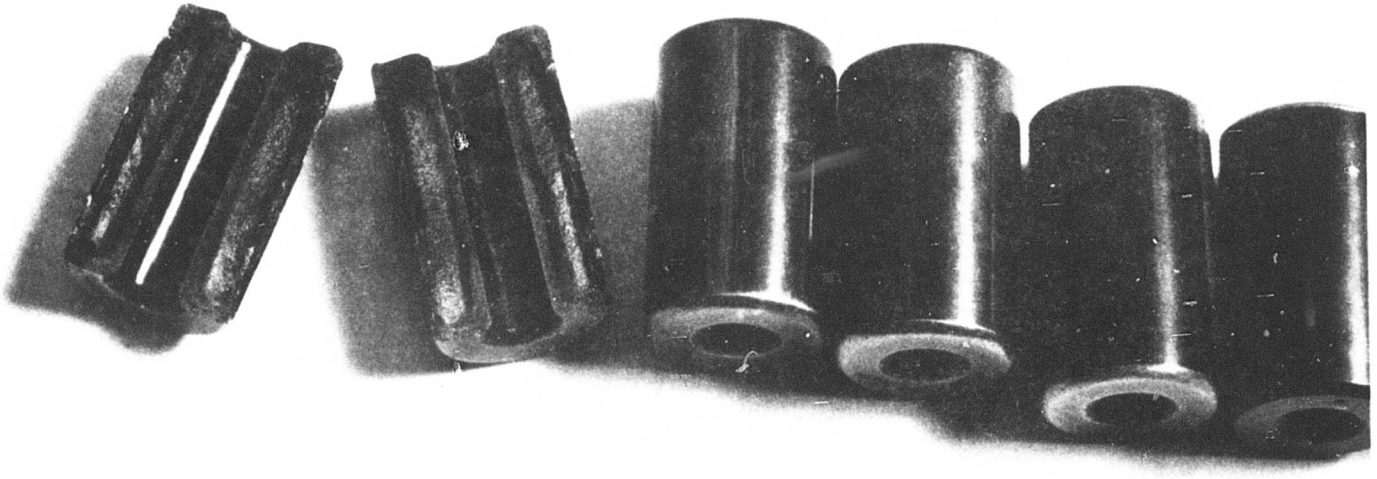

Figure 30. Roller Fatigue Fracture, Static Cyclic Test.

the surface of the hole under the load as shown in Appendix II. The calculated roller stresses at the test load were 250,000 ± 35,000 psi. These stresses are below the endurance limit for the roller material.

In aircraft use, the roller does not remain in the locked position for 10 million cycles. Surface breakdown will not occur in a concentrated contact zone since the rollers are "polished" during overrunning. It is concluded, therefore, that the roller fatigue fracture will not occur in aircraft application because:

1. Fatigue fracture originated on outside of roller due to tungsten-carbide plating breakdown which created stress concentrations. Outside of roller is not the maximum roller stress point.

2. Stress concentrations will not occur in rollers of aircraft ramp roller clutch since overrunning will "heal" any start of this condition.

3. Fatigue test at twice design load was at accelerated load conditions not likely to occur for 10 million cycles in ramp roller clutch life.

A composite of housing, cam, and rollers is shown in Figure 31. None of the roller clutch components other than the housing, cam, and rollers showed signs of wear, fretting, or yielding in any areas. The roller fracture may have occurred at approximately 8 million cycles, where the slope of clutch creep versus cycles increases as shown in Figure 27. Since no other rollers were cracked as determined by magnetic particle inspection, it can be assumed the failure was at the later stages of testing at high cycle count.

Overload

Two static overload tests were conducted on the ramp roller clutch static test installation. Load was applied through a hydraulic cylinder monitored by calibrated load cell. The initial test was conducted with a ramp roller clutch with case-carburized outer housing, and the second test was conducted with a ramp roller clutch with tungsten-carbide flame-plated outer housing. The tests were not carried to complete destruction but were stopped at 24,000 inch-pounds torque, which is greater than six times design load. In both tests the hollow rollers were the weak link, with all rollers experiencing diametral cracks across the contacting surfaces. Cracking sounds were detected in both tests between 17,000 and 18,000 inch-pounds. A yielding of 0.3 degree at 18,000 inch-pounds torque indicated that the rollers failed at this point.

Torsional spring rate, or clutch angular deflection versus torque, is shown in Figure 32 for the flame-plated housing. Identical results were obtained with the carburized housing.

Outer housing radial deflection was recorded for both tests as a function of clutch torque and is shown in Figure 33. Note the yielding at 18,000 inch-pounds torque, indicating roller cracking.

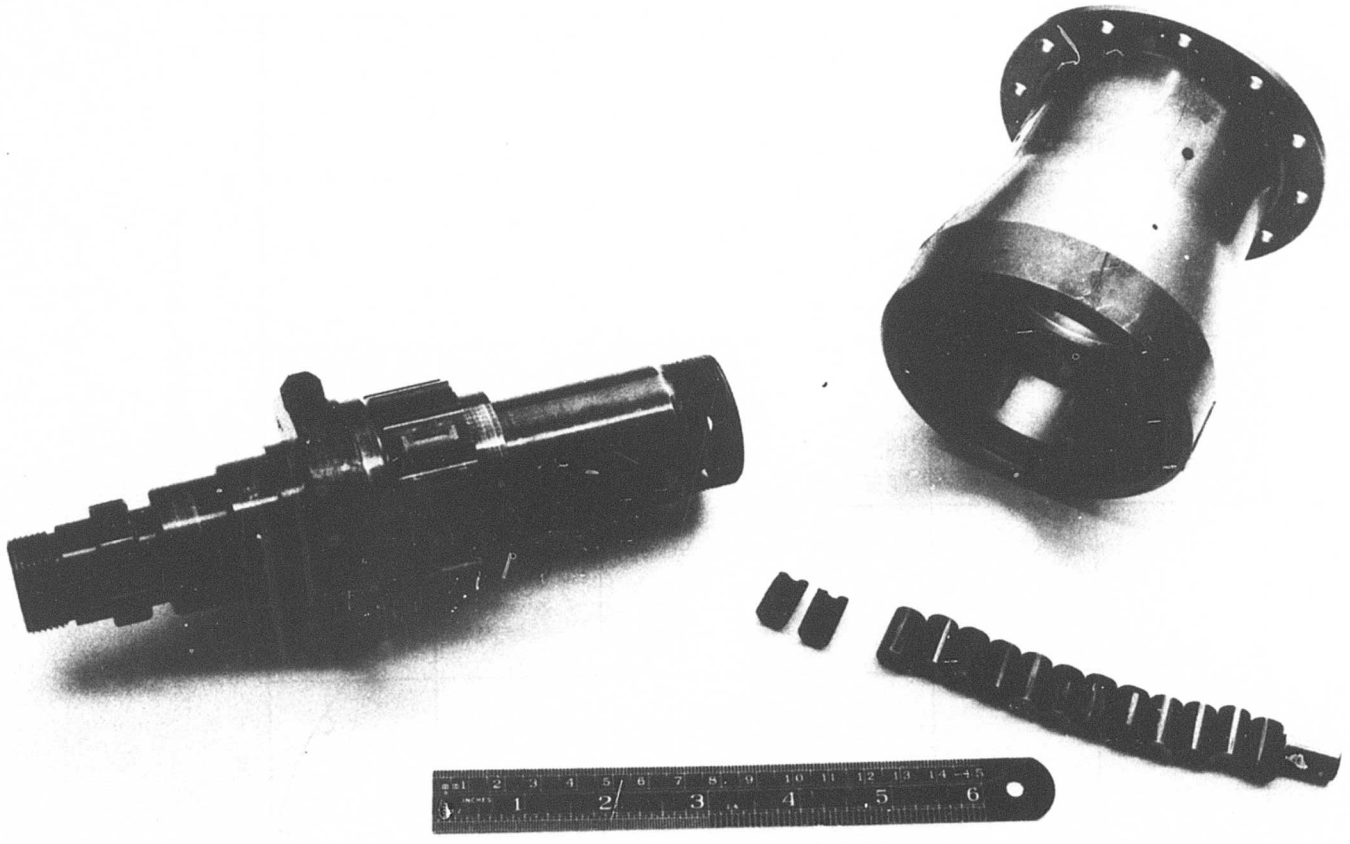

Figure 31. Clutch Components After Static Cyclic Test.

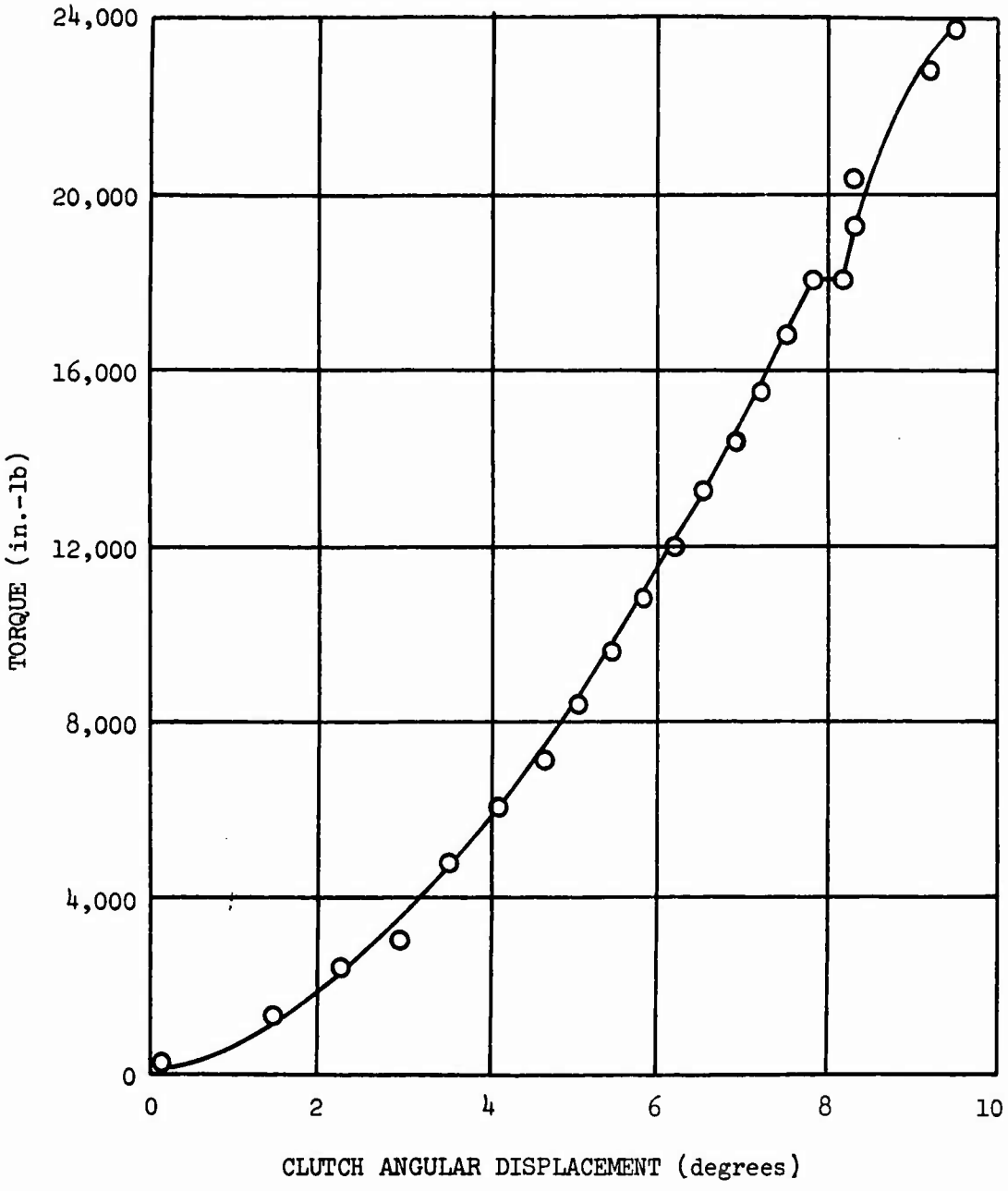

Figure 32. Ramp Roller Clutch Torsional Spring Rate.

The roller contact angle is calculated using the actual measured angular displacement. Knowing the true roller contact angle and torque, the actual roller load may be determined. At 18,000 inch-pounds torque, the roller load was found to be 11,000 pounds at a roller contact angle of 8 degrees 49 minutes. The calculated roller bending stress at this load is 360,000 psi. The hollow roller obviously yielded prior to reaching this stress, as the minimum tensile stress of the roller material is 300,000 psi. The 360,000-psi bending stress may be thought of as a modulus of rupture for the hollow roller. At 24,000 inch-pounds torque, the roller load was found to be 12,650 pounds. For a solid roller with a 12,650-pound load, the calculated Hertzian compressive surface stress is 897,000 psi between roller and housing. There is no known theoretical derivation of the contact stresses for hollow rollers. Since the flame-plated clutch housing did not fail and the allowable surface stress is in the order of 500,000 to 600,000 psi, the stresses were obviously lower in the hollow roller owing to its greater flexibility. This is a major advantage in using hollow rollers in a ramp roller clutch. It is conservatively estimated that surface contact stresses between roller and cam and between roller and outer housing are reduced by 50 percent due to greater flexibility of hollow rollers as compared to solid rollers.

With solid rollers, "spit out" usually occurs when the coefficient of friction on the rollers becomes less than the tangent of the roller contact angle. Previous experience has shown that roller spit-out generally occurs at approximately 8 degrees. With this test, rollers of the ramp roller clutch did not spit out with roller contact angles of 10 degrees 19 minutes. This capacity for spit-out is also attributed to greater area of contact from increased flexibility of hollow rollers. Thus, another important advantage of hollow rollers in the ramp roller clutch is the use of higher allowable roller contact angles. This leads to a reduction in roller load by the ratio of cotangent of one-half of the roller contact angle. For example, if an allowable roller contact angle of 8 degrees is used for hollow rollers versus 6 degrees for solid rollers, the roller load will be decreased by 25 percent.

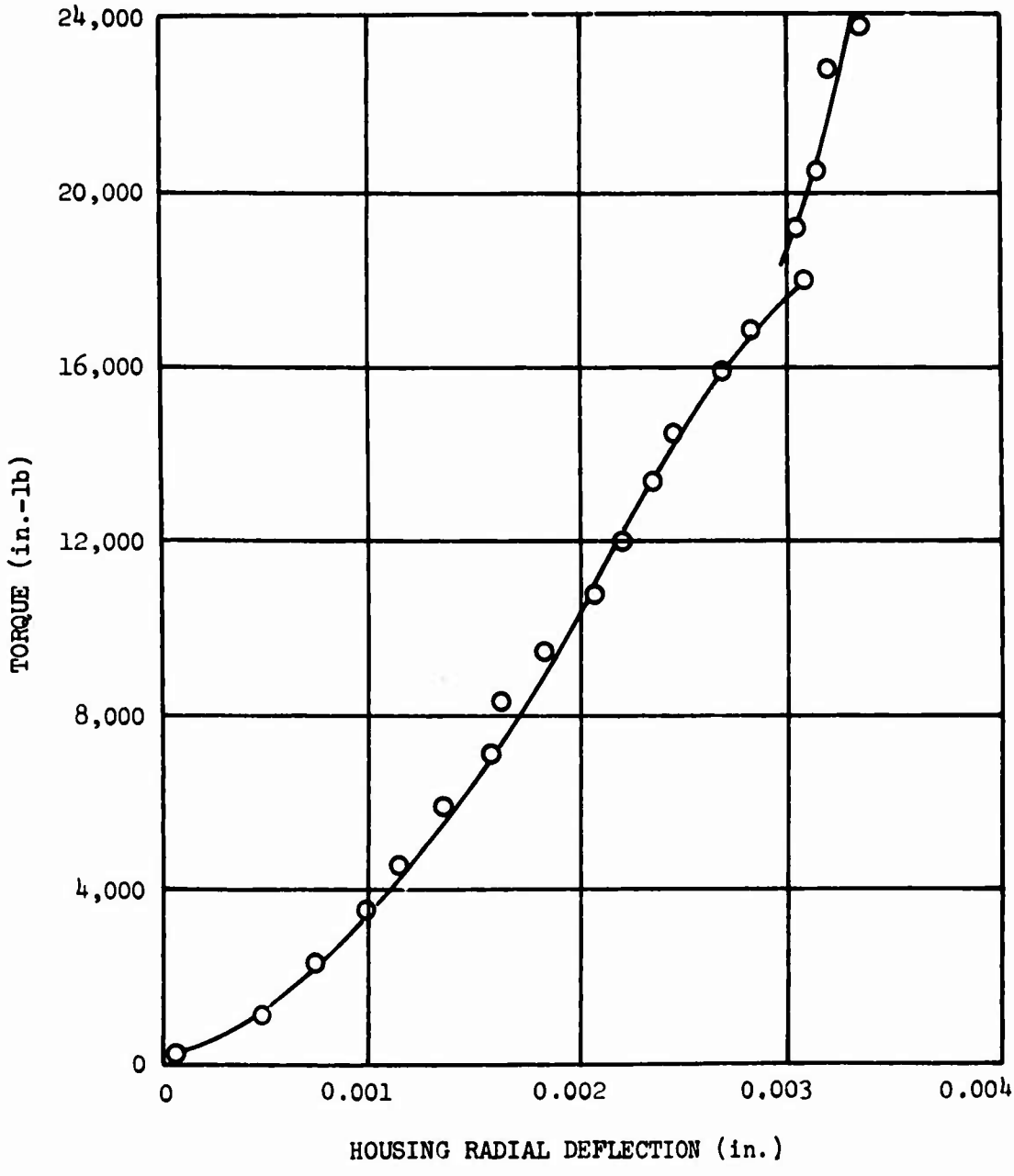

Figure 33. Ramp Roller Clutch Outer Housing Radial Spring Rate.

METALLURGICAL EVALUATION

PROCEDURE

The following procedures were used to determine the mode of failure, origin of failure, microstructure of case and core, chemical composition, case depth, and hardness of the case and core for one test sample of each major ramp-roller clutch component:

1. Fractures, wear patterns, spalling, and brinnelling were visually examined with a low-power stereo-microscope to determine the mode and origin of failure.

2. One each of cam shaft, outer housing, roller retainer, adapter shaft, and several hollow rollers were further examined as follows:

    a. The Rockwell hardness was determined for the case and core.

    b. A section from each component was mounted, etched with 2-percent nital solution, and examined on a metallograph to determine the microstructure of the case and core.

    c. Total case depth was determined by examination of the etched mounts under a Brinell microscope. The effective case depth was determined in terms of "Knoop" hardness on a Tukon microhardness tester. The case-core transition point was taken at KHN 542 (approximately equal to R_c 50). The results presented have been converted to R_c readings.

    d. Material chemical composition was analyzed on a spectrograph to determine conformity with the material specifications.

RESULTS

The hardness data for the major clutch components examined are listed in Table VII.

The cam shaft drawing specified an additional hardness requirement of R_c 60 to be maintained for a minimum depth of 0.030 inch. Microhardness readings taken at 0.030 inch indicated a hardness of R_c 60. Surface hardness was R_c 62.

A spectrographic analysis was conducted on all the major clutch components. This analysis indicated that the material of all components was 9300 series steel. Metallographic examination of the mounted sections of clutch components revealed typical martensitic structure with no evidence of excessive carbides or retained austenite.

TABLE VII. RAMP ROLLER CLUTCH COMPONENT HARDNESS DATA

Part Name	Case Hardness		Core Hardness		Effective Case	
	Actual (R_c)	Required (R_c)	Actual (R_c)	Required (R_c)	Actual (in.)	Required (in.)
Cam Shaft	62	60-64	39	30-45	.061	.060-.090
Outer Housing	55	52-58	35	30-40	.050	.050-.090
Roller Cage	60	58-64	39	30-45	.021	.010-.025
Roller	60	59-64	41	30-45	.038	.030-.060

Results of the stereo-microscope examination are discussed in the "TEST RESULTS" section of this report.

The results of tests and examinations indicated that all parts conformed to the drawing requirements.

CONCLUSIONS

1. The ramp-roller clutch, in its present configuration, operated at 26,500 rpm, but under its most critical operating condition (differential-speed overrunning) it experienced high roller and housing wear.

2. The pressurized lubrication system used to lubricate the rollers of the ramp-roller clutch allowed designing of the cam as the input or driving member by assuring lubrication without centrifugal force assist. Centrifugal effects on the rollers during full-speed overrunning were eliminated, resulting in a highly successful full-speed overrunning operation.

3. The straddle-mounted roller retainer that was used trapped oil around the rollers and the cam, which reduced cam wear resulting from roller sliding.

4. The use of hollow rollers in place of solid rollers in the ramp-roller clutch gave the following advantages:

   a. The surface contract stresses between rollers, cam, and outer housing were reduced because roller flexibility created a larger contact area.

   b. The allowable maximum roller contact angle was increased to 8 degrees, thus reducing roller loads and resulting stresses because the hollow rollers had higher resistance to "spit-out". The flattened contact area of hollow rollers had a greater resistance to skidding than solid rollers.

   c. Increased roller flexibility resulted in improved load sharing.

   d. The lower mass of the hollow rollers reduced the centrifugal load of the rollers on the outer housing during differential speed overrunning. This lower centrifugal load reduced wear of rollers and housing.

5. The tungsten-carbide flame-plating process used on the ramp-roller clutch outer housing broke down in all tests, due to its susceptibility to shock or impact loads. These loads were assumed to have been created by vibrations of the rollers at high pitch-line velocities. It was also assumed that particles from the tungsten-carbide coating acted as an abrasive compound on the rollers, thus accelerating wear.

6. The design load of the roller retainer return-spring-pin assembly was insufficient when the centrifugal effects became more pronounced. Also, the lack of the return-spring-pin assembly load did not allow the rollers to overrun in the proper position, in contact with the cam and housing at all times.

7. Additional exploratory development effort is required to minimize or eliminate the excessive wear experienced at the differential overrunning speed condition. Specific areas requiring additional development effort are

surface treatment of outer housing and roller retainer return-pin-spring assembly.

LITERATURE CITED

1. Roark, Raymond J., FORMULAS FOR STRESS AND STRAIN, Third Edition, New York, N.Y., McGraw Hill Book Company, 1954.

2. Sikorsky Aircraft, SIKORSKY AIRCRAFT STRUCTURES MANUAL, Stratford, Connecticut, United Aircraft Corporation, January 1968.

3. Sauzedde, R.E., ROLLER CLUTCH DESIGN, SAE Publication 208B, September, 1960.

4. Horger, O.J., FATIGUE TESTS OF SOME MANUFACTURED PARTS, Proceedings of the Society for Experimental Stress Analysis, Vol. III, No. II, 1946.

5. Seeley, Fred B., and Smith, James O., ADVANCED MECHANICS OF MATERIALS, Second Edition, New York, John Wiley and Sons, Inc., 1966, pp. 177-182.

6. SKF Computer Program AE66Y004, ANALYSIS OF DYNAMIC PERFORMANCE CHARACTERISTICS OF CYLINDRICAL ROLLER BEARINGS UNDER RADIAL LOAD, King of Prussia, Pennsylvania, SKF Industries, Inc.

7. Harris, T.A., and Aaronson, S.F., AN ANALYTICAL INVESTIGATION OF CYLINDRICAL ROLLER BEARINGS HAVING ANNULAR ROLLERS, ASLE Transactions 10, 1967.

8. Battelle Memorial Institute, ANALYSIS OF A ROLLER BEARING ASSEMBLY WITH HOLLOW ROLLERS, Columbus, Ohio, Battelle Memorial Institute.

APPENDIX I

STRUCTURAL ANALYSIS, RAMP ROLLER CLUTCH

FULL-LOAD ROLLER CONTACT ANGLE

This analysis determines the roller contact angle, commonly called the nip angle, for the fully loaded ramp roller clutch. The analysis includes the expansion of the housing and the contraction of the cam. The following nomenclature is used for the ramp roller clutch analysis:

b	= 1.875 in.	=	housing outside radius
R	= 1.503 in.	=	housing bore radius
K	= 1.125 in.	=	cam flat to cam center line
d	= .800 in.	=	cam inside radius
ρ	= .1875 in.	=	roller radius
l	= .560 in.	=	roller effective length
N	= 14	=	number of rollers
ν	= .32	=	Poisson's ratio

Figure 34 shows the loads imposed on the roller.

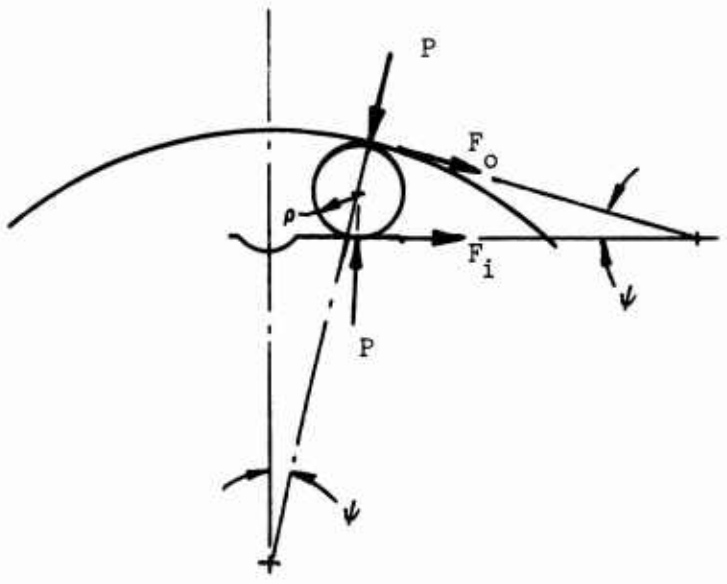

Figure 34. Loads Imposed on Roller.

$$T = \frac{63025\ hp}{rpm} \quad (1)$$

$$T = \frac{63025\ (1500)}{26500}$$

$$T = 3570\ \text{in.-lb}$$

For equilibrium of the roller,

$$F_o\ \rho = F_i\ \rho \quad (2)$$

$$F_o = F_i$$

Also from Figure 35,

$$F_i + F_o \cos \psi - \rho \sin \psi = 0 \quad (3)$$

which reduces to

$$P = F_o \cot \left(\frac{\psi}{2}\right) \quad (4)$$

To determine the cam and roller contact angle,

$$l_h = 1 + b - R \quad (5)$$

$$l_h = .560 + 1.875 + 1.503$$

$$l_h = .932$$

$$A_h = 2 \pi R\ l_h \quad (6)$$

$$A_h = 2 \pi\ (1.503)(.932)$$

$$A_h = 8.801 = \text{effective expansion area of housing}$$

$$l_c = 1 + K - d \quad (7)$$

$$l_c = .560 + 1.125 - .800$$

$$l_c = .855$$

$$A_c = 2 \pi K\ l_c \quad (8)$$

$$A_c = 2 \pi\ (1.125)(.885)$$

$A_c = 6.256$ = effective contraction area of cam

The radial contraction of the cam as given by Reference 1:

$$\mu_c = \frac{-K P_c}{E} \left[\frac{K^2 + d^2}{K^2 - d^2} - \nu \right] \tag{9}$$

$$P_c = \frac{P N}{A_c} \tag{10}$$

$$= \frac{F_o N}{A_c} \left(\cot \frac{\psi}{2} \right)$$

$$= \frac{T}{R A_c} \left(\cot \frac{\psi}{2} \right)$$

$$\mu_c = \frac{-T}{E A_c} \left(\frac{K}{R} \right) \left[\frac{K^2 + d^2}{K^2 - d^2} - \nu \right] \cot \frac{\psi}{2} \tag{11}$$

$$= W \cot \frac{\psi}{2} \tag{12}$$

where $$W = \frac{-T}{E A_c} \left(\frac{K}{R} \right) \left[\frac{K^2 + d^2}{K^2 - d^2} - \nu \right]$$

The radial expansion of the housing as given by Reference 1:

$$\mu_h = \frac{R P_h}{E} \left[\frac{b^2 + R^2}{b^2 - R^2} + \nu \right] \tag{13}$$

$$P_h = \frac{T}{R A_h} \left(\cot \frac{\psi}{2} \right) \tag{14}$$

$$\mu_h = \frac{T}{E A_h} \left[\frac{b^2 + R^2}{b^2 - R^2} + \nu \right] \cot \frac{\psi}{2} \tag{15}$$

$$= X \cot \frac{\psi}{2} \tag{16}$$

where $$X = \frac{T}{E A_h} \left[\frac{b^2 + R^2}{b^2 - R^2} + \nu \right]$$

Substituting for W and X gives the following:

$$W = \frac{-3570}{29 \times 10^6 (6.256)} \left(\frac{1.125}{1.503}\right) \left[\frac{1.125^2 + .800^2}{1.125^2 - .800^2} - .32\right]$$

$$W = -40.2 \times 10^{-6}$$

$$X = \frac{3570}{29 \times 10^6 (8.801)} \left[\frac{1.875^2 + 1.503^2}{1.875^2 - 1.503^2} + .32\right]$$

$$X = 68.7 \times 10^{-6}$$

Now

$$\cos \frac{\psi}{2} = \frac{K + \mu_c + \rho}{R + \mu_h - \rho} \qquad (17)$$

Substituting for μ_c and μ_h gives the following:

$$\left[\frac{R - \rho}{2}\right] \sin 2\psi + \left[X \cos\psi + W\right]\left[1 + \cos\psi\right] = \sin\psi\left[K + \rho\right] \qquad (18)$$

$$\left[\frac{1.503 - .1875}{2}\right] \sin 2\psi + 10^{-6}\left[68.7 \cos\psi - 40.2\right]\left[1 + \cos\psi\right] = \sin\psi\left[1.125 + .1875\right]$$

By an iterative solution procedure, ψ in Equation (18) is solved for the full-load contact angle, giving

$$\psi = 5 \text{ deg } 11 \text{ min}$$

A full-load roller contact angle of less than 8 degrees at the maximum design horsepower has been shown by experience to be sufficient to retain the rollers in position and prevent roller spit-out. A full-load angle greater than 2 degrees has been shown by experience to be sufficient to prevent self locking. Hence, the ramp roller clutch assembly meets the design requirements for roller contact angle.

By the same method, the roller contact angle for twice the above design torque is found to be 6 degrees 3 minutes.

RAMP ROLLER CLUTCH HOUSING

The ramp roller clutch housing is subjected to bending and tensile stresses induced by roller loads. The housing is analyzed as a ring subjected to 14 equally spaced loads reacted at the output flange as a uniform shear flow. A typical load point is shown in Figure 35.

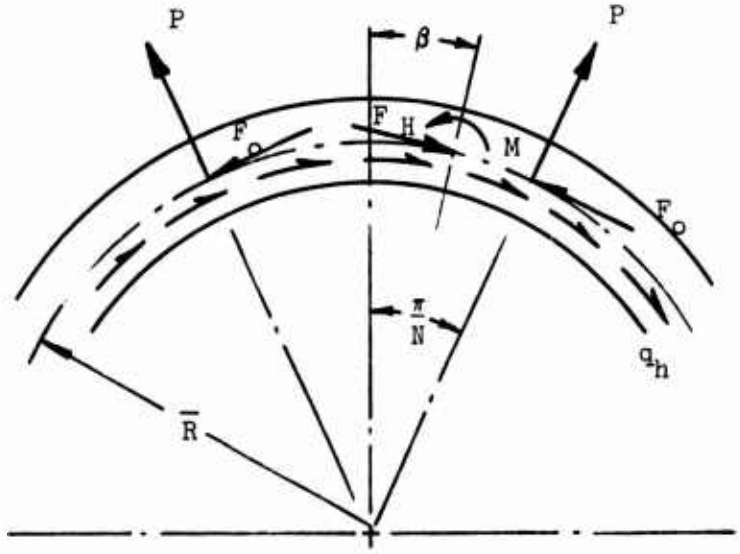

Figure 35. Roller Contact Loads on Outer Housing.

The roller loads are found from

$$F_o = \frac{T}{R\,N} \qquad (19)$$

$$F_o = \frac{3570}{1.503\ (14)}$$

$$F_o = 170 \text{ lb}$$

$$P = F_o \cot \frac{\psi}{2} \qquad (20)$$

$$P = 170 \cot \frac{5 \text{ deg } 11 \text{ min}}{2}$$

$$P = 170\ (22.1)$$

$$P = 3760 \text{ lb}$$

$$q_h = \frac{T}{2\pi R_r^2} \tag{21}$$

where q_h = shear flow, lb/in.

q_h = radius to intersection of output flange and housing, lb

$$q_h = \frac{3570}{2\pi\ 1.584^2}$$

$$q_h = 227 \text{ lb/in.}$$

The critical sections through the housing are at the roller contact points ($\theta = \beta = \pi/N$)

$$\theta = \frac{\pi}{N} = \frac{\pi}{14} = .2244 \text{ rad} = 12 \text{ deg } 51 \text{ min} = \beta$$

The maximum bending moment at these points as given by Reference 2:

$$M_{max} = \frac{P\,\bar{R}}{2}\left(\frac{1}{\theta} - \frac{\cos\beta}{\sin\theta}\right) + \frac{F_o\,\bar{R}\sin\beta}{2\sin\theta} - q_H \cdot R_r^2\,\beta \tag{22}$$

where $\bar{R}$ = radius to centroid of effective housing area, in.

$$M_{max} = \frac{3760(1.702)}{2}\left(\frac{14}{\pi} - \frac{\cos .2244}{\sin .2244}\right) + \frac{170(1.702)}{2}$$

$$-277(1.584)^2\,(.2244)$$

$$M_{max} = 249 \text{ in.-lb}$$

The internal tensile load as given in Reference 2:

$$F_H = \frac{P\cos\beta}{2\sin\theta} - \frac{F_o\sin\beta}{2\sin\theta} \tag{23}$$

$$= \frac{3760}{2}\left(\frac{\cos\ (.2244)}{\sin\ (.2244)}\right) - \frac{170}{2}$$

$$= 8160 \text{ lb}$$

The maximum bending stress occurs at the outside of the housing and is given by

$$f_b = \frac{M_{max}\ Y_o}{I_H} \qquad (24)$$

where I_H = moment of inertia of effective housing area about centroid, $in.^4$

Y_o = radial distance from centroid of housing area to outside fiber, in.

$$f_b = \frac{249\ (.173)}{.00531}$$

$$f_b = 8110 \text{ psi}$$

The axial stress is given by

$$f_a = \frac{F_H}{A_H} \qquad (25)$$

where A_H = housing cross-sectional area, $in.^2$

$$f_a = \frac{8160}{.563}$$

$$f_a = 14{,}500 \text{ psi}$$

The material of the ramp roller clutch housing is AMS 6260 heat-treated, Rc 30-45, which has the following material properties:

$$F_{tu} = 136{,}000$$

$$F_{ty} = 115{,}000$$

$$F_{bu} = 180{,}000$$

The margin of safety is given by

$$M.S._{ult} = \frac{1}{1.5\left[\frac{f_a}{F_{tu}} + \frac{f_b}{F_{bu}}\right]} - 1 \qquad (26)$$

$$M.S._{ult} = \frac{1}{1.5\left[\frac{14{,}000}{136{,}000} + \frac{8110}{180{,}000}\right]} - 1$$

$$M.S._{ult} = +3.4$$

RAMP ROLLER CLUTCH CAMSHAFT

The ramp roller clutch camshaft is analyzed in a manner similar to the outer housing but with loading inward instead of outward as shown in Figure 36. Ring formulas are used with 14 equally spaced loads and uniform shear flow acting at the radius to the centroid R_r of the input torque flange.

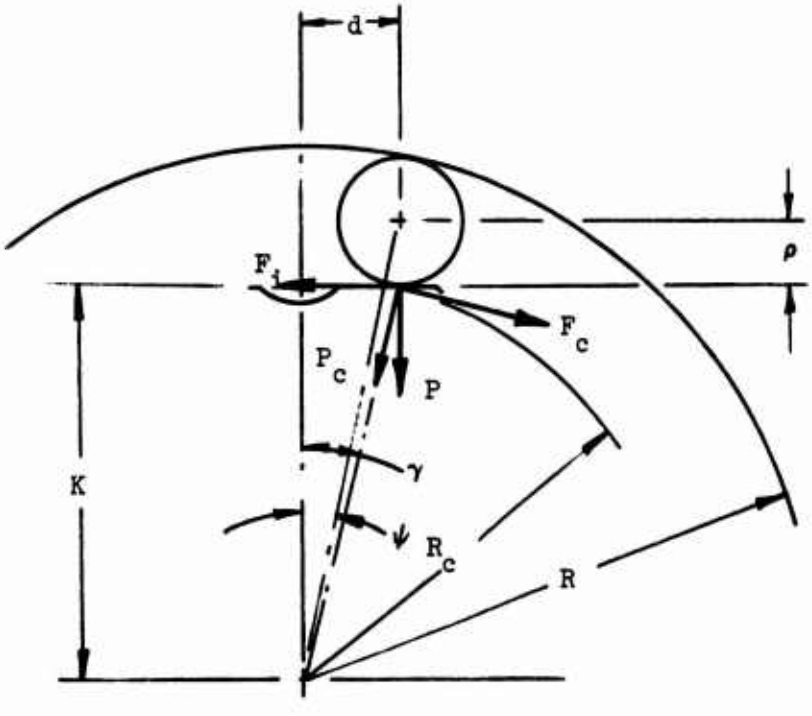

Figure 36. Roller Contact Loads on Inner Cam.

The roller loads are identical to those on the housing and are

$$F_i = F_o = 170 \text{ lb}$$

$$P = 3760 \text{ lb}$$

The radial and tangential cam loads P_c and F_c are found as follows:

$$d = (R-\rho) \sin \psi = (1.503 - .1875) \sin 5 \text{ deg } 11 \text{ min} = .1188 \tag{27}$$

$$\gamma = \tan^{-1}\left(\frac{d}{K}\right) = \tan^{-1}\left(\frac{.1188}{1.125}\right) = 6 \text{ deg } 5 \text{ min} \tag{28}$$

$$R_c = \frac{K}{\cos \gamma} = \frac{1.125}{\cos 6 \text{ deg } 5 \text{ min}} = 1.131 \tag{29}$$

$$P_c = P \cos \gamma + F_i \sin \gamma \tag{30}$$

$$= 3760 \cos 6 \text{ deg } 5 \text{ min} - 170 \cos 6 \text{ deg } 5 \text{ min}$$

$$= 3760 \text{ lb}$$

$$F_c = P \sin \gamma - F_i \cos \gamma \tag{31}$$

$$= 3760 \sin 6 \text{ deg } 5 \text{ min} - 170 \cos 6 \text{ deg } 5 \text{ min}$$

$$= 230 \text{ lb}$$

$$q_c = \frac{T}{2\pi F_r^2} \tag{32}$$

where q_c = shear flow lb/in.

R_r = radius to centroid of input torque flange

$$q_c = \frac{3570}{2\pi (.798)} = 890 \text{ lb/in.}$$

The critical sections through the cam are at the roller contact points ($\theta = \beta = \pi/N$):

$$\theta = \frac{\pi}{N} = \frac{\pi}{14} = .2244 \text{ rad.} = 12 \text{ deg } 51 \text{ min} =$$

$$M_{max} = \frac{-P_c \bar{R}}{2}\left[\frac{1}{\theta} - \frac{\cos\beta}{\sin\theta}\right] - \frac{F_c \bar{R} \sin}{2 \sin\theta} + q_c R_r^2 \beta \qquad (33)$$

$$= \frac{-3780(.843)}{2}\left[\frac{14}{\pi} - \frac{\cos(.2244)}{\sin(.2244)}\right] - \frac{230(.843)}{2}$$

$$+890(.797)(.2244)$$

$$= -53 \text{ in.-lb}$$

The internal compressive load is given by

$$F = \frac{-P_c \cos\beta}{2 \sin\theta} + \frac{F_c \sin\beta}{2 \sin\theta} \qquad (34)$$

$$= \frac{-3760 \cos(.2244)}{\sin(.2244)} + \frac{230}{2}$$

$$= -8130 \text{ lb (compression)}$$

The maximum bending stress occurs at the inside of the cam and is given by

$$f_b = \frac{M_{max} Y_i}{I_c} \qquad (35)$$

where I_c = moment of inertia of effective cam area about centroid, in^4.

Y_i = radial distance from centroid of cam area to inside fiber, in.

$$f_b = \frac{-53(.281)}{.0148}$$

$$f_b = -1000 \text{ psi}$$

The axial stress is given by

$$f_a = \frac{F}{A_c} \tag{36}$$

where A_c = cam cross-sectional area, $in.^2$

$$f_a = \frac{-8130}{.562}$$

$$f_a = -14{,}500 \text{ psi}$$

The material of the ramp roller clutch cam is AMS 6260, heat-treated, R_c30-45, which has the following material properties:

$$F_{tu} = 136{,}000$$

$$F_{ty} = 115{,}000$$

$$F_{bu} = 180{,}000$$

The margin of safety is given by

$$M.S._{ult} = \frac{1}{1.5\left[\frac{f_a}{F_{tu}} + \frac{f_b}{F_{bu}}\right]} - 1$$

$$M.S._{ult} = \frac{1}{1.5\left[\frac{14{,}500}{136{,}000} + \frac{1{,}000}{180{,}000}\right]} - 1$$

$$M.S._{ult} = +4.9$$

RAMP ROLLER CLUTCH ROLLER

The rollers transmit power to the outer housing from the cam and are subjected to a maximum compressive stress when transmitting the maximum design horsepower.

$P = 3760$ = load at maximum hp

$\rho = .1875$ = roller radius

$l = .56$ = roller effective length

The compressive stress on the rollers is calculated as shown in Reference 1:

$$f_c = .591 \sqrt{\frac{P\,E}{2\,l\,\rho}} \qquad (37)$$

$$f_c = .591 \sqrt{\frac{3760\ (29 \times 10^6)}{2\ (.56)(.1875)}}$$

$$f_c = 425{,}900 \text{ psi}$$

The allowable compressive stress is given in Reference 3:

$$f_c \text{ allowable} = 600{,}000 \text{ psi}$$

$$\text{M.S.} = \frac{600{,}000}{425{,}900} - 1 = +.41$$

RAMP ROLLER UNIT, DYNAMIC ANALYSIS, ROLLER RETAINER PIN SPRING ASSEMBLY

The pin and spring assembly as shown in Figure 37, exerts a force on the roller retention cage which causes the rollers to contact the outer housing and ramp roller cam at all times. Improper design can cause the torque on the roller retention cage to reverse under dynamic conditions due to centrifugal forces. This phenomenon is critical when the cam and rollers are in the freewheel position, i.e., initial contact angle. P_p as shown in Figure 37, is the total force on the roller retention cage due to static and dynamic forces. In the ideal design, P_p should remain constant under all conditions of rpm.

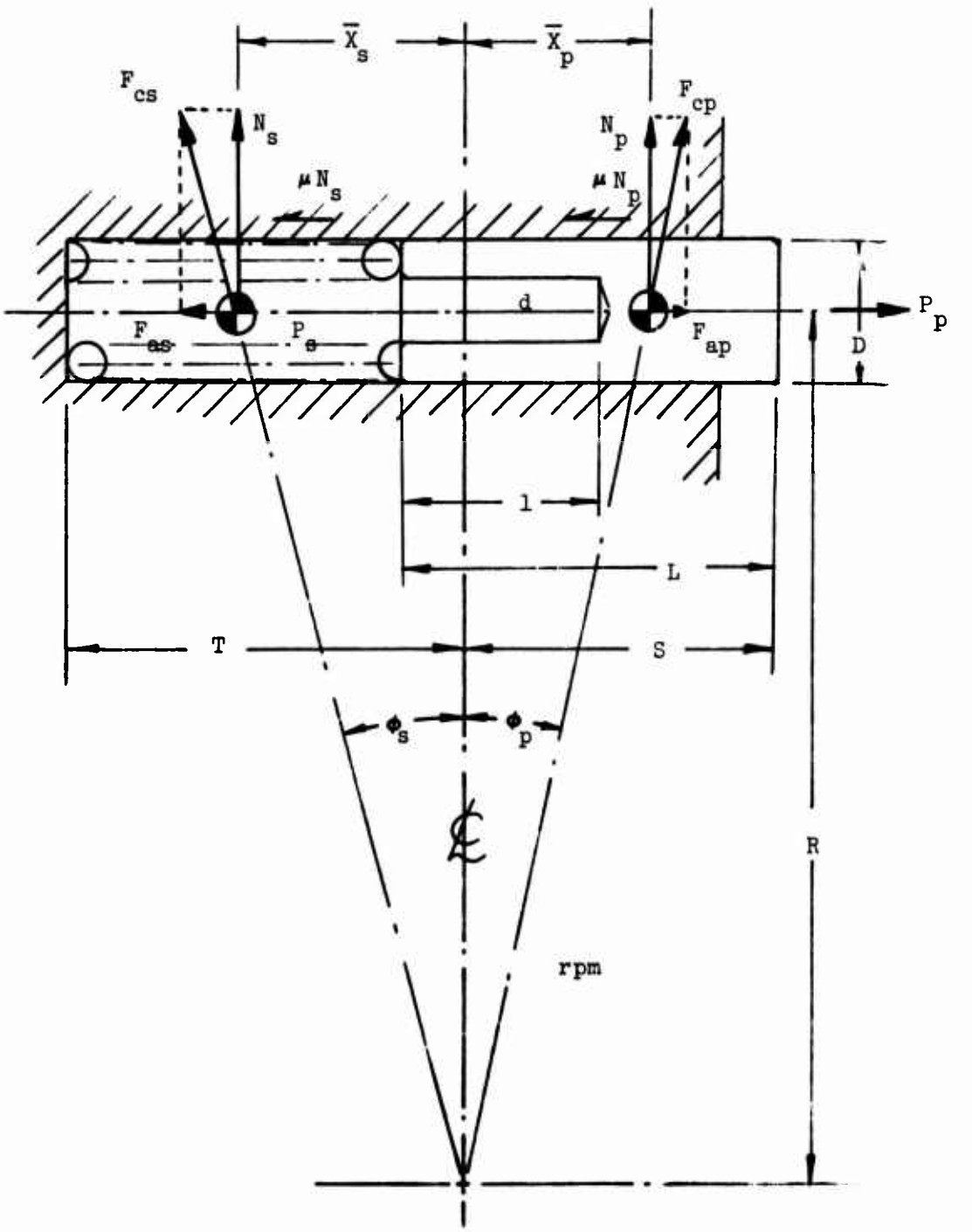

Figure 37. Roller Retainer Return-Pin-Spring Assembly Geometry and Dynamic Forces.

The spring analysis is given below.

f_s = 1.00 = free length of spring

K_s = 4.00 lb/in. = spring rate

W_s = .0004567 = weight of spring

$$\bar{X}_s = \frac{T - S + L}{2} \tag{38}$$

$$= \frac{.881 - .494 + .625}{2}$$

$$= .506$$

The centrifugal force acting on the spring is given as

$$F_{cs} = \frac{\pi^2 W_s \ rpm^2}{900\ g} \sqrt{R^2 + \bar{X}_s^2} \tag{39}$$

$$= \frac{\pi^2 (.0004567)(rpm)^2}{900\ (386)} \sqrt{1.280^2 + .506^2}$$

$$= 1.786 \times 10^{-8}\ rpm^2$$

The normal spring force is found from

$$N_s = F_{cs} \frac{R}{\sqrt{R^2 + \bar{X}_s^2}} \tag{40}$$

$$= 1.786 \times 10^{-8}\ rpm^2 \frac{1.280}{\sqrt{1.280^2 + .506^2}}$$

$$= 1.661 \times 10^{-8}\ rpm^2$$

The axial spring force is found from

$$F_{as} = N_s \frac{\bar{X}_s}{R} \tag{41}$$

$$= 1.661 \times 10^{-8} (rpm)^2 \frac{.506}{1.280}$$

$$= .656 \times 10^{-8} \ rpm^2$$

The spring force at the installed position is

$$F_s = K_s (f_s - T - S + L) \tag{42}$$

$$= 4.00 (1.000 - .881 - .474 + .625)$$

$$= 1.000 \text{ lb}$$

The resultant spring force acting on the pin in the axial direction is

$$P_s = F_s - (F_{as} + \mu N_s) \tag{43}$$

$$= 1.000 - (.656 \times 10^{-8} \ rpm^2 + \mu \, 1.661 \times 10^{-8} \ rpm^2)$$

$$= 1.000 - rpm^2 \times 10^{-8} \ (.656 + 1.661 \mu)$$

If the rpm and μ in the above equation are such that P_s is negative, the spring will not act on the pin but will be forced in the opposite direction. In the ramp roller clutch design, the spring becomes inactive at 12,300 rpm regardless of μ.

The analysis of the pin is given below.

D = .125 in.

L = .625 in.

d = .0625 in.

l = .375 in.

W_p = .001845 lb = pin weight

$$\bar{X}_p = \frac{DL^2 - dl^2}{2\,(DL - dl)} + S - L \tag{44}$$

$$= \frac{.125(.625)^2 - .0625(.375)^2}{2\,[.125\,(.625) - .0625(.375)]} + .494 - .625$$

$$= .235$$

The centrifugal force exerted on the pin in the radial direction is

$$F_{cp} = \frac{\pi^2 \; W_p \; rpm^2}{900\; g} \sqrt{R^2 + \bar{X}_p^2} \tag{45}$$

$$= \frac{\pi^2(.001845)\; rpm^2}{900\;(386)} \sqrt{1.280^2 + .235^2}$$

$$= 6.821 \times 10^{-8} \; rpm^2$$

The pin normal load is found from

$$N_p = \frac{F_{cp} \cdot R}{\sqrt{R^2 + \bar{X}_p^2}} \tag{46}$$

$$= \frac{6.821 \times 10^{-8} \; rpm^2 \; (1.280)}{\sqrt{1.280^2 + .235^2}}$$

$$= 6.709 \times 10^{-8} \; rpm^2$$

The pin axial component of centrifugal force is given as

$$F_{ap} = N_p \frac{\bar{X}_p}{R} \tag{47}$$

$$= 6.709 \times 10^{-8} \text{ rpm}^2 \quad \frac{.235}{1.280}$$

$$= 1.232 \times 10^{-8} \text{ rpm}^2$$

The resultant pin force on the ramp roller carrier is given as

$$P_p = P_s + F_{ap} - \mu N_p \tag{48}$$

$$= P_s + \text{rpm}^2 \times 10^{-8} \left[1.232 - 6.709 \mu \right]$$

where P_s = resultant spring force on pin and can never be negative.

Examination of Equation (48) reveals that $P_p = 0$ when the coefficient of friction μ is greater than .18 and the rpm is such that $P_s = 0$. Figure 38 is a plot of resultant pin load versus rpm for various values of coefficient of friction. It shows that for a range of practical values of μ, the resultant pin load is always positive.

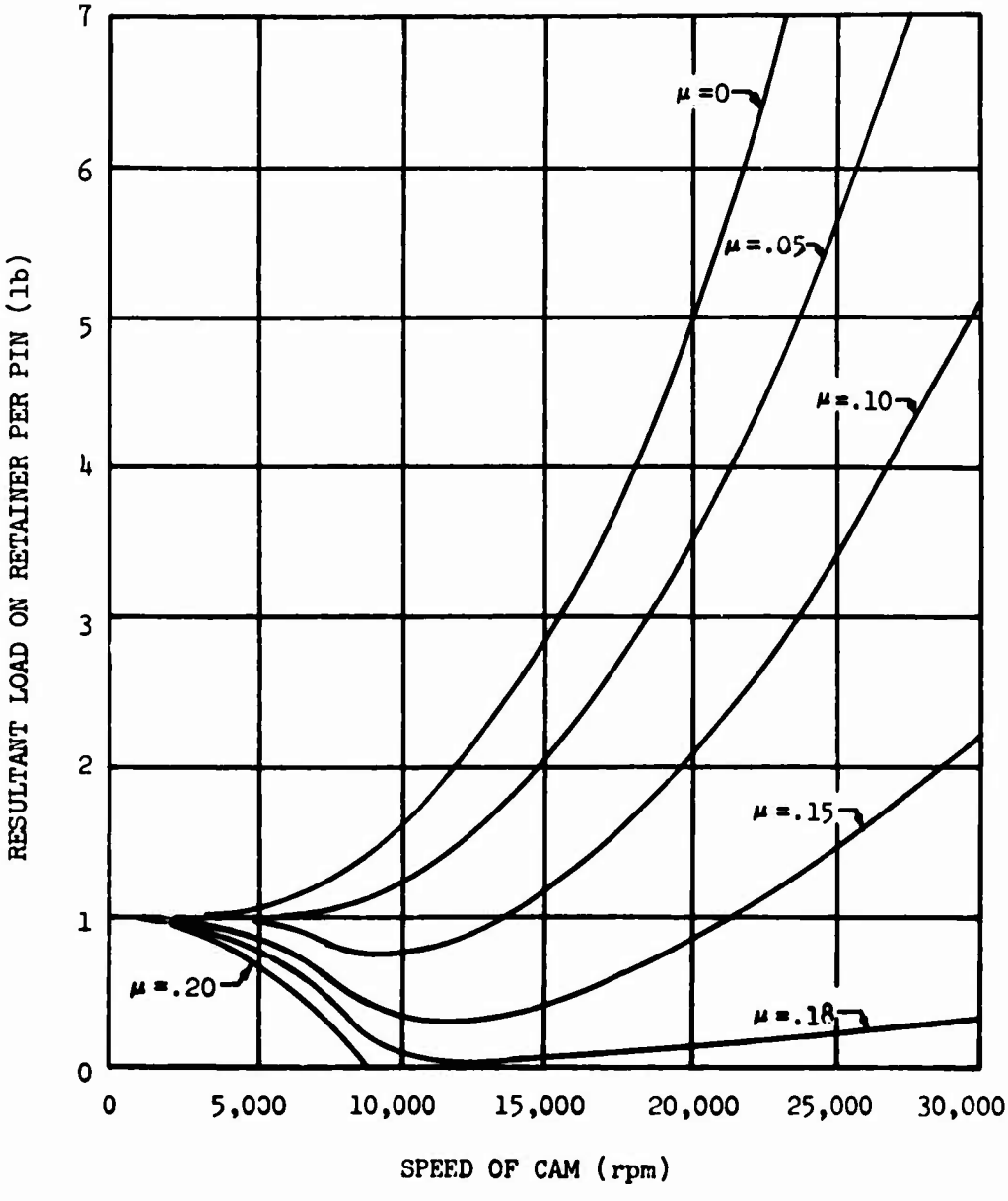

Figure 38. Resultant Pin Load on Retainer for Various Values of Coefficient of Friction.

APPENDIX II

HOLLOW ROLLER ANALYSIS, RAMP ROLLER CLUTCH

Hollow rollers have recently been investigated for applications in roller bearings. Cylindrical roller bearings having annular rollers offer several advantages over bearings having solid rollers, particularly in high-speed applications. The chief advantage is the reduction of centrifugal roller load due to lower roller weight. In high-speed applications, the centrifugal roller loading may become more significant than the applied bearing loads; thus the use of hollow rollers may improve bearing life substantially. Another advantage of the annular roller is the improved heat dissipation of the bearing by allowing additional collant flow through the centers of the rollers. Hollow rollers also offer improved load sharing and may retard cage skidding due to the higher flexibility afforded. These advantages must be compared with the increased bearing deflections and bending stress which affect the bearing fatigue life.

In the ramp roller clutch, annular rollers offer many of the same advantages as the cylindrical roller bearing. A significant factor at high speed is centrifugal roller loading during differential overrunning, which is reduced with hollow rollers. Centrifugal roller loading is a direct cause of wear in the rollers and housing of a ramp roller clutch. In the ramp roller clutch of this program, the roller centrifugal load at full rpm exceeds 25,000 g's. Improved heat dissipation during overrunning and improved load sharing are also important advantages of annular rollers in the ramp roller clutch. Roller stresses are vibratory in the cylindrical roller bearing and steady in the ramp roller clutch. Since rollers of the ramp roller clutch carry steady loads only, it would appear that the advantage of reduced centrifugal loading with hollow rollers is enhanced. In practice, however, the applied roller loads are much higher in the ramp roller clutch than in roller bearings, which offsets the advantages of static stress design. Thus, in the ramp roller clutch of this program, the practical upper limit for the 0.375-inch-diameter roller is a hole of 0.125 inch diameter which reduces centrifugal load by 12.5 percent. A larger hole will reduce centrifugal load significantly but will increase resultant roller stress levels.

There are several methods available for determining hollow roller stresses analytically. From the method of Reference 4, the stresses at various positions on the inside and outside of the hollow rollers are given by

$$f = K \frac{4P}{\pi D} \tag{49}$$

where
- P = roller unit load, lb/in.
- D = outer roller diameter, in.
- K = a factor dependent upon the position at which the stress is required and on the ratio of roller hollowness H (ratio of inner to outer roller diameter)
- f = annular roller tangential stress, psi

The stress multiplication factor K is determined from photoelastic studies and is given in Reference 4. The point of maximum stress is on the inside of the hollow roller at a point directly under the applied load.

A second method which uses curved beam theory is given in Reference 5 and is similar to the methods of References 6, 7, and 8. The stress at a point on the inside of the roller and directly under the load is given by

$$f = \frac{2P}{\pi D}\left[\frac{1}{2ZH} - \frac{1}{(1-H)}\right] \tag{50}$$

where $H = d/D$ = ratio of inner to outer roller diameter

$$Z = -1 + \left[\frac{(1+H)}{2(1-H)}\right] \ln\left(\frac{1}{H}\right) \tag{51}$$

For the roller of the ramp roller clutch, a comparison of the results of these two methods for calculating stresses is presented in Figure 39. Note that as H becomes small in Figure 39, the curved beam theory is inaccurate since the stress is infinite for H = 0. The photoelastic method is more accurate for small values of H.

Although the rollers of the ramp roller clutch are designed statically, maximum stress dictates hollow roller design. The rollers are fabricated from CEVM 8620 steel and heat-treated to R_C 59 minimum. This represents an ultimate tensile strength in excess of 300,000 psi. At the maximum operating condition, the allowable stress for hollow rollers can be in the order of 150,000 psi. This value is chosen on the basis of low cycle fatigue considerations. Referring to Figure 39, with an allowable stress of 150,000 psi, the ratio H is approximately .32 for the curved beam theory and .38 for the photoelastic analysis method; hence, a 0.125-inch-diameter hole (H=.33) is about the maximum practical diameter for use in the annular roller of the ramp roller clutch design presented herein.

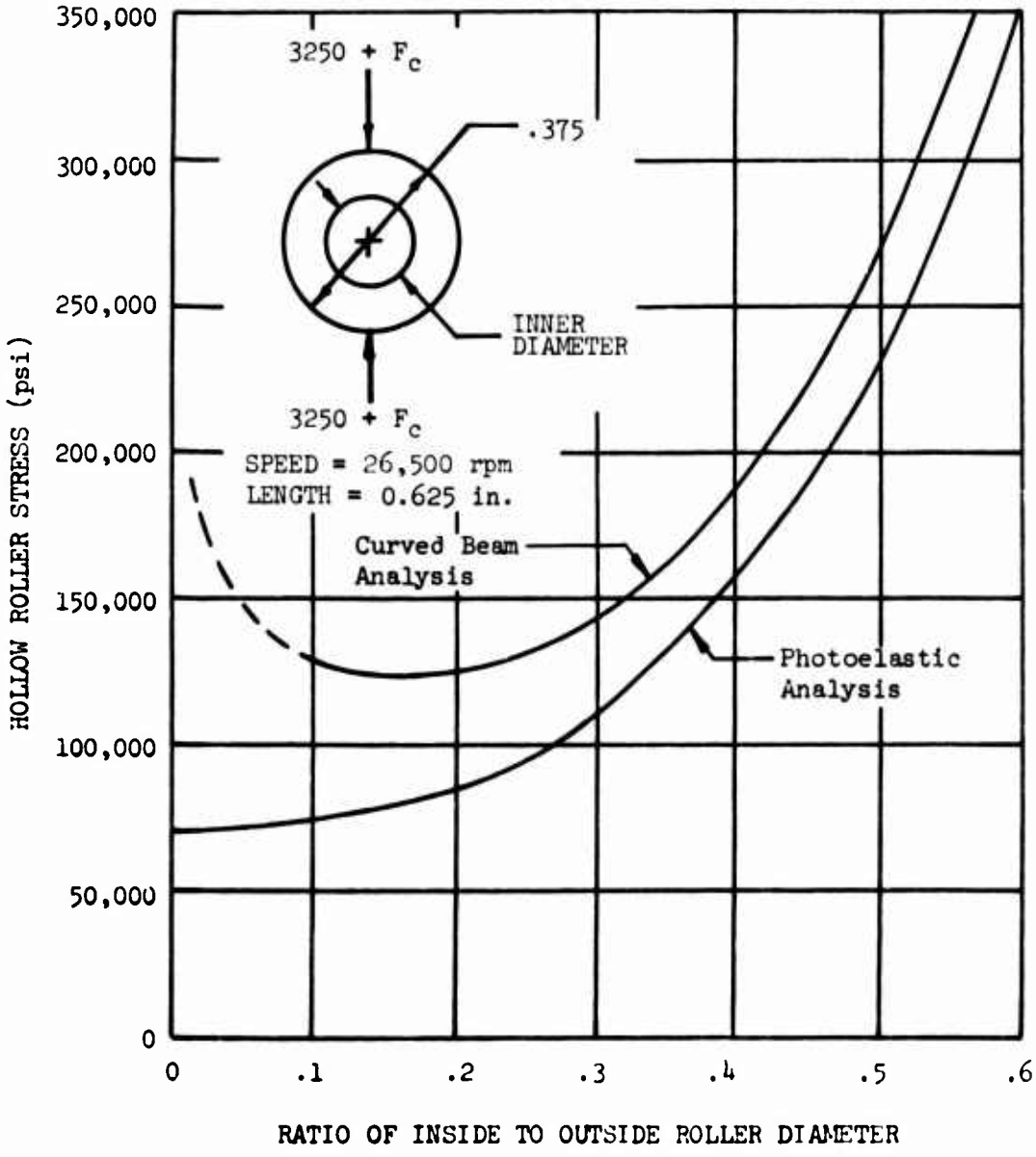

Figure 39. Hollow Roller Bending Stresses for 3570 In.-Lb Design Condition.

APPENDIX III

DYNAMIC TEST DRAG TORQUE DATA

Full speed overrunning test drag torque data is presented in Figures 40 and 41. The drag torque of Figure 40 was measured by spring scale and arm whereas the drag torque shown in Figure 41 was measured by temperature rise of the oil.

Drag torque data for the differential speed overrunning tests is shown in Figure 42.

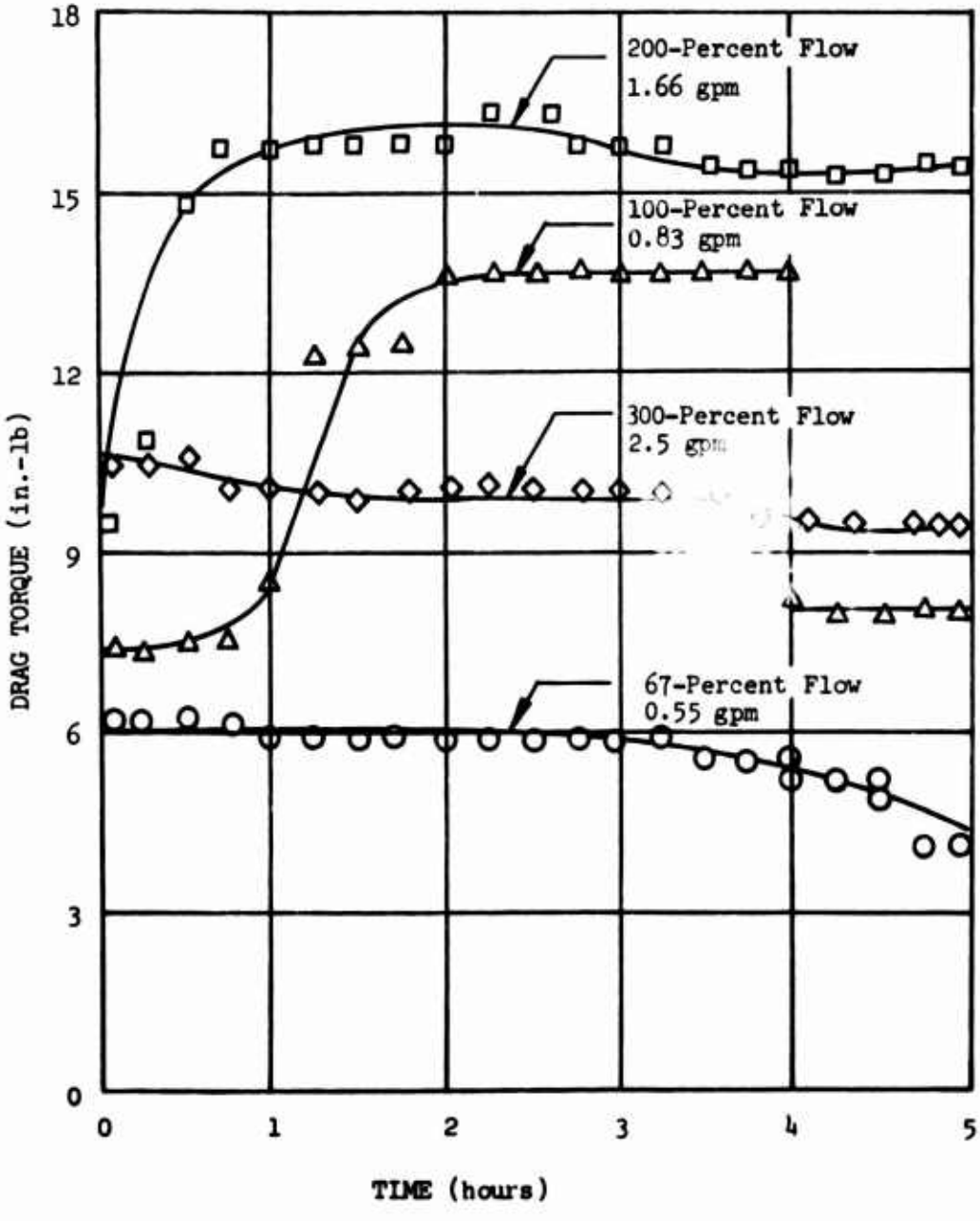

Figure 40. Full-Speed Overrunning Test Drag Torque Data Measured by Spring Scale and Arm.

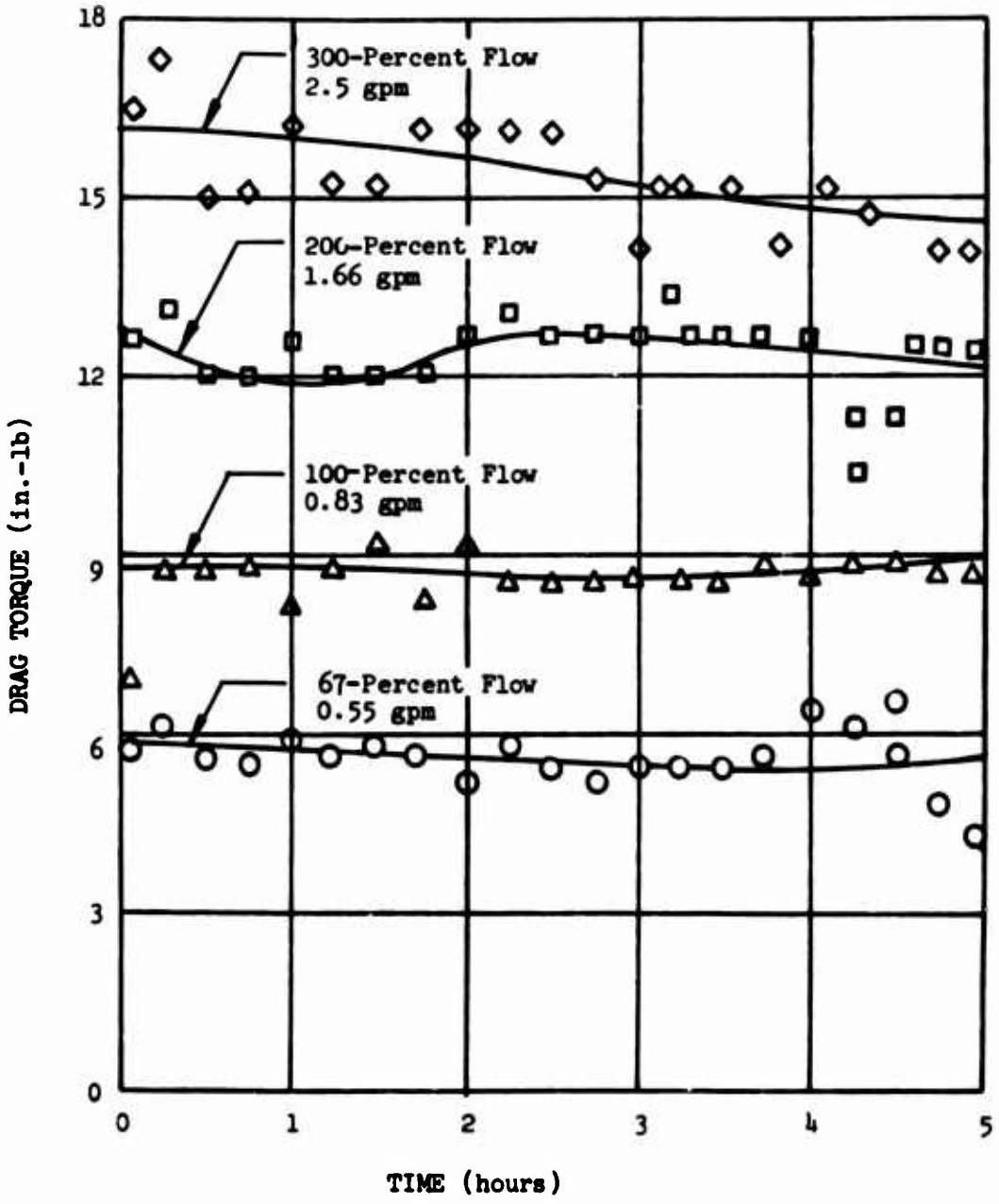

Figure 41. Full-Speed Overrunning (Input Stationary - Output 26,500 RPM) Test Drag Torque Data Measured by Heat Absorbed in Oil.

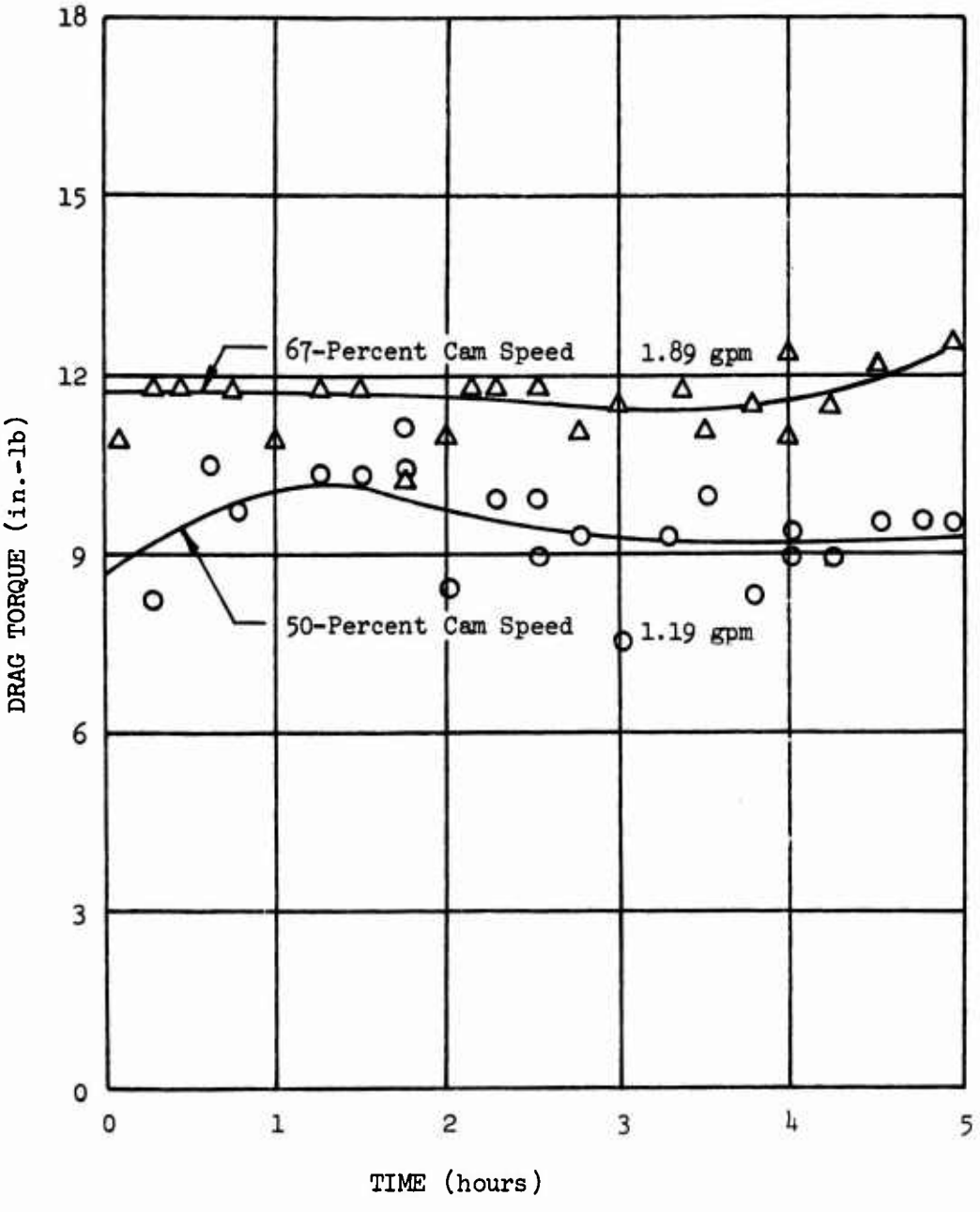

Figure 42. Differential-Speed Overrunning Test, Drag Torque Data.